UNIVERSITÀ DEGLI STUDI DI TRIESTE

XXXIII CICLO DEL DOTTORATO DI RICERCA IN NANOTECNOLOGIE

Biophysical and biomolecular analysis of EVs and their interaction with target cells

Settore scientifico-disciplinare: FIS/03 – Dipartimento di Fisica

DOTTORANDA
Beatrice – Senigagliesi

COORDINATORE
PROF. Alberto – Morgante

SUPERVISORE DI TESI
Dr. Pietro – Parisse

CO-SUPERVISORE DI TESI
Dr. Loredana - Casalis

ANNO ACCADEMICO 2019/2020

UNIVERSITÀ DEGLI STUDI DI TRIESTE

XXXIII CICLO DEL DOTTORATO DI RICERCA IN NANOTECNOLOGIE

Biophysical and biomolecular analysis of EVs and their interaction with target cells

Settore scientifico-disciplinare: FIS/03 – Dipartimento di Fisica

DOTTORANDA
Beatrice – Senigagliesi

COORDINATORE
PROF. Alberto – Morgante

SUPERVISORE DI TESI
Dr. Pietro – Parisse

CO-SUPERVISORE DI TESI
Dr. Loredana - Casalis

ANNO ACCADEMICO 2019/2020

ABSTRACT

Triple negative breast cancer (TNBC) is one of the most aggressive, invasive breast cancer subtypes with a poor prognosis. Despite the constant progress in this field, development of metastases in TNBC remains a highly complex and poorly understood process with a relatively poor outcome. In light of that, clarifying biological mechanisms of the metastatic process in TNBC is crucial in finding new therapeutic approaches for effective interventions.

Metastasis is thought to be easier for more deformable and, therefore, soft cancer cells, which can migrate through narrow pores of extracellular matrix and vessels. Extracellular vesicles (EVs) derived from TNBC, by sharing oncogenic molecules, have been shown to promote proliferation, drug resistance migration, and metastatic capability in target cells proportional to properties of donor ones.

Considering all these evidences, we wondered if small extracellular vesicles (small-EVs) could also transfer information to target cells about biomechanical properties of the donor cell.

Small-EVs were isolated through ultracentrifuge from metastatic MDA-MB-231 cells (TNBC) and characterized by using a multi-technical approach (SEM, AFM, NTA, Western blot). The functionality and activity of isolated vesicles were tested in non-invasive MCF7 cells, as target cells. Cell stiffness changes in MCF7 cells upon the addition of MDA-MB-231-derived small-EVs were studied via AFM force spectroscopy, cytoskeleton rearrangements via fluorescence analyses, and Yap activity via RT-qPCR analyses.

Our results showed that the addition of TNBC-derived small-EVs can directly decrease cell stiffness (Young's modulus), induce cytoskeleton and nuclear rearrangements, and increase Yap activity in MCF7 cell line as target cell, by making them similar to donor cells.

Therefore, in this study, we highlighted a new mechanism through which TNBC-derived small-EVs could be able to contribute to progression and metastatic processes in breast cancer; this new knowledge could be used in diagnostic and therapeutic field.

NanoInnovation Laboratory, lead by Dr. Loredana Casalis, Elettra-Sincrotrone Trieste S.C.p.A, and Pietro Parisse, CNR-IOM.

TABLE OF CONTENTS

INTRODUCTION

Extracellular vesicles

A new communication paradigm

Intercellular communication represents a crucial process for all living organisms (Simeone *et al.*, 2020). Cell-cell communication has been considered for long time exclusively mediated by direct cell-cell contact/interactions or by the release of soluble factors (i.e. chemokines, cytokines, and growth factors) (Ahmed and Xiang, 2011)(Yoon, Kim and Gho, 2014). However, in the last decades an alternative mechanism to those already known, represented by the release of membrane-derived vesicles, has been described and has gained much interest (Peinado, Lavotshkin and Lyden, 2011)(Pitt, Kroemer and Zitvogel, 2016). For several years, lipid vesicles released by cells were not considered to be of biological significance, but only cellular waste or debris. With the improvement of the research tools and thanks to the new knowledge about the exocytosis, this idea and also the relative interest have been completely reversed. Vesicle isolation, characterization, imaging and experimentally supported activity revealed their role as carriers able to transfer bioactive molecules and signals to both neighboring and distant cells (Margolis and Sadovsky, 2019). These vesicles released from donor cells are now classified by the term "Extracellular Vesicles" (EVs). International Society for Extracellular Vesicles (ISEV) "*endorses EV as the generic term for particles naturally released from the cell that are delimited by a lipid bilayer and cannot replicate, i.e. do not contain a functional nucleus*" (Thery *et al.*, 2018). The secretion of EVs appears to be conserved among species; in fact, it has been identified basically in all eukaryotes and in many prokaryotes (Raposo and Stoorvogel, 2013). The new intercellular crosstalk mediated by EVs concerns almost all the cell types of the body and controls both physiological and pathological conditions.

What are the Extracellular Vesicles?

EVs are nano-sized particles (from 30 up to 5000 nm in diameter) delimited by a lipid bilayer capable of transferring functional cargos, such as proteins, nucleic acids, metabolites, and lipids. Cell culture media and body fluids are replete with extracellular vesicles, some of which are presumably en route from their source to their physiological target. Extracellular vesicles are present in all body fluids. In fact, they can be isolated from blood, urine, saliva, milk, tumor exudates, cerebrospinal fluid, and amniotic fluid (Li *et al.*, 2019). Several published reports

confirmed that extracellular vesicles transfer functional biological elements from donor cell to target cell/cells by moving through the extracellular space both in vitro and in vivo (Raposo and Stahl, 2019), as shown in **Figure 1**. The vesicle data have indicated that cargo of EVs is highly heterogeneous and dynamic and depends directly on the donor cell, state and environmental conditions (Yáñez-Mó *et al.*, 2015). Furthermore, there seems to be a specificity between EVs and target cells: vesicles have transmembrane receptors, integrins and cell-adhesion molecules that seem to bind specific microdomains of the plasma membrane of the target cells, in order to transmit their information after different uptake mechanisms (Fais *et al.*, 2016). It is known that EVs mediate most, if not all, physio-pathological processes, including tumor invasion/metastasis, neural signal transduction, immunoregulation, embryofetal development, ageing, and repair/regeneration, etc. (Zheng *et al.*, 2020)(Kawahara and Hanayama, 2018)(Xie *et al.*, 2020)(Szekeres-Bartho, Šućurović and Mulac-Jeričević, 2018)(Panagiotou *et al.*, 2018)(Bjørge *et al.*, 2018). Thus, vesicles can be released constitutively from donor cell, or their production can take place even after activation, due to inflammation, hypoxia, oxidative stress, cell death, etc. (Helmke and Vietinghoff, 2016)(Almeria *et al.*, 2019)(Bodega *et al.*, 2019)(Kakarla *et al.*, 2020).

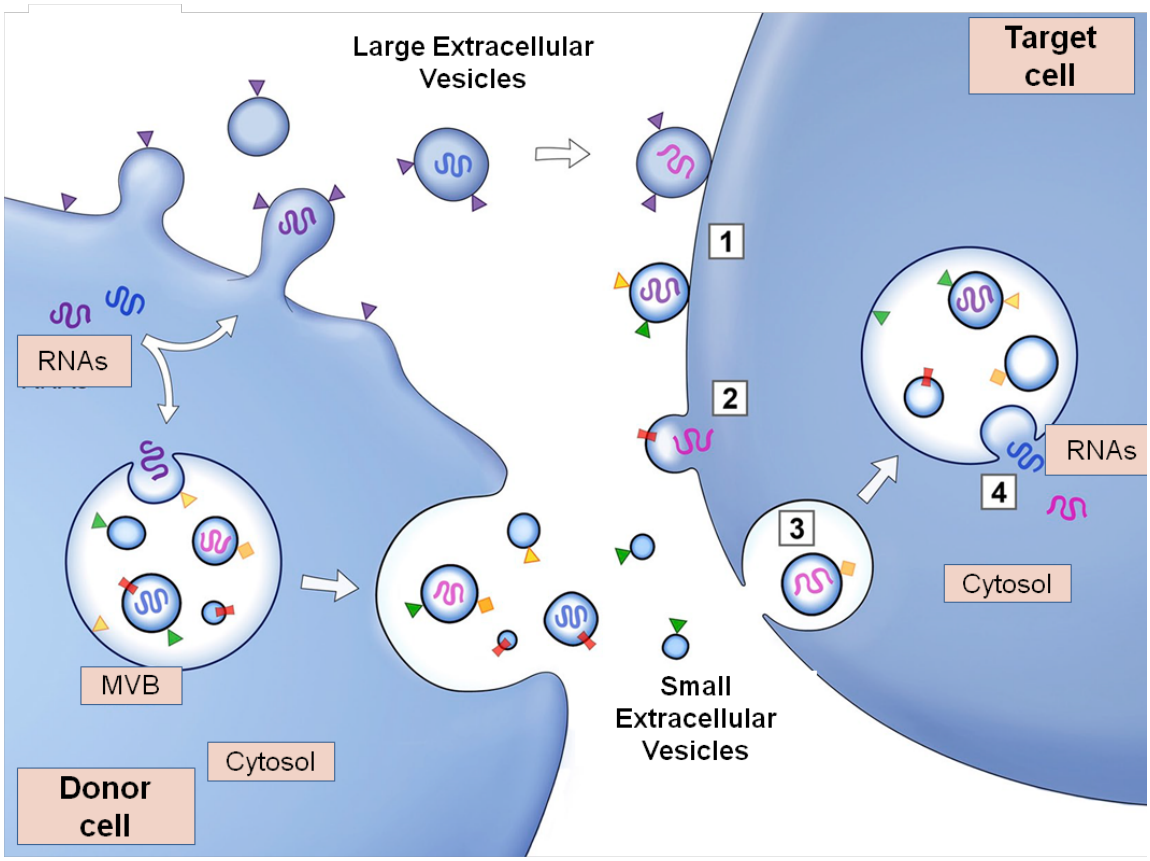

Figure 1. A new cell-cell communication paradigm: via Extracellular vesicles. Schematic representation of EV release from donor cell and interaction with target cell.

Role in diagnosis

In body fluids, there is a mixture of EVs originating from various tissues, including some vesicles that can provide information on specific pathological conditions present in the body. The lipid membrane of EVs encapsulates and protects their contents from the degrading enzymes present in the body fluids (Yáñez-Mó *et al.*, 2015). The EV stability at different conditions (with and without protease inhibitors at 37°C, 4°C, −20°C and −80°C) was assessed and it seems that EVs are stable at least for 3 months (Sokolova *et al.*, 2011). Therefore, the stability of disease-derived EVs in body fluids offers excellent opportunities to exploit these vesicles as reservoirs of disease biomarkers. Based on their utility in practice, vesicle analysis as biomarker could provide insights on early diagnosis, prognosis, regression or response to treatment of a disease. Moreover, body fluid-derived EV analysis represents a non-invasive methods of analysis, very useful especially in cases of tumours or inaccessible diseased tissues (e.g., neurodegenerative diseases) (Boukouris and Mathivanan, 2015). Hence, for clinicians and diagnosticians, EV-based tests available for clinical use are gaining increasing interest; for example the prostate intelliscore test was approved by the Food and Drug Administration (FDA) (Tschuschke *et al.*, 2020). Several technologies, such as fluorescence labeling, micro imaging and microfluidic chip, are successfully employed for single extracellular vesicles (SEV) detection and new detection strategies SEV are developing (Wang *et al.*, 2020).

Role in therapy

In addition to being an excellent diagnostic resource, these nanocarriers, given their biocompatible characteristics might be potentially used also in therapeutic field (Stremersch, De Smedt and Raemdonck, 2016). EVs can be used as drug delivery system (DDS) of various chemical and biological entities (endogenous and/or exogenous), including small molecules, anti-cancer agents, anti-inflammatory compounds, miRNA, mRNA, proteins, and growth factors, etc. (Burnouf, Agrahari and Agrahari, 2019). Currently, liposomes and polymeric nanoparticles are most commonly used for the administration of drugs and genes (anti-cancer drugs, anti-fungal drugs, and analgesics). Both liposomes and nanoparticles are synthetic or semi-synthetic and, therefore, they have limitations, including the short half-life in the circulatory system, varying biocompatibility, and long-term toxicity (Tschuschke *et al.*, 2020). Instead, extracellular vesicles have promising long circulating half-life, minimal side effects, intrinsic capability to target specific tissues or even cells, low immunogenicity and tend to have innate homing capacity (Lai *et al.*, 2013). Extracellular vesicles are an important mode of communication between neurons and glia in Central Nervous System, making them crucial for

the physiological modulation of neuronal processes (Saeedi *et al.*, 2019). As a matter of fact, EVs can cross the blood-brain barrier in both directions, propagating inflammation across the blood brain barrier (BBB), mediating neuroprotection, and modulating regenerative processes (Ciccocioppo *et al.*, 2019). Therefore, EVs may also be genetically engineered to pass through the blood-brain barrier and penetrate into tissues, in order to carry numerous types of drug molecules and genes, such as proteins, lipids, RNAs and DNAs, protecting them from degradation (Ha, Yang and Nadithe, 2016). In addition, researchers demonstrated that EVs can promote heart repair and that they can be used as nano-therapeutic agents in autoimmune diseases and neurodegenerative diseases (Wang *et al.*, 2020).

EV publications

Therefore, EVs appear to be ideal nanovectors for theranostics (therapy and diagnosics), which includes the early detection of diseases, the monitoring of therapeutic responses, and the targeted delivery of therapeutic agents (Fais *et al.*, 2016).

Considering their important role as mediators of cell signalling and their precious potential in theranostic field, the last decade has seen a sharp increase in the number of scientific publications about EV studies (Nazarenko, 2020), as shown in **Figure 2**.

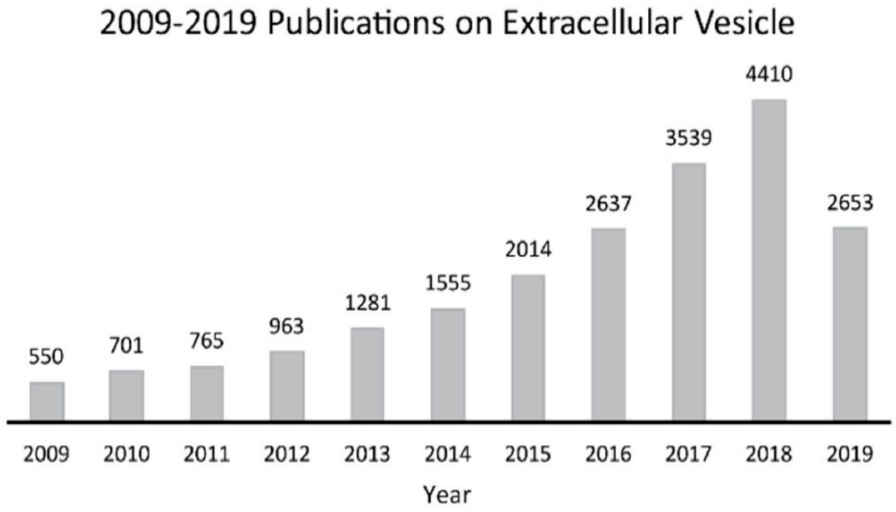

Figure 2. Publication trends on extracellular vesicle studies from 2009 to 2019. Publications were selected by searching the keyword "extracellular vesicle" in the Web of Science. *X axis*: year; *Y axis*: number of publications (Li *et al.*, 2019).

Biogenesis

Although knowledge on extracellular vesicles is continuously increasing, several "unsolved mysteries" (i.e. size diversity, cargo loading, target specificity, cell delivery, function in health and disease etc.) remain elusive, mainly due to their high intrinsic heterogeneity (Lötvall *et al.*, 2014)(Margolis and Sadovsky, 2019). However, extracellular vesicles can be subdivided into several subtypes depending on physical characteristics, biochemical compositions, conditions or cell of origin. The International Society for Extracellular Vesicles, ISEV, (Thery *et al.*, 2018) adopts a classification that refers to their physical/size characteristics; therefore, EVs are subdivided into two main classes: "small-EVs" (sEVs) and "medium/large-EVs" (m/lEVs), with ranges defined, respectively, < 200 nm and > 200 nm.

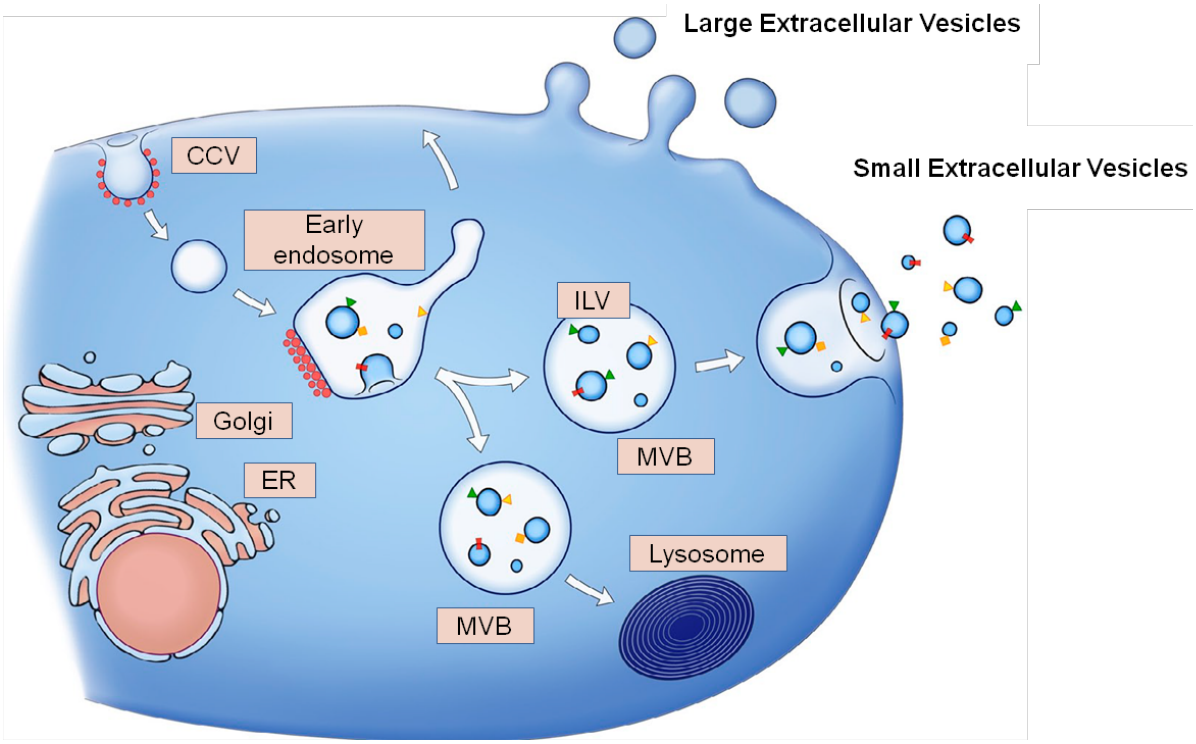

Figure 3. Release of large-EVs and small-EVs from donor cell. The first bud directly from the plasma membrane, whereas the second are formed as the ILV by budding into early endosomes and MVBs and are released by fusion of MVBs with plasma membrane. Other MVBs fuse with lysosomes. Red spots represent clathrin associated with vesicles at the plasma membrane (clathrin-coated vesicles [CCV]) or bilayered clathrin coats at endosomes (Raposo and Stoorvogel, 2013).

Small extracellular vesicles

Small-EVs have, usually, an endocytic biogenesis formed through sequential invaginations of endosomal membrane that results in early endosome formation, which maturates into a type of late endosome, called multivesicular bodies (MVBs), as shown in **Figure 3**.

The MVBs, leading to generation of intraluminal vesicles (ILVs), later fuse with plasma membrane and release the ILVs, which in turn become sEVs upon cellular exit (Bebelman *et al.*, 2018)(Tschuschke *et al.*, 2020). Numerous molecules and pathways are involved in the MVB and ILV formation. Endosomal Sorting Complex Required for Transport (ESCRT) (e.g. the tumor susceptiblity gene 101 protein, TSG101) is an ubiquitin-dependent mechanism important for sorting ubiquitinated proteins in the ILVs. However, MVB and ILV formation can occur also with ESCRT-independent pathways, such as pathways related to tetraspanin family composed to four-transmembrane domain proteins (cluster of differentiation proteins, e.g. CD9, CD63, and CD81). Moreover, several proteins facilitate and control the MVB fusion with plasma membrane and participate in processes concerning vesicle transport within cells (such as GTP-ase RAB proteins or soluble NSF-attachment protein receptors, SNAREs). In addition to these proteins, also cytoskeleton directly contributes to the budding and the release of EVs. The vesicle secretion requires altered actin polymerization under the plasma membrane followed by the actomyosin contraction in a process orchestrated by the small GTPase RhoA (Granger *et al.*, 2014)(Antonyak, Wilson and Cerione, 2012). Cortical actin depolymerization probably allows MVB docking to the plasma membrane for vesicle release. Also microtubule network is necessary for the MVB transport to plasma membrane (Jackson *et al.*, 2017). The composition of extracellular vesicles reflects most of the time the composition of MVBs and, therefore, can give clues about the pathway involved in their release. Moreover, proteins useful for MVB and ILV formation found in vesicles are accepted as specific extracellular vesicle markers (e.g. TSG101, CD9/63/81, RAB proteins etc.) (Kim *et al.*, 2013)(Hessvik and Llorente, 2018)(Tschuschke *et al.*, 2020).

Medium/Large extracellular vesicles

Instead, medium/large-EVs are usually generated by the direct outward budding of plasma membrane and, therefore, they resemble plasma membrane composition of the donor cell (Yoon, Kim and Gho, 2014)(Tschuschke *et al.*, 2020)(Kalluri and LeBleu, 2020), as shown in **Figure 3**. The medium/large-EVs can be generated via multiple distinct mechanisms that partially can overlap with those involved in small-EV biogenesis, and vice versa.

As a matter of fact, these are general indications but there is no clear and standard classification for the different types of extracellular vesicles. EVs have dimensions, cargo, membrane composition, biogenesis and, above all, extremely heterogeneous biological functions.

Cargo loading

Extracellular vesicles may deliver specific molecules to target cells and, therefore, functional activity of vesicles directly depends on their cargo loading, mainly composed by proteins, lipids and nucleic acids, as shown in **Figure 4**.

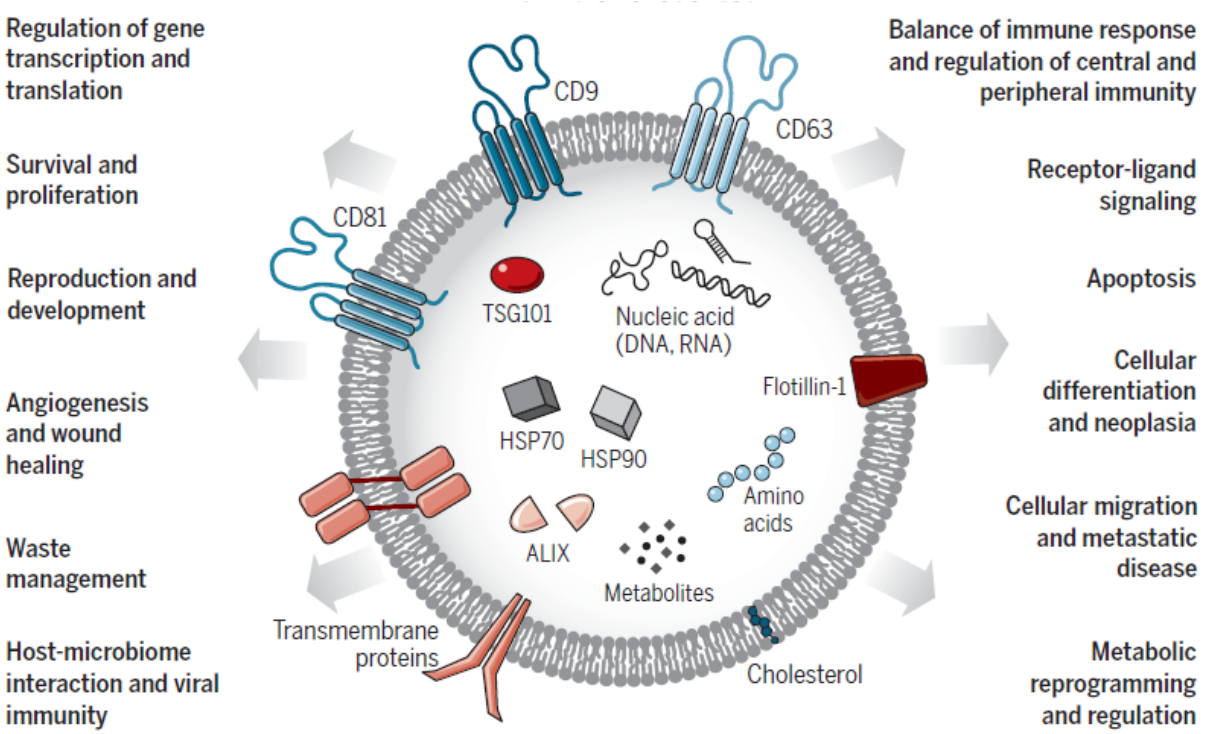

Figure 4. Hallmarks of EVs. Extracellular vesicles generated by all cells carry nucleic acids, proteins, lipids, and metabolites to target cells (Kalluri and LeBleu, 2020).

Proteins

No universal protein marker of EVs has been identified, to date. However, proteomic studies on EVs derived from different cell types suggest the presence of common vesicle proteins, mainly involved in vesicle structure, biogenesis, and trafficking: tetraspanins (CD9, CD63, and CD81), adhesion proteins (integrins), transporter and channels, vesicle trafficking-related proteins (Annexine, TSG101 and Alix), cytoskeleton proteins (actins, cofilin-1, ezrin/radixin/moesin, profilin-1, and tubulins), and cytosolic proteins (heat shock proteins and metabolic enzyme) (Choi *et al.*, 2013). However, as mentioned before, biogenesis of different EV classes determines the enrichment of endosomal-associated proteins and plasma membrane proteins in

small-EVs and medium/large-EVs, respectively. Cytoskeleton proteins, in both case, are crucial for EV release, structure, and motility (Morhayim, Baroncelli and Van Leeuwen, 2014). Proteins present in the plasma membrane and cytoplasm are more commonly sorted into EVs if compared with nuclear ones (Raimondo *et al.*, 2011). Furthermore, EVs also contain cell type-specific proteins. For example, melanoma-derived EVs contain tumor-associated antigen (MART1), while epithelial cell-derived EVs contain epithelial cell adhesion molecule (EpCAM) (Yoon, Kim and Gho, 2014). A growing number of studies suggest that breast cancer-derived EVs are enriched in various cancer-associated molecules, such as oncogenic proteins (HER2, EGFR, FAK, survivin, EMMPRIN, CD24, and EpCAM) and miRNAs when compared with healthy controls (Rontogianni *et al.*, 2019). Vesicular proteins seems to be sorted by the endosomal-sorting complexes (e.g. tetraspanins and heat shock proteins that cluster at the site of exocytosis; plasma membrane budding act as sorting machineries to target proteins into EVs (Morhayim, Baroncelli and Van Leeuwen, 2014)), by protein-lipid interactions, (e.g. proteins associated with lipid rafts like flotillin, glycosylphosphatidylinositol-anchored proteins and annexin (Wubbolts *et al.*, 2003)), or by the internalization of cytosolic proteins (Choi *et al.*, 2013).

Lipids

Lipids are known to play key roles in the rigidity, stability, function, intracellular fusion, and budding processes of extracellular vesicles (Yoon, Kim and Gho, 2014) and protect vesicle cargo from degradation before the uptake in target cell. Lipidomic analyses of extracellular vesicles derived from different cells and biological fluids reveal the presence of membrane lipids (sphingomyelin, phosphatidylcholine, phosphatidylethanolamine, phosphatidylserine, ganglioside GM3, and phosphatidylinositol), prostaglandins (E2, F2, J2, and D2), and lysobisphosphatidic (Laulagnier *et al.*, 2004)(Subra *et al.*, 2007)(Subra *et al.*, 2010). However, the vesicle membrane does not exactly reflect plasma membrane of the donor cell. In fact, if compared to the cellular plasma membrane, EV lipid bilayer comprises more phospholipids, sphingomyelin, cholesterol, ganglioside GM3, phosphatidylserine, and hexosylceramides, at the expense of phosphatidylcholine and phosphatidylethanolamine (Raposo and Stoorvogel, 2013); as well as lower amount of phosphatidylinositol in comparison to releasing cell (Hessvik and Llorente, 2018). Sphingomyelin and cholesterol allow the tight packing of lipid bilayers and increase the vesicle rigidity and stability (Ramstedt and Slotte, 2002)(Needham and Nunn, 1990). Also the ganglioside GM3 increases the vesicle stability and, moreover, prevents the recognition of EVs by blood components and the uptake by the reticuloendothelial system (Allen *et al.*, 1991)(25). Furthermore, phosphatidylserine facilitates the vesicle fusion and

fission and helps to assemble the curved vesicular shape of EVs (Chernomordik and Kozlov, 2003). As the cellular plasma membrane, vesicle membrane contains lipid rafts that are detergent-resistant domains containing specific components (e.g., glycolipids, Src tyrosine kinases or glycosylphosphatidylinositol, GPI-anchored proteins, (Moreau *et al.*, 2019)). Lipid rafts are involved in vesicle formation and secretion of specific molecules into extracellular space (Tschuschke *et al.*, 2020). The biogenesis pathway greatly affects the lipid composition of each EV class. Small-EVs are enriched with endosomal phospholipid bis-monoacylglycero-phosphate, whereas medium-EVs contain phosphatidylcholine and are devoid of phospholipid bis-monoacylglycero-phosphate (Morhayim, Baroncelli and Van Leeuwen, 2014). In 2002 a biological activity evidence of vesicular lipid was reported for the first time (Kim *et al.*, 2002): tumor-derived extracellular vesicles can have an angiogenic activity promoting endothelial cell migration, tube formation and neovascularization in vitro and in vivo and their capability is mediated mainly by sphingomyelin. Furthermore, EV-bound prostaglandins were found to activate signaling pathways in basophil leukemia cells of rat (Subra *et al.*, 2010). Moreover, the transfer of vesicular lipids to target cells could lead to changes in cell homeostasis due to their accumulation and of their associated enzymes (Morhayim, Baroncelli and Van Leeuwen, 2014).

Nucleic acids

Extracellular vesicles derived from different cells and body fluids contain also nucleic acids. Significant quantities of vesicular mRNA and miRNA have been reported in extracellular vesicles (Choi *et al.*, 2013). Transfer of vesicular mRNAs and miRNAs can directly lead to the activation of signaling molecules and receptors or epigenetic reprogramming of target cells (Fabbri *et al.*, 2012)(Valadi *et al.*, 2007). Analyses of the vesicular mRNAs and miRNAs in diseased conditions may potentially be useful as diagnostic tool (Skog *et al.*, 2008). Interestingly, a review suggested how the vesicular miRNAs represents a very marginal proportion as compared to small RNAs (<200 nt) present in EVs, species including various small non-coding RNAs, lncRNAs, and mRNA fragments (Turchinovich, Drapkina and Tonevitsky, 2019). Moreover, extracellular vesicles also contain rRNA, tRNA, mitochondrial DNA, and short DNA sequences of retrotransposons (Yoon, Kim and Gho, 2014). The different RNAs are enclosed in the vesicular structure in order to escape from the mix of RNAases present in body fluids. Vesicle RNA differs from donor cell RNA content, which proves the existence of specific mechanisms and proteins controlling RNA sorting into EVs, such as the RNA binding complex ESCRT-II (Irion and St Johnston, 2007)(Rahbarghazi *et al.*, 2019). Conversely, several studies have described the existence of a vesicle DNA that probably undergoes a random sorting

process, completely reflecting the genomic DNA of donor cell (Thakur *et al.*, 2014). On the contrary, another study suggests that DNA is more likely released through endosomal mechanisms and autophagy (Jeppesen *et al.*, 2019).

Biophysical properties

In addition of their content, vesicle size represents a fundamental parameter for the uptake kinetics and biological functions of EVs (Caponnetto *et al.*, 2017). This physical parameter and morphological integrity remain unaltered up to a long storage time (i.e., till three months in plasma under -80 °C freezing conditions (Kalra *et al.*, 2013)) (Kumeda *et al.*, 2017), but can be affected by the isolation methods used for EV purification, as they are mainly based on dimensional separation. A growing number of studies have taken advantage of different EV sizes to distinguish different pathological contexts. For example, Zhang et al. demonstrated that the sizes of EVs derived from normal ovarian epithelial cells differed from those of cancer cell-produced EVs: the normal-cell-derived EVs were significantly larger than those derived from malignant cells (Zhang *et al.*, 2016). In another work, results suggested that the presence of large-diameter EVs represent a cancer-related signature (Santana *et al.*, 2014). EVs analyzed in the study were isolated from glioblastoma, metastatic mammary gland adenocarcinoma, and pancreatic adenocarcinoma cell lines.

So far, most characterization approaches for evaluating the isolated EV rely heavily upon particle size and count determinations (Paolini, Zendrini and Radeghieri, 2018). But, recently, some studies are focusing on the determination of structure, surface topography, adhesiveness or elasticity/stiffness of single EVs (Sharma *et al.*, 2020). In fact, beside the size also the mechanical properties of nanoparticles (synthetic or natural) can modulate their transport, internalization and externalization by cells, and adhesion to surfaces (LeClaire, Gimzewski and Sharma, 2021). Whitehead et al. demonstrated that EVs derived from isogenic malignant non-metastatic and metastatic bladder cells have a similar size, but exhibit a significantly reduced stiffness (95 MPa and 280 MPa), when compared with that derived from non-malignant ones (1.5 MPa) (Whitehead *et al.*, 2015).

Such biophysical information could represent a new opportunity to compare EVs of different origins, but also to evaluate nanoscale effects of isolation strategies used and are instrumental for the use of EVs in. New knowledge in biophysical characterization field is needed for their use in diagnostics and clinical medicine.

Uptake in target cells

Functional activity of vesicles in physiological and pathological processes depends directly on their ability to interact with recipient cells and deliver inside their contents of proteins, lipids, and nucleic acids (Raposo and Stoorvogel, 2013). There are both direct and indirect evidences that suggest the EV internalization (uptake) into target cells (Mulcahy, Pink and Carter, 2014). It is unknown whether the extracellular vesicle cargo, size and/or surface molecules can define a different mode of vesicle uptake in distinct localization, degradation, and/or functional outcomes in target cells (Mathieu *et al.*, 2019). For example, micropinocytosis is in theory compatible with the capture of small-EVs, but not with large-EVs or small-EV aggregates, which are too large (Mathieu *et al.*, 2019). Furthermore, it is to consider that pathways of vesicle secretion from donor cell and uptake in target cells may intersect, resulting in a mixed production of extracellular vesicles composed of both endogenously produced and recycled vesicles (Kalluri and LeBleu, 2020). It could be possible that the "rate" for internalization of vesicular cargo varies depending on the nature of the cargo and on the target cell's metabolic status. Several techniques were used in conjunction with EV uptake assays to tease out the molecular mechanisms of vesicle uptake (Mulcahy, Pink and Carter, 2014)(Mathieu *et al.*, 2019), including the use of antibodies to test the involvement of specific ligands/receptors and the use of chemical inhibitors to block specific uptake pathways (Mulcahy, Pink and Carter, 2014). Researchers discovered many vesicle proteins that interact with membrane receptors of target cells allowing the subsequent vesicle internalization in some cases or the lack of internalization in others. Tetraspanin proteins of target cells have been discovered to have a key role in vesicle uptake, considering also their high abundance on EV surface (Morelli *et al.*, 2004). Tetraspanins can create clusters of proteins (Tetraspanin-enriched microdomains) together with other tetraspanins, adhesion molecules and transmembrane receptor proteins of the raft-like structures in the plasma membrane that are involved in several processes, including vesicular and cellular fusion (Hemler, 2005). Also integrins and immunoglobulins can be involved in vesicle-target cell interaction. These proteins regulate cell-cell adhesions, cell signalling and antigen presentation (Aplin *et al.*, 1998). Moreover, proteoglycans, glycoproteins and lectins modulate the vesicle uptake in recipient cells. In addition to proteins, the vesicle-target cell docking can occur via different molecular interactions, involving sugars or lipids (Mathieu *et al.*, 2019). The membrane fluidity (high cholesterol, sphingomyelin, and saturated fatty acid) of vesicles and the pH of the environment (neutral pH) can contribute to the vesicle rigidity and prevent the fusion with target cells (Morhayim, Baroncelli and Van Leeuwen, 2014).

Mechanism used for vesicle uptake

The mechanisms used for the extracellular vesicle uptake in target cells can be summarized in two main subgroups: mediated by endocytosis or cell surface membrane fusion.

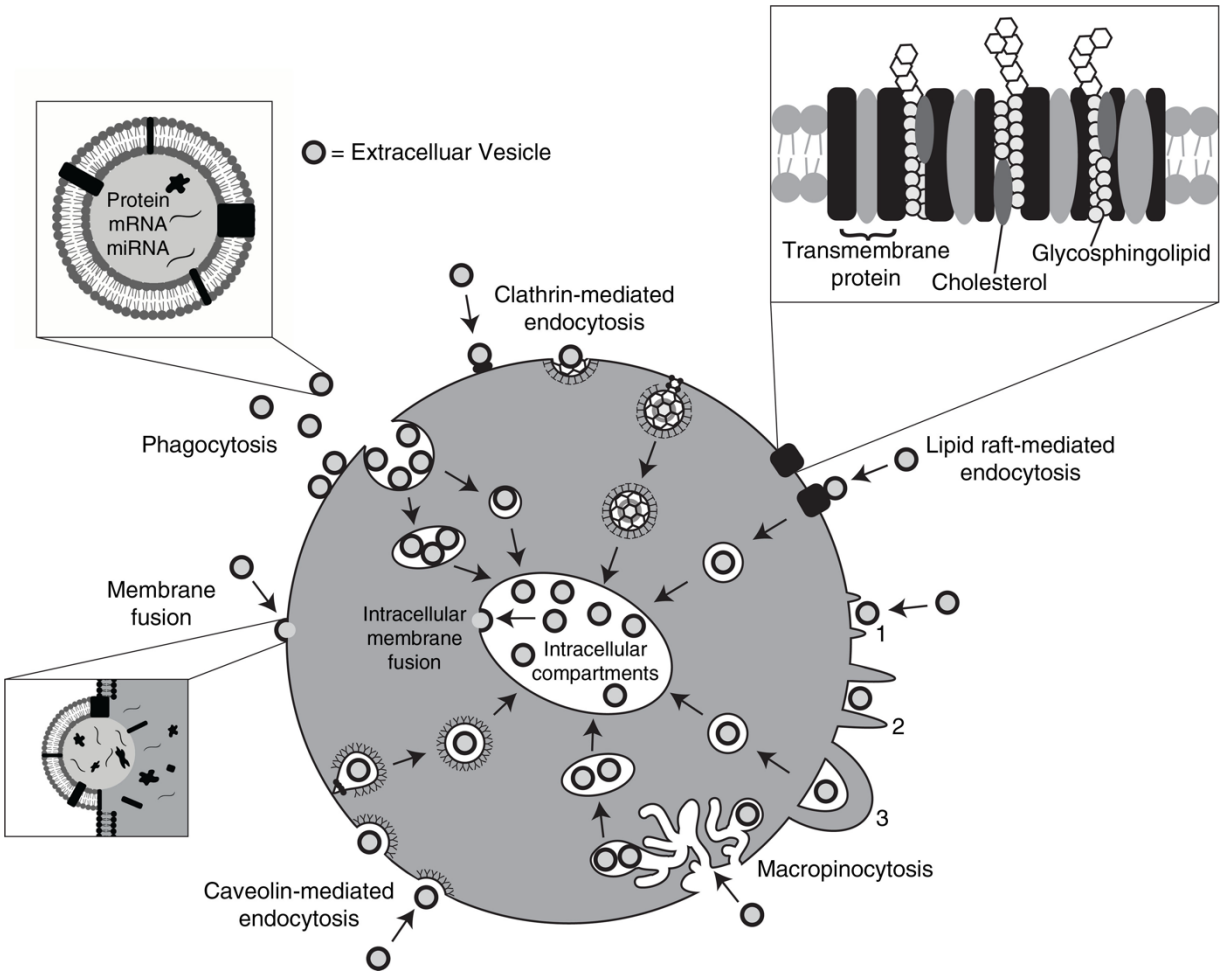

Figure 5. Pathways that participate in vesicle uptake in recipient cells. EVs may deliver their cargo by entering thorugh endocytosis, or by fusion with the plasma membrane using different molecular interactions (membrane-exposed proteins, sugars or lipids) (Mulcahy, Pink and Carter, 2014).

Most vesicle studies suggest that the preferred route for the uptake is the endocytosis mechanism (Mulcahy, Pink and Carter, 2014). This uptake is extremely fast: vesicles were observed inside the target cell after 15 minutes from the addition (Feng *et al.*, 2010). The endocytic pathway is an energy-dependent process (temperature dependent) that requires a functioning cytoskeleton. The endocytosis process includes different molecular internalization pathways: clathrin-mediated andocytosis and clathrin-independent endocytosis, including caveolin-dependent endocytosis, macropinocytosis, phagocytosis, and lipid rafts-mediated (Mulcahy, Pink and Carter, 2014), as shown in **Figure 5.** Another uptake mechanism is the cell surface membrane fusion, which consists of a direct fusion of the vesicle membrane with the target cell plasma

membrane, thanks to several proteins (such as SNAREs, Rab proteins, and Sec1/Munc-18 related proteins (SM-proteins) (Jahn and Südhof, 1999). Different inhibitors have been used to block the different vesicle uptake pathways and the frequent failure to completely abrogate internalization is due to the fact that the EV uptake occurs through more than one mechanism.

Critical steps: vesicle isolation and characterization

As mentioned above, there are different sizes and origin of extracellular vesicles, the cargo loading changes and the vesicle uptake can occur through different mechanisms (Raposo and Stahl, 2019). Great difficulties occur in isolation and characterization of extracellular vesicles considering

that, in reality, classifications and subpopulations are not so defined, but there is a considerable overlapping in size and cargo between different populations of EVs (Gardiner *et al.*, 2016). Moreover, no specific markers are currently available to distinguish the origin of extracellular vesicles and distinguish between vesicles of similar size isolated together (Sunkara, Woo and Cho, 2016). Several reports have shown that tetraspanins (i.e. CD9, CD63, and CD81), in addition to being abundant in small-EVs, may also be present in medium-EVs, complicating the discrimination among different types of EVs (Willms *et al.*, 2018). Furthermore, characterization techniques revealed that pure isolation of vesicles are hampered by the presence of non-vesicular macromolecular contaminants present in culture supernatant or body fluids. Moreover, EVs derived from different sources can contain differences in protein/lipid loading, intraluminal content or non-specific component aggregation to their surface; all these variability can lead to different sedimentation properties (Taylor and Shah, 2015). In conclusion, vesicle heterogeneity makes it difficult to compare data from different vesicle studies.

Isolation techniques

In addition to the inherent heterogeneity of EVs, several studies demonstrated how the vesicle isolation method directly impacts amount, type and purity of EVs recovered (Van Deun *et al.*, 2014)(Taylor and Shah, 2015)(Takov, Yellon and Davidson, 2019). The most common approach used to separate EVs from other molecules is to use differential centrifugation, which involves several centrifugations and ultracentrifuge (UC) steps, in order to finally isolate EVs based on sedimentation rate, according to their size and buoyant density (Momen-Heravi *et al.*, 2013)(Konoshenko *et al.*, 2018). Isolation methods can be subdivided into three major classes, based on their separation principle: density, size and immunoaffinity-based methods (Sunkara, Woo and Cho, 2016). The density-based techniques enable the EV concentration rather than the

isolation; this class includes density gradient ultracentrifugation (UC) and regular centrifugation with precipitation reagents including commercialized kits (such as ExoQuick or Exo-Spin). In density gradient UC, vesicles are separated by combining ultracentrifuge and density gradient in order to exclude molecules with different densities from EVs (Wu *et al.*, 2017). In the precipitation kits, the reagents reduce the vesicle solubility by lowering their hydration and lead to EV precipitation. With this method EVs are separated at lower g force and with higher yield than ultracentrifuge, but they are highly expensive and give low purity (co-precipitation of protein contaminants). The most used size-based technique is the size exclusion chromatography (SEC), in which a column containing small porous polymer beads is able to track extracellular vesicles; in detail, when the solution passes through the column larger particles travel more quickly through the column by eluting at an earlier time point, while the small ones, which initially remain retained by the column, reach the end at a later time (Willms *et al.*, 2018). Finally, the immunoaffinity-based isolation methods, such as paper microfluidic devices or immunomagnetic beads, are based on the antibody recognition of typical EV markers (Sunkara, Woo and Cho, 2016).

As mentioned above, ultracentrifugation technique is the most widely used isolation method, considering one hundred and ninety-six responses in the first case or three hundred and fifty-seven responses in the second one collected from individual researchers of different countries (Gardiner *et al.*, 2016)(Royo *et al.*, 2020), as shown in **Figure 6**. After the ultracentrifuge, the respondents uses SEC or a combination of different isolation methods. The other relatively well-used isolation technique are: density gradient centrifugation, filtration, precipitation, and others. Most researchers who choose the precipitation method use it in combination with other techniques and the 84% uses it to perform RNA analyses on EVs. The starting sample volume is an aspect to consider during the choice of the isolation techniques to use. Researchers with larger starting volume use ultracentrifuge protocol, compared with respondents with limited sample volume.

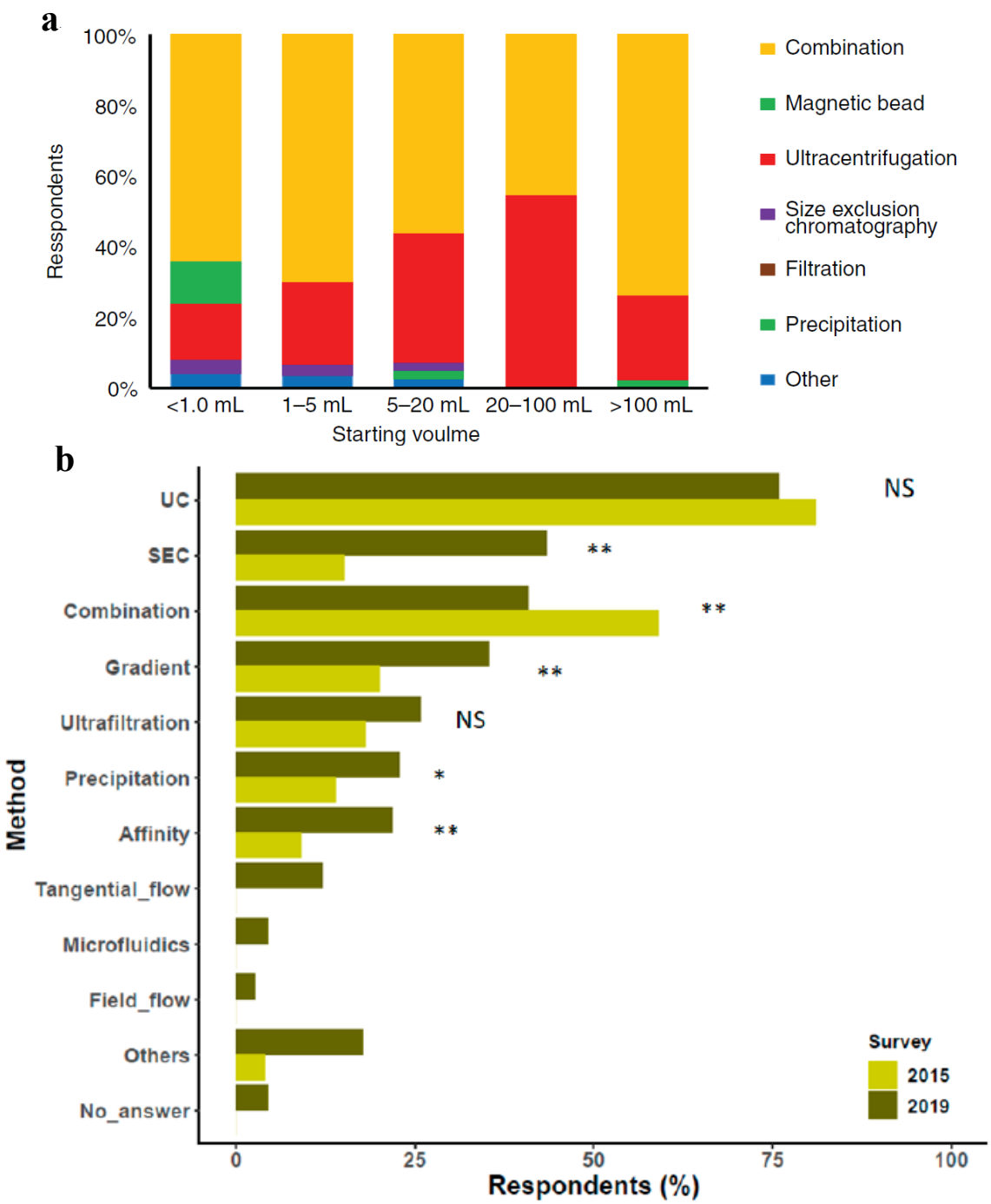

Figure 6. a) Isolation methods based on different initial volumes (Gardiner *et al.*, 2016). **b) Isolation methods compared with results of Gardiner et al.**. Results are based on 357 responses. Differences between proportions were tested by a z test, and *p* values were obtained by a chi-square test (NS, non-significant, * $p < 0.05$, ** $p < 0.01$. Affinity capture (Affinity), Combination of methods (Combination), Density gradient (Gradient), Field flow fractionation (Field_flow), Microfluidics (Microfluidics), Precipitation methods (Precipitation), Size exclusion chromatography (SEC), Tangential flow filtration (Tangential_flow), Ultracentrifugation (Royo *et al.*, 2020).

Characterization techniques

In order to evaluate method/s used for EV isolation, characterization techniques are needed to study the size, identity, concentration, and purity of the EVs. Nowadays, there is no single method allowing accurate identification for the whole range of EV types (Xu *et al.*, 2016), as **Figure 7** shows. Several techniques are available and a combination of different methods is used for EV identification, quantification, and characterization (Sunkara, Woo and Cho, 2016). Moreover, their nanometric dimensions, low refractive index (RI), and polydispersity make their characterization difficult for techniques currently used in research. In fact, it is reported that the choice of characterization technique can influence the measured vesicle size (Khatun *et al.*, 2016).

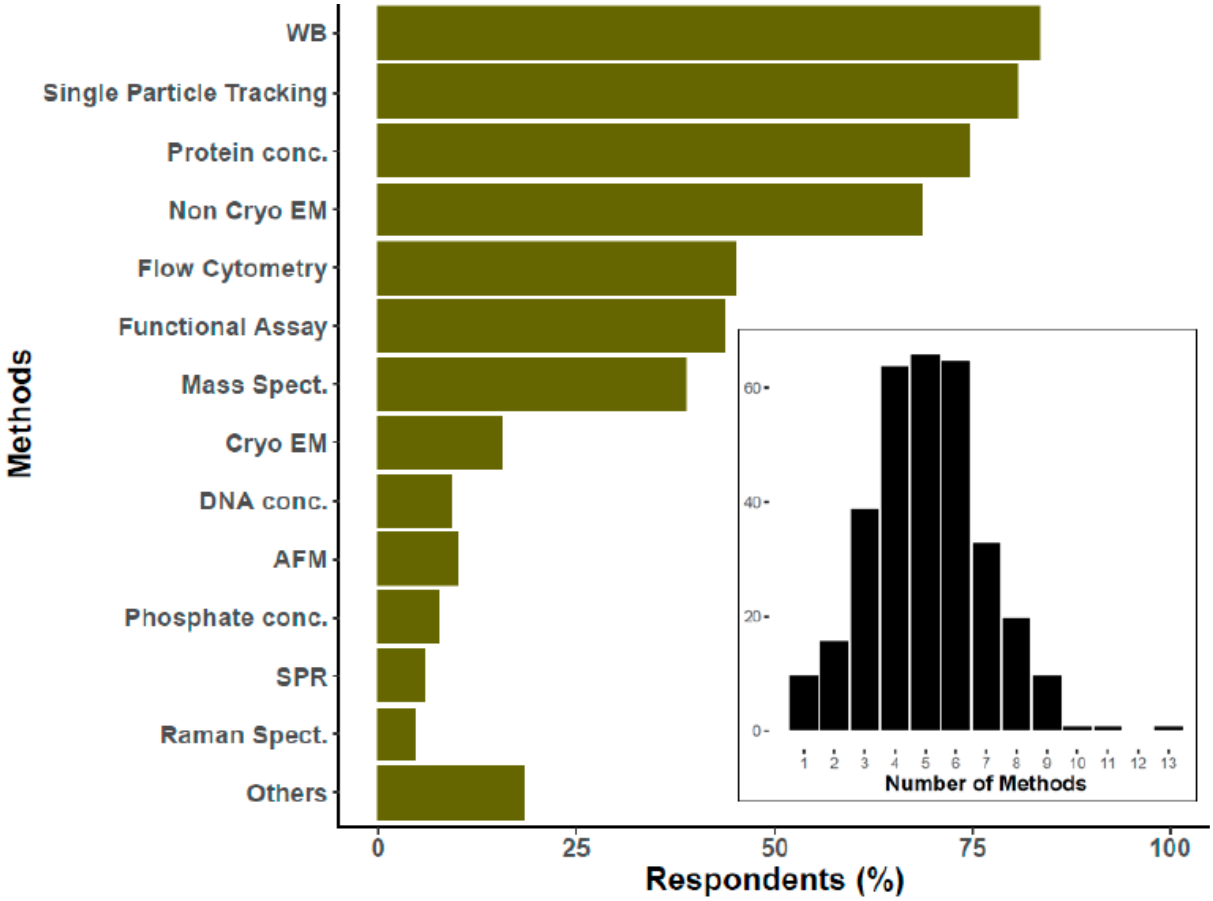

Figure 7. EV characterization methods. Results are based on 326 responses. Atomic force microscopy (AFM), Cryogenic electron microscopy (Cryo EM), DNA concentration (DNA conc.), Flow cytometry, Functional assays (Functional Assay), Mass spectroscopy (Mass Spect.), others (including among others ELISA, Colorimetric nanoplasmonic, and Next Generation Sequencing), Particle tracking (Single Particle Tracking), Phosphate/phospholipids concentration (Phosphate conc.), Protein concentration (Protein conc.), Raman spectroscopy (Raman), Surface plasmon resonance (SPR), Transmission or scanning electron microscopy (Non Cryo EM),Western blotting (WB). The histogram at the bottom of the graph reflects the number of researchers (Y-axis) that use the specified number of methods to characterize EVs (X-axis) (Royo *et al.*, 2020).

Characterization methods of EVs can be grouped into three major categories namely: biophysical methods, molecular methods and microfluidic-based methods (Khatun *et al.*, 2016). Biophysical methods are normally used to characterize the size distribution of EVs present in the sample, without any molecular information. High-resolution imaging through electron microscopy (cryo, transmission or scanning electron microscopy) or atomic force microscopy (AFM) can give size and morphological information of the EVs. Light scattering techniques (nanoparticle tracking analysis and dynamic light scattering) determine the relative size distribution, the concentration and the zeta potential of the EVs in solution (Sunkara, Woo and Cho, 2016). Molecular methods, including enzyme-linked immunosorbent assay, western blotting, bradford's assay, and flow cytometry, allow the identification of molecular vesicle markers present on the surface or inside of EVs (Sunkara, Woo and Cho, 2016). This characterization type allows to obtain information about the vesicle secretion, uptake and subtype (Khatun *et al.*, 2016). Microfluidic methods are primarily used for isolation of EVs in suspension, but can also categorized as characterization methods due to their multifunctional nature; in the isolation process, microfluidics channels or magnetic nanoparticles are functionalized/immobilized with antibodies against vesicle surface proteins that specifically bound EV subtypes that then are eluted allowing to indirectly quantify the number of vesicle protein markers. Furthermore, in fluidic channels the filter pore sizes can be changed allowing characterization of EVs of different sizes (Khatun *et al.*, 2016).

Nowadays, there are no "standard" isolation and characterization techniques that allow the optimal purification of vesicle subpopulations (Gardiner *et al.*, 2016)(Royo *et al.*, 2020).

MISEV2018: Minimal Information for Studies of Extracellular Vesicles

Despite the great theranostic potential of vesicles and the still growing progresses in EV field, standardization of isolation and characterization methods remains limited and represents one of the main challenges of this period. Taking into account that, the International Society for Extracellular Vesicles (ISEV) has attempted to address some of these issues through the publication in 2018 of the Minimal information for Studies of Extracellular Vesicles (MISEV2018) guidelines (Thery *et al.*, 2018). This position paper gives the minimal experimental requirements for definition of EVs and of their function, including suggested protocols and steps to follow. The authors propose experiments and controls suitable for most experimental situations based on EVs produced by all organisms and cells; in the meantime, they suggest also alternatives for particular situations in which not all guidelines could be strictly

followed. The ISEV does not assign specific markers of EV subtypes, such as endocytic origin for small-EVs or plasma-membrane origin for medium-EVs, since the vesicle assignment to a particular biogenesis pathway is difficult, unless the EV is captured in the act of release by specific techniques. Therefore, ISEV suggests to consider use of operational terms for EV subtypes that refer to: physical characteristics of EVs as described above, biochemical composition (CD63+/CD81+-EVs, Annexin A5-stained EVs, etc.) or descriptions of conditions or cell of origin (podocyte EVs, hypoxic EVs, large oncosomes, apoptotic bodies). They point out that several factors, including in principle the experimental conditions used for cell growth, could affect the EV recovery and the final EV sample obtained. Therefore, it is crucial to fine tune experimental procedures and standardize them as much as possible, in order to maximize the number of known and reportable parameters. It is to be noted that the EV recovery depends not only on EV release, but also on re-uptake by cells in culture, which may vary based on culture density. Therefore, the ISEV highlights the importance to maintain the same culture and harvesting conditions, such as passage number and seeding confluence. Moreover, regular checks for mycoplasma contamination must be performed on cells, not only for cellular responses to contamination, but also because contaminating species can release EVs. Furthermore, the culture medium composition and preparation could alter the EV composition and purity. For example for cell culture studies, supplements like glucose, antibiotics and growth factors can affect EV production and/or composition. Also the serum (fetal calf/bovine serum, FCS/FBS), which is a normal medium component, is likely to contain its own extracellular vesicles or others protein contaminants that could alter downstream analyses. However, the protocol should be chosen based on downstream use of EVs. Then, the ISEV suggests to use the most suitable isolation methods depending on the subsequent experiments. Furthermore, authors underline the importance to assess the results of isolation method (with the characterization), in order to establish the probability that biomarkers or functions are associated with EVs and not with other co-isolated materials. First of all, the ISEV recommends that each preparation of extracellular vesicles should be quantified in each experiment by the total starting volume of biofluid/number of cells or by the quantification of molecules, such as proteins, lipids, that can be used as a proxy for quantification of EVs. Moreover, the authors suggest to perform a characterization of single vesicles using at least these two different but complementary techniques: techniques that provide images of single EVs at high resolution (electron microscopy or scanning-probe microscopy, including atomic force microscopy) and single particle analysis techniques that estimate biophysical features of EVs: by light scattering properties (e.g. nanoparticle tracking analysis and high resolution flow cytometry), resistive

pulse sensing or Raman spectroscopy. Finally, the ISEV suggests to test the presence of components associated with EV subtypes: check at least the presence of proteins associated with plasma membrane and/or endosomes (e.g. transmembrane tetraspanin proteins) and one cytosolic proteins (e.g. TSG101 as ESCRT complex protein, ALIX or Flotillins-1). Moreover, they recommend to evaluate the purity controls that include proteins found in most common co-isolated contaminants of EV preparations (i.d. albumin or lipoproteins) (Thery *et al.*, 2018).

In this research work, we set ourselves the aim of following as much as possible the guidelines and suggestions indicated by the update of the MISEV2018.

Extracellular vesicles in breast cancer

Role in breast cancer progression and metastasis

An increase of EV concentration was observed in plasma of patients with breast cancer, and in particular of patients with triple-negative subtype, compared to the concentration of healthy controls (Galindo-Hernandez *et al.*, 2013)(Stevic *et al.*, 2018). This increase of vesicle release in cancer cells could be due to an up-regulation of a p53-regulated product (TSAP6) that modulates the vesicle secretion (Yu, Harris and Levine, 2006). The increase in vesicle secretion into circulation represents an important resource in diagnosis and treatment of breast cancer (Goh *et al.*, 2020). Extracellular vesicles secreted by cancer cells can have different proteins and microRNA (miRNA) profile compared to healthy cells, therefore EV characterization can serve as "fingerprints" of their cells of origin (Kogure, Kosaka and Ochiya, 2019). Researchers observed that EVs isolated from the triple negative breast cancer cells by changing the expression of genes and miRNAs can induce proliferation and drug resistance in non-tumorigenic breast cells (Ozawa *et al.*, 2018). Moreover, vesicle studies demonstrated the in vivo and in vitro activation of angiogenesis by extracellular vesicles derived from cancer cells. For example, the vesicular lipid component sphingomyelin can trigger cell migration and neovascularization in target cells (Yoon, Kim and Gho, 2014). As a matter of fact, extracellular vesicles can be exploited to share oncogenic molecules among cells directly modifying the cell signaling and metabolic state (Maia *et al.*, 2018); this ability makes them one of the main suspects of the elusive mechanisms of metastatic spreading (Peng *et al.*, 2018). Willms et al. demonstrated that extracellular vesicles are involved in the communication between tumor-tumor cells and tumor-stromal cells (non-malignant cells that surround the primary tumor) of the primary tumor formation, but also in progression and metastasis formation of breast cancer

(Willms *et al.*, 2018). EVs, by travelling through the systemic circulation to reach distant target cells, have been shown to contribute to the formation of pre-metastatic niche, facilitating metastatic outgrowth (modulation of intratumour heterogeneity, immunological responses, production of cancer associated fibroblast and angiogenesis) (Tschuschke *et al.*, 2020). It has been shown that small-EVs are also involved in organ-specific metastatic processes (organotropism). For example, the MDA-MB-231 cell line (TNBC) metastasises primarily into the lung, and, in fact, MDA-MB-231-derived small-EVs express integrins (α6β4/β1 and αvβ5), which specifically mediate liver tropism (Hoshino *et al.*, 2015). Moreover, extracellular vesicles can also make the cancer cells drug resistant. For example, the chemotherapeutic drugs can be expelled from cancer cells via EVs (Shedden *et al.*, 2003).

Breast cancer

Classification and Triple Negative Breast cancer

Breast Cancer is the most frequently diagnosed malignancy and ranks as the leading cause of cancer mortality in women worldwide (Momenimovahed and Salehiniya, 2019). Similarly to other tumors, breast cancer is a multifactorial disease. This disease is widespread all over the world, but its progression, mortality and survival rates vary widely between different areas of the world. For example, these variations can depend on population structure (i.e. age, race and ethnicity), lifestyle, environment, genetic factors and access to high-quality care (Hortobagyi *et al.*, 2005). Moreover, breast cancer is a disease with a complex and heterogeneous genetic and biochemical background. Long before the advent of modern molecular techniques, histopathologists discovered that breast cancer was heterogeneous also through morphological observations and that classification was based on histological type, tumour grade and lymph node status (Holliday and Speirs, 2011). Subsequently, thanks to the advent of the new molecular techniques (i.e. gene expression profiling and immunohistochemistry), breast cancer has been shown to express the oestrogen receptor (ER), progesterone receptor (PR) and/or human epidermal growth factor receptors 2 (HER2) (Holliday and Speirs, 2011). The expression of these factors combined to other clinicopathological variables, including tumor grade and size, nodal involvement, and sirurgical margins, allows to predict disease prognosis and manage treatment (Vallejos *et al.*, 2010). According to their gene expression signatures and their citokeratins expression, breast cancer can be classified in different molecular subtypes: Luminal A (ER+/PR+/HER2-/lowKi-67), Luminal B (ER+/PR+/HER2-/+/high Ki-67), HER2-overexpression (ER-/PR-/HER2+), and triple negative breast cancers/TNBCs (ER-/PR-/HER2-

). Basal-like subtype of breast cancer, referred to as TNBC, was found to be positive for basal marker (CK5/6) expression (Al-thoubaity, 2020). The Luminal A subtype responds to hormone therapy and is usually linked to an excellent prognosis, while the Luminal B has a worse prognosis, even if it is still better than the one of pure HER2+. Despite HER2+ is identified among the more aggressive breast cancer subtypes, it could be still treated with monoclonal antibodies targeting HER2 receptor (Trastuzumab) (Navarro Vilar *et al.*, 2017). The triple negative subtype, as a result of expression of markers associated with the epithelial–mesenchymal transition (features associated with breast cancer stem cells, e.g. CD44+CD24–/low phenotype and high incidence of metastasis), is the most aggressive subtype and with a poor prognosis (Haffty *et al.*, 2006)(Holliday and Speirs, 2011). Moreover, due to the absence of specific targeted treatments, both neo/adjuvant systemic treatment and systemic palliative therapy for triple negative subtype is limited to chemotherapy (Yeo, 2015). Furthermore, triple negative breast cancer patients have an high risk of disease relapse compared with the others subtypes (Bianchini *et al.*, 2016). The therapy of patients with TNBC, which are approximately 15-20% of breast cancer cases diagnosed annually worldwide (Gu *et al.*, 2020), is complex due to its intrinsic molecular heterogeneity; in fact, researchers identified TNBC sub-classifications based on biomarkers and gene signatures that include basal-like tumours, *BRCA*-mutant and BRCAness subtypes, and Claudinlow subtype (Yeo, 2015). The risk of relapse and response to chemotherapy in TNBC is also influenced by the vast heterogeneity of immune environment, which shows a full range of different levels of lymphocyte and monocyte infiltration and activation of inhibitory checkpoints, including PD-1/PD-L1 (Bianchini *et al.*, 2016).

Carcinogenesis

In all cancer types, there is the differentiation from a healthy cell to a cancer one, a process called carcinogenesis, in which the cell acquires different capabilities. First of all, cancer cells are able to proliferate in absence of external growth stimulatory signals (e.g. vascular endothelial growth factor/VEGF, and epidermal growth factor/EGF); instead, in healthy cells these signals are detected in extracellular matrix by specific receptors that, by activating in turn signal transduction pathways (such as Ras/MAPK, Akt/PKB or STAT-3), promote cellular proliferation. Moreover, tumor cells are able to divide by escaping the contact-dependent inhibition of growth. Cancer cells have developed different strategies to elude apoptosis, such as increased synthesis of anti-apoptotic factors or loss-of-function mutations in pro-apoptotic genes. As intensely proliferating tissues, tumors need small capillaries for an adequate supply of both nutrients and oxygen and for the removal of their metabolic waste products. This process

of tumor vascularization, called neoangiogenesis, is regulated and drived by pro- and anti-angiogenetic factors (e.g. VEGF, PDGF, FGF, angiostatin, endostatin, and thrombospondins) secreted in the environment by tumor cells. Furthermore, cancer cells do not carry out senescence or apoptosis programs after a certain number of cell division events (~50 mitoses, Hayflick limit), which instead happens in normal cells for the loss of genetic stability due to telomere shortening. Tumor cells can activate the telomerase, a reverse transcriptase, which elongates the telomeres overcoming this pitfall and becoming immortalized (Leber and Efferth, 2009).

Metastasis

Despite tumor cells acquire all these capabilities, the presence of a primary tumor is not directly related to patient's death, but mortality is linked to metastases (primary cause of death for >90% of patients with cancer) (Kozłowski, Kozłowska and Kocki, 2015). In particular, it has been established that breast cancer patients develop deadly metastases, which also occur decades after the time of diagnosis and prior removal of the tumor, with a 25-50% probability (Kozłowski, Kozłowska and Kocki, 2015). The term metastasis in botany refers to the interaction between a "seeds" (tumour cells) and its "congenial soil" (the metastatic microenvironment). The new colonized tissue can undergo some changes and contributes to the progressive outgrowth of tumour cells at the secondary site by altering cellular composition, immune status, blood supply, ECM composition and many other aspects (Steeg, 2016). Metastasis is the spread of cancer cells from the site of primary tumor to a different location, where they originate a secondary tumor site. This process may begin early or late with respect to primary tumour formation and may be fed by genomic instability that consists of a progressive loss of the checks on normal chromosome stability, DNA repair, and gene expression regulation. This instability is supposed to give rise to a heterogeneous cellular population in primary tumor with some cells enabled to progress in the metastatic cascade (Steeg, 2016). The classical simplification of metastatic disease in a sequence of steps helps to understand the biological complexity of this process, as shown in **Figure 8**. These steps are:

1) *escape of cancer cells from primary tumor site and local invasion*. Individual cells or cluster of tumor cells, thanks to the secretion of several enzymes, such as matrix metalloproteinases (MMPs), which degrade extracellular matrix (ECM) and facilitate migration, escape from the primary tumor site and invade adjacent healthy tissues;

2) *intravasation into blood or lymphatic vessels*. Cancer cells attach themselves via adhesion molecules to the endothelial cells and infiltrate blood vessels or lymphatic system;

3) *survival in circulation and adhesion of the circulating tumor cells (CTCs) to the endothelium of the capillaries of the target organ site*. Tumoral cells have to resist to the high concentration of oxygen and cytotoxic lymphocytes present in vessels. This is a sort of selection for resistant and aggressive tumor cells;

4) *extravasation from vessels and invasion of surrounding basement membrane and target organ tissues*. Cancer cells leave blood stream, penetrate the endothelium, and settle in a second organ or tissue by developing the pre-metastatic niche;

5) *growth of secondary tumor mass at the target organ site*.

(Leber and Efferth, 2009)(Kozłowski, Kozłowska and Kocki, 2015).

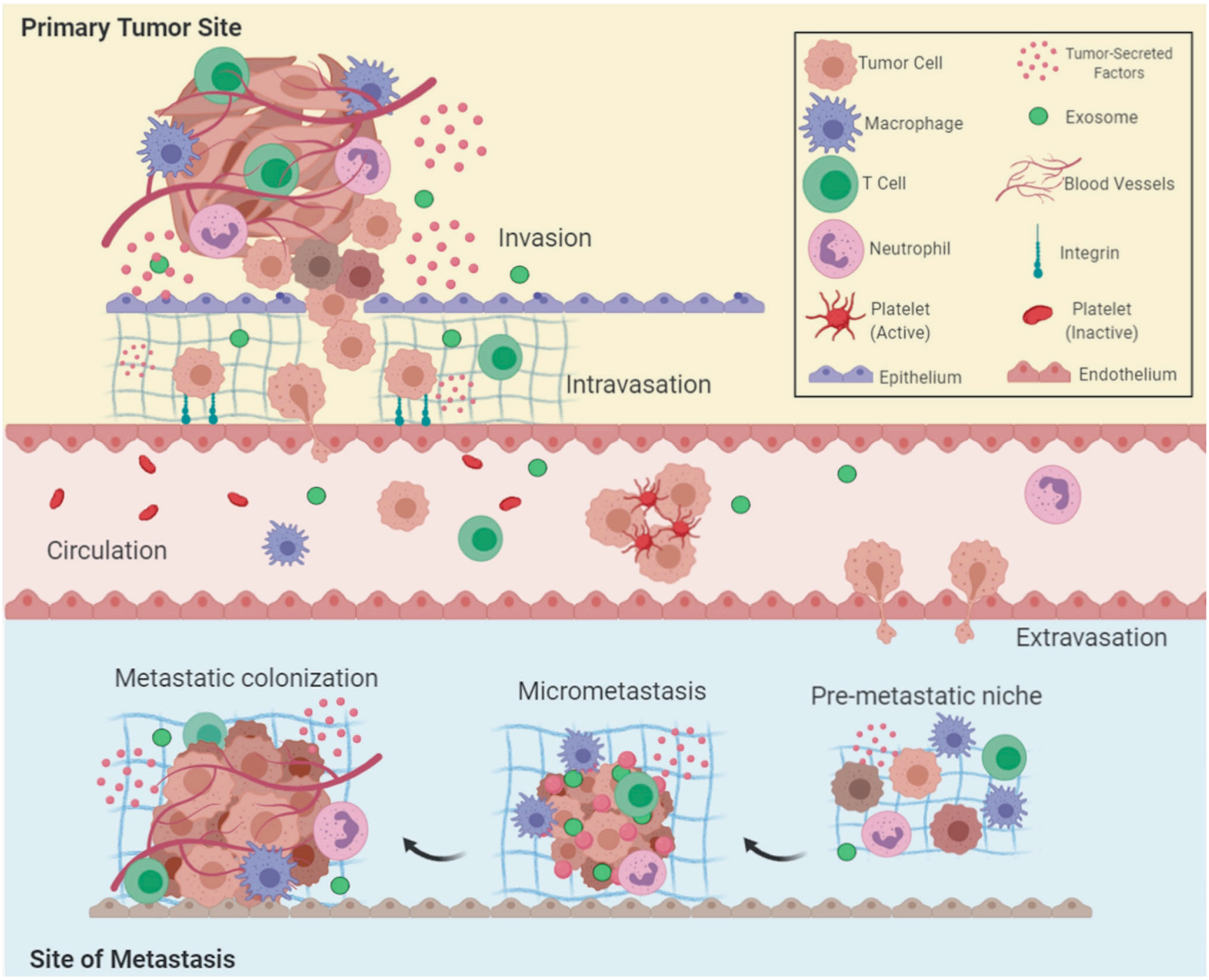

Figure 8. Complete overview of the metastatic process starting from the escape of tumor cells originating from the primary tumor to the formation of the secondary tumor mass. The five key steps of metastasis include local invasion, intravasation, circulation, extravasation, and colonization (Fares *et al.*, 2020).

Epithelial-mesenchymal transition

It seems that the onset of metastasis requires the epithelial–mesenchymal transition (EMT), whereas the opposite process of mesenchymal–epithelial transition (MET) is needed for metastatic progression and takes place when the metastasis is being formed in a secondary specific organ. Moreover, EMT process could be a central role also in resistance to chemotherapy (Fares *et al.*, 2020). The majority of cancers, including breast cancer, originate from epithelial tissues. In metastasis, tumor cells in order to leave the primary tumor and invade surrounding ECM need to diminish their tight cell-cell adhesion and interactions with neighboring extracellular matrix. In fact, cadherins, adhesion molecules involved in tight intercellular adhesion by interacting with the actin component, was found altered in tumor cells who underwent the transition (Kozłowski, Kozłowska and Kocki, 2015). In EMT process, it was observed a down-regulation of E-cadherin, a cell-cell junction, which leads to a reduction of the adhesion between epithelial breast cancer cells and other epithelial cells, and, at the same time, an increase in N-cadherin, a mesenchymal cadherin, which permits the adhesion of cancer cells to stromal cells and, subsequently, the invasion (Scully *et al.*, 2012). Moreover, the EMT mechanism involves the loss of epithelial polarity, the achievement of a mesenchymal morphology, and elevated levels of Twist and Slug, which are EMT-inducing transcription factors. Furthermore, in epithelial breast cancer cells was observed also the expression of vimentin, a mesenchymal marker indicating shorter postoperative survival of patients. The transition from one state to another is governed by several others factors, including growth factors, signaling pathways, transcriptional, chromatin, and RNA elements, epigenetic and post-translational modulators (Fares *et al.*, 2020). The reduction of cell-cell contacts and the acquisition of a mesenchymal (fibroblastoid) spindle-shape morphology is connected with increased invasiveness that result in the release of single cells from a solid epithelial primary tumor (Kozłowski, Kozłowska and Kocki, 2015). The described EMT process is shown in **Figure 9**.

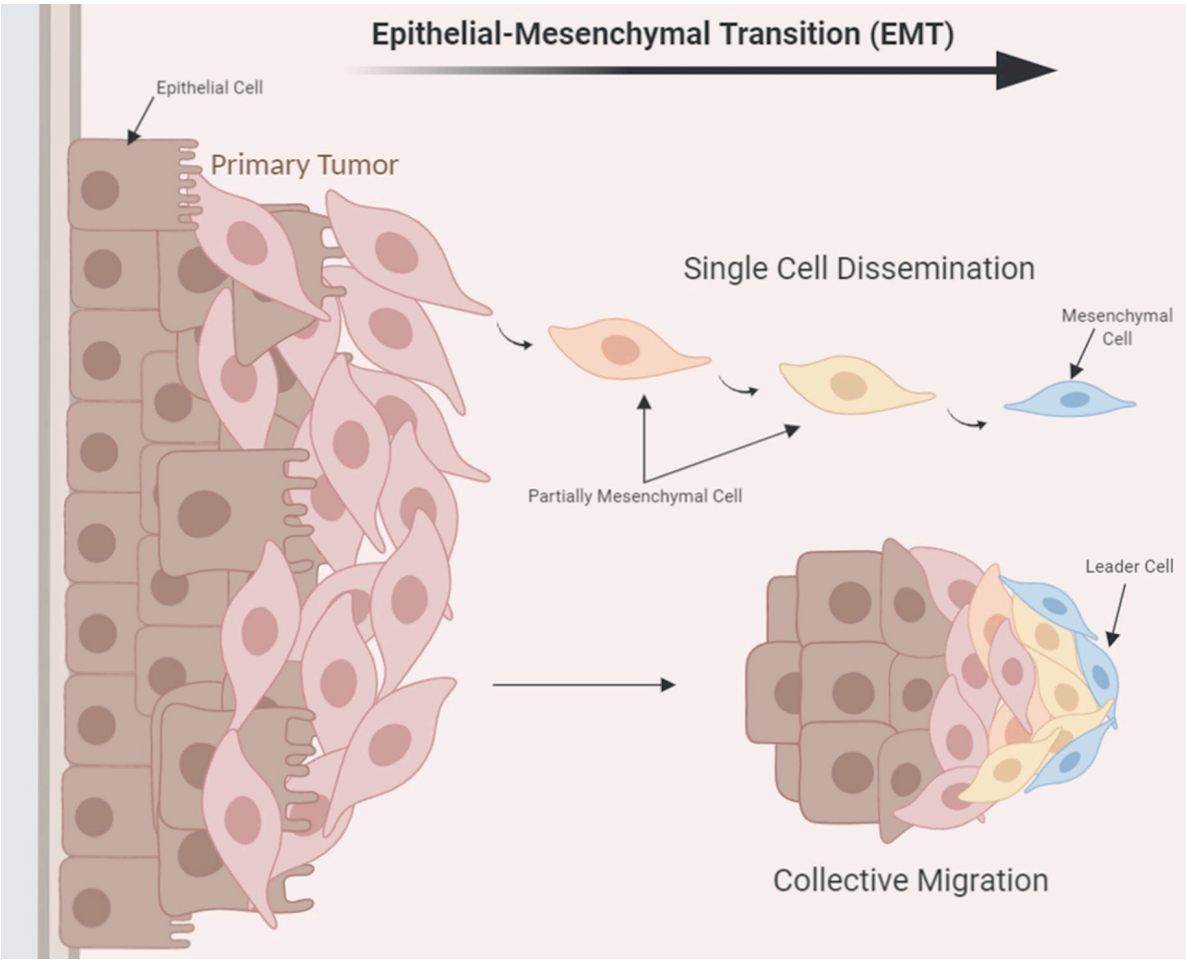

Figure 9. Epithelial–mesenchymal transition that occurs through single-cell dissemination or through collective migration. The process consists of several transition stages starting from the initial epithelial cell up to the invasive mesenchymal cell (Fares *et al.*, 2020).

Cytoskeleton organization in healthy cells

Loss of cell-cell adhesion, the consequent increase in cell motility, which promotes migration, invasion and metastasis of cancer cells are often related with cytoskeletal changes (Lambrechts, Van Troys and Ampe, 2004). In normal physiological conditions, the cytoskeleton allows cells to resist to deformation, transport intracellular cargo, and move changing their shape (Fletcher and Mullins, 2010). Cytoskeleton can be subdivided into three main classes, namely microtubules, microfilaments, and intermediate filaments, that are assembled into networks to carry out their tasks (**Figure 9**). Microtubules, hollow cylindrical polymers made up of α- and β-tubulin heterodimers, allow trafficking of molecules, chromosomal segregation during cell division, and maintenance of the cell shape (Ong *et al.*, 2020). Microfilaments are composed of actin. Three main groups of actin isoforms (α-, β-, and γ-actin) have been identified. Actin can be found as globular monomer, G-actin, or filamentous polymer, F-actin. In normal cells, polymerisation and depolymerisation of actin filaments are tightly regulated to drive cell

morphology, adhesion, motility, exocytosis, and endocytosis. Actin filaments can also interact with myosin to form acto-myosin bundles, namely actin stress fibres, which have a critical role in cell adhesion to the extracellular matrix (ECM) (Ong *et al.*, 2020). Although actin filaments are softer than microtubules, high concentrations of actin stress fibers, which are anisotropy (the organization is not in all directions, but parallel), promote the assembly of highly organized rigid structures (Fletcher and Mullins, 2010) that increase and are proportional to cell stiffness (Rajagopal et al., 2018). Intermediate filaments, subdivided into several classes (including cytokeratin, vimentin, desmin, neurofilaments, nuclear lamins or nestins), if cross-linked to each other or to other molecules can contribute to the mechanical integrity of cells, as well as regulation of the cellular space (Ong *et al.*, 2020). Cytoskeleton interacts with other molecules, including integrins. Integrin are transmembrane proteins that via their extracellular domains interact with the substrate, while via their intracellular ones link various proteins, in order to assemble complex structures, called focal adhesions (FAs) (Dasgupta and McCollum, 2019). Focal adhesions, therefore, act as a bridge between integrin-ECM connection and the cytoskeleton (Dasgupta and McCollum, 2019). In fact, FAs are frequently associated with stress fibres at one or both ends. Focal adhesions are structures that allow the adhesion to the underlying matrix and, by assembling and disassembling, regulate cell migration. Many studies demonstrated that FAs are mechanosensitive and that, in particular, mechanical tension and actin polimerization lead to their assembly (FA growth, maturation and size) (Burridge and Guilluy, 2016). Previous studies demonstrated that Yes-associated protein (YAP) has a role in regulation of the acto-myosin network (Qiao *et al.*, 2017)(Dobrokhotov *et al.*, 2018) and focal adhesions (Nardone *et al.*, 2017). Yap is a transcriptional co-activator that has many roles in tissue homeostasis (promote cell proliferation, survival, and maintenance of stem cell fate) (Dasgupta and McCollum, 2019) and it is regulated, and can regulate, mechanical cues of cell microenvironments, such as adjacent cells and the extracellular matrix. Negative regulation, via phosphorylation (with consequent nuclear export or degradation), of the Hippo pathway has been identified as canonical mechanism for modulation of YAP activity (Dobrokhotov *et al.*, 2018).

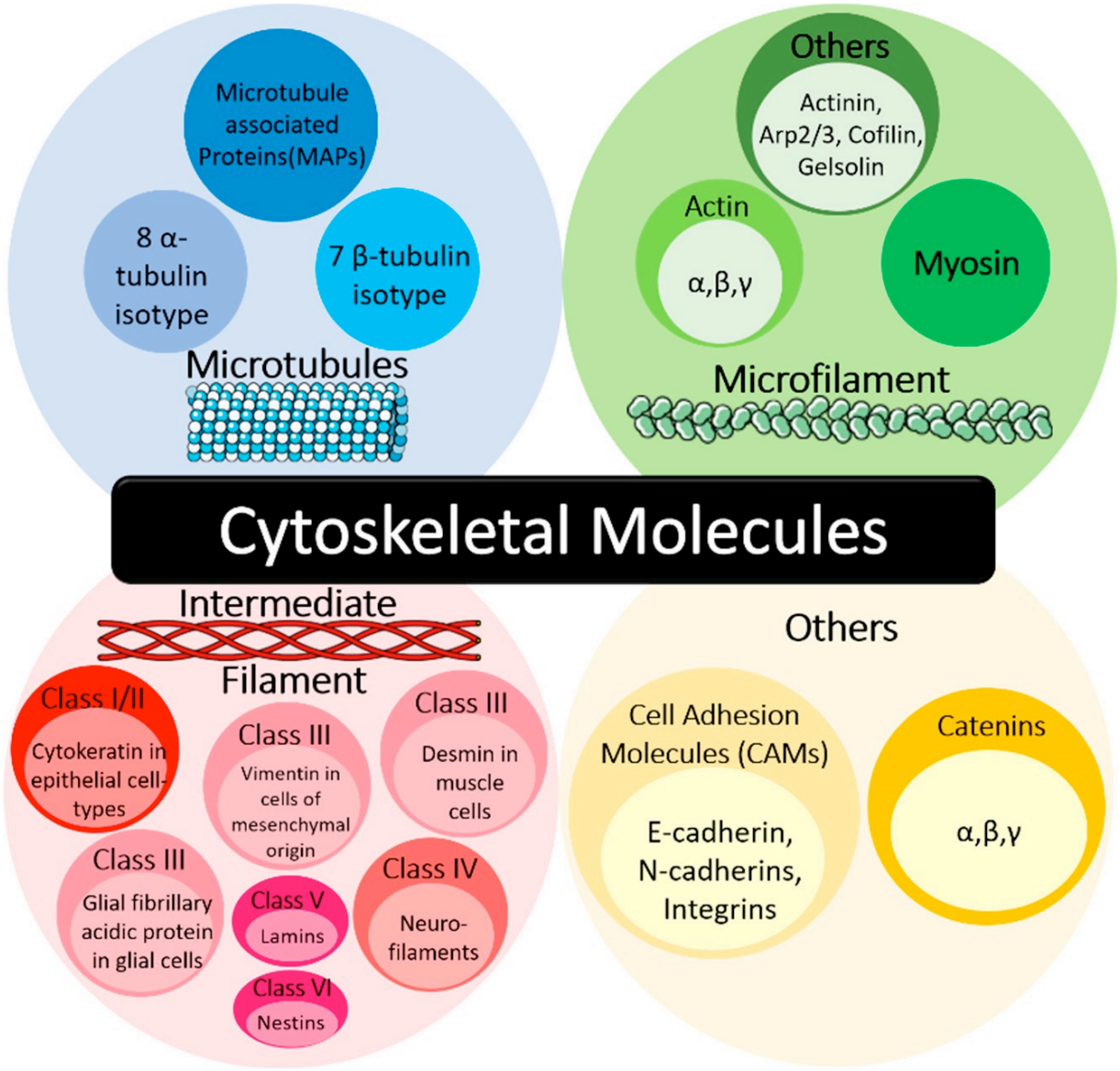

Figure 9. Classification of cytoskeletal molecules. The cytoskeletal molecules can be classified into three main classes: microtubules, microfilaments and intermediate filaments (Ong *et al.*, 2020).

Nuclear organization in healthy cells

The cytoskeleton is not the only regulator of cellular biomechanics; also the nucleus, 2-10 times stiffer than the cytoplasm and by occupying the majority of the cell volume, has a fundamental role in biomechanics and metastasis. Nuclear Envelope (NE), a sub-domain of the endoplasmic reticulum, defines the nucleus and it is composed of Inner Nuclear Membrane (INM) and Outer Nuclear Membrane (ONM) (Gorjánácz, 2014). Under the INM there is the nuclear lamina, composed of intermediate lamin filaments. Lamin proteins, in vertebrates, are divided into two groups: A-type lamins (lamin A and C are splice variants) and B-type lamins. Nuclear lamins confer shape, elasticity, and stiffness to the NE. In fact, lamin variants correlate with the mechanical stress of tissues: B-types are constitutively expressed in all tissues and less correlate

with the nuclear stiffness, while A/C-type lamins are low expressed in soft tissues (like liver or brain) and high expressed (increasing up to 30 folds) in stiff tissues (like heart or muscle). Therefore, A-type lamins are very important for biomechanic characteristics of tissues. In addition to regulate nuclear stiffness, lamins tether the chromatin to the NE, contributing to the non-random chromatin organization within the nucleus. Nuclear lamina can modulate gene expression indirectly, through influencing chromatin organization (interacting with histones and heterochromatin-associated proteins), or directly, through interacting with transcription factors that regulate cellular proliferation, differentiation and apoptosis (Gorjánácz, 2014). Lamins are mechanically connected to cytoskeletal proteins via the Linker of Nucleoskeleton and Cytoskeleton (LINC) complex, composed of two protein domanis (i.e. SUN and KASH, expressed in proteins known as nesprins) (Bouzid *et al.*, 2019), as shown in **Figure 10**. LINC complex can regulate chromatin, nucleus morphology, cell migration and polarization, and allows to detect mechanical changes of the environment (Bouzid *et al.*, 2019). Therefore, proteins found at the NE have been shown to play a key role in modulating the transfer of biomechanical information between cell surface, cytoskeletal structures, and the nucleus.

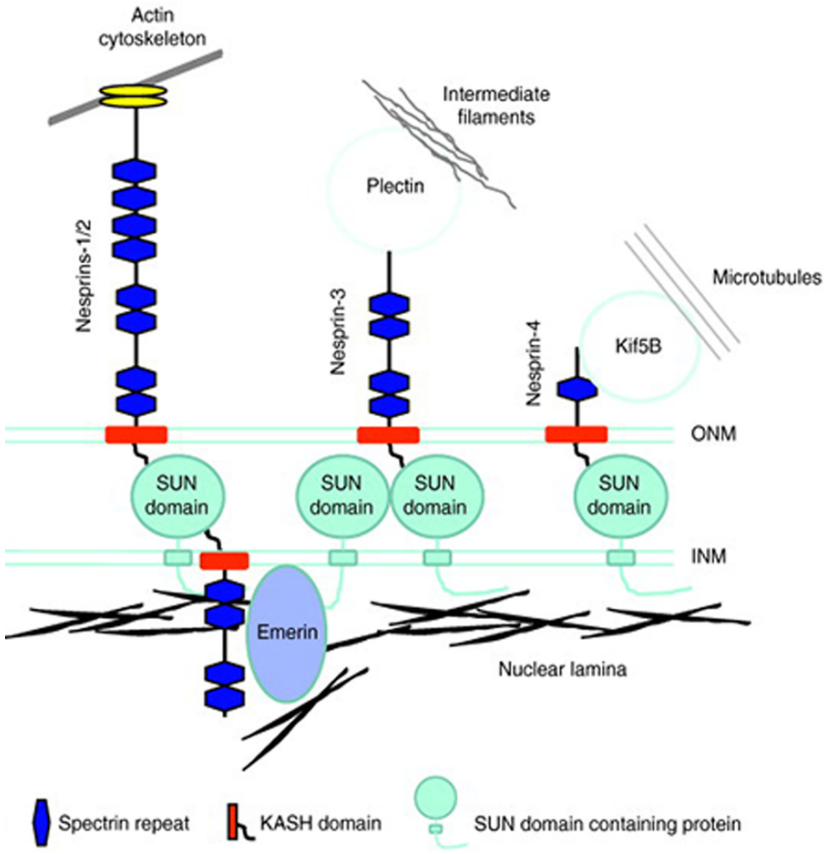

Figure 10. Linker of the nucleoskeleton and the cytoskeleton (LINC) complex. LINC complex is formed by SUN and KASH proteins that pass through nuclear envelope and connects the nucleus to forces generated in the cytoplasm (Bouzid *et al.*, 2019).

Nuclear and cytoskeleton organization in cancer cells

In tumor cells, rearrangements of cytoskeletal proteins and their associated signalling pathways can occur, in order to promote tumour cell survival growth, aggressiveness and invasion, resulting in the acquiring of all cancer hallmarks (Ong *et al.*, 2020). Moreover, the metastatic potential of cancer cells is directly related to their motility, which is a bidirectional interplay between the actin and microtubules organization and expression (Etienne-Manneville, 2004). High expression of tubulin isotypes (e.g. βI-, βII-, βIII-, βIVa-, and βV-tubulin) has been associated with tumor progression, aggressiveness, chemotherapy drug resistance, and poor prognosis (Parker *et al.*, 2017). Instead, disorganization of the actin cytoskeleton with an increase in the G:F actin ratio is usually observed in aggressive cancer cells; moreover, in invasive tumor cells, actin stress fibres are usually less evident for the purpose of stimulating cellular migration (Ong *et al.*, 2020). Nevertheless, other papers showed less cortical actin but more stress fibers with membrane protrusions (lamellipodia and filopodia) in pre-invasive breast cancer cells (Tavares *et al.*, 2017) and in tumor cells that undergo EMT (Liu *et al.*, 2019). No significant differences in actin organization between MCF7 and MDA-MB-231 breast cancer cells were reported from previous studies (Calzado-Martín *et al.*, 2016)(Schierbaum, Rheinlaender and Schäffer, 2017). Conflicting results have been obtained in cancer cell lines also regarding the focal adhesions. Several articles showed a direct correlation between metastatic/aggressive potential of cancer cells and an high number and small focal adhesion complexes with higher contractile forces (Rönnlund *et al.*, 2013)(Gad *et al.*, 2012)(Kraning-Rush, Califano and Reinhart-King, 2012). Instead, other studies observed that invasive cells are characterized by large dynamic adhesion sites and less traction forces to migrate (Peschetola *et al.*, 2013)(Tavares *et al.*, 2017). FAs are widely composed of tyrosine kinases and their substrates. Among these, the focal adhesion kinase (FAK), which is active when recruited and phosphorylated at Tyr397 (phospho-FAK), has been demonstrated to be a major participant in focal adhesion dynamics. Phospho-FAK, recruiting other signalling molecules, promotes the assembly of focal adhesion complexes (Shen *et al.*, 2018). This protein has been observed to have an oncogenic role in many types of human cancers (Shen *et al.*, 2018). Moreover, increased expression and activity of FAK have often been associated with metastasis and poor prognosis in breast cancer (Luo and Guan, 2010). Although focal adhesions and FAK in breast cancer have been widely studied, it is not yet perfectly clear how FAs are regulated in tumour progression and metastasis. As mentioned before, Yap can regulate actio-myosin network and FAs. Yap is an oncoprotein and abnormally accumulation of nuclear YAP has been observed in many types of cancer, including breast cancer (Qiao *et al.*, 2017)(Dobrokhotov *et al.*, 2018). In particular,

an increase in Yap activity can drive the lack of contact/density-dependent inhibition of growth (Dasgupta and McCollum, 2019), the increase in cell motility, invasion, and metastasis (Wang *et al.*, 2014), a marked increase in FA formation (Nardone *et al.*, 2017)(Shen *et al.*, 2018), and a promotion of FAK phosphorylation (Shen *et al.*, 2018). Contrasting results regarding how the Yap oncoprotein regulates actin cytoskeleton were obtained. In the study of Qiao et al., Yap seems to drive an actin depolymerization with consequent cell softening in human gastric cancer cells (Qiao *et al.*, 2017), while in the study of Nardone et al. it seems to promote stress fibers with consequent cell stiffening in adipose tissue-derived mesenchymal stem (Nardone *et al.*, 2017). These conflicting results could be probably due to the way Yap regulates acto-myosin systems: it promotes the expression of both a RhoA activator (ARHGEF17) and RhoA inhibitors (ARHGAP18/29) (Dobrokhotov *et al.*, 2018). Therefore, the regulation of the actin by Yap seems to be cell-specific. Shen et al. observed that YAP promotes focal adhesion dynamics, but they did not reported any significant actin changes in breast cancer cells (MCF7 and MDA-MB-231) upon Yap overexpression or silencing (Shen *et al.*, 2018).

Furthermore, in cancer cells, the nucleus morphology and stiffness is altered if compared with healthy cells (Denais & Lammerding, 2014). In particular, nuclear irregularity, deformity, and softening, as result of nucleoskeleton (including Lamin proteins) and nucleus-cytoskeleton interactions, are associated to high tumoral invasiveness of cancer cells (Chiotaki, Polioudaki and Theodoropoulos, 2014)(Senigagliesi *et al.*, 2019). In cancer, often there are mutations or downregulation of lamins or lamin-associated proteins, which lead to disorganized lamin filaments, deformed, multi-lobulated and fragile nuclei and to an altered nuclear mechanotransduction and cellular functioning (Capo-Chichi *et al.*, 2011)(Toh, Ramdas and Shivashankar, 2015)(Gorjánácz, 2014).

Biomechanical properties of normal and cancer cells

It has been known for a long time that changes in cellular cytoskeleton and nucleus are associated to malignant transformation and neoplasia. Moreover, several papers demonstrated that the main malignant tumor processes (uncontrolled growth, invasion and metastasis) require active and passive biomechanical changes of the tumour cells and their stroma (Fritsch *et al.*, 2010). Cancer cells detect and respond to mechanical properties of their microenvironment and, consequently, generate other forces (Alibert, Goud and Manneville, 2017). In the early dysplasia, cell softening was observed for increased cell proliferation. This biomechanical phenotype is attributed to the disappearance of the prominent fibrous actin of the interphase when the cell enters in mitosis; the fibrous actin is replaced by a diffuse distribution of actin

throughout the cytoplasm. Besides, tumor cell lines with high metastatic potential show significant cytoskeletal and biomechanical changes. These changes provide advantages to invasive cancer cells that can individually move through the tumor/cell-cell boundary and extracellular matrix creating then metastases. Invasion of the surrounding tissues, intravasation, extravasation and dissemination to other organs are thought to be facilitated for more deformable tumor cells (Alibert, Goud and Manneville, 2017). Several papers demonstrated that invasive cancer cells, if compared with non-invasive or normal ones, appear to be softer so as to easily pass through narrow environmental constrictions (Lekka, 2016; Luo *et al.*, 2016; Alibert, Goud and Manneville, 2017), as shown in **Figure 11**. Moreover, cell softening can increase the aggressiveness and the rate of lamellipodial motility of individual malignant cells (Fritsch *et al.*, 2010). The reason of biomechanical differences is still to be completely understood. Several cellular elements are involved in cellular biomechanical changes, including cellular microenvironment, cytoskeleton, nucleus and plasma membrane (Alibert, Goud and Manneville, 2017). These results may appear in contradiction to the macroscopically detected stiffening of several tumors, such as breast cancer ones, as shown **Figure 11**; in fact, solid tumors are detectable in microscale by palpation, since malignancy is correlated with solid tumor stiffness. This phenomenon is explained by mechanical property changes of the extracellular matrix: the extracellular matrix of malignant tissues is stiffer as compared to the extracellular matrix of non-malignant ones (Goetz *et al.*, 2011).

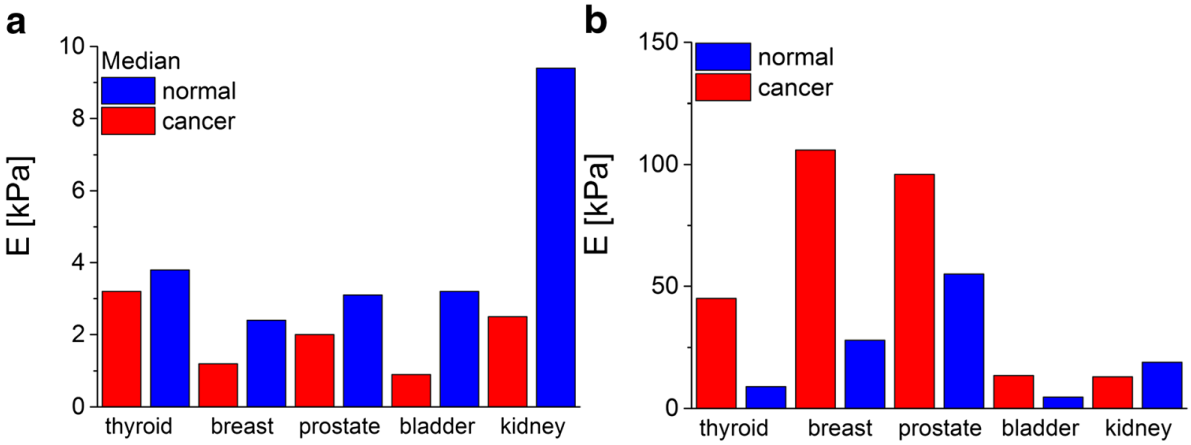

Figure 11. Young's modulus (stiffness) comparison determined for various cancers at a) single cell and **b)** tissue levels (Lekka, 2016)**.**

Thus, considering the fundamental role of biomechanical properties for invasive cancer cells during metastasis, it is relevant to deeply investigate this mechanism and understand if this phenotype could be regulated by extracellular vesicle activity.

Atomic Force Microscopy

AFM is a scanning probe microscope based on the detection of forces acting between a sharp tip and atoms of the sample surface. The AFM technique measures surface topography at high resolution providing a three-dimensional space reconstruction of the sample. The sharp AFM probe tip (the tip radius of curvature is about 10 nm for standard probes) is attached at the end of a micro-sized cantilever spring. AFM tips and cantilevers are micro-fabricated from silica or silicon nitride. When the tip is in contact or near contact with the surface of interest, small forces are produced between the probe and the surface, which induce a deflection of the cantilever beam. As a matter of fact, the cantilever could be considered as a spring and the force, which can be described using Hooke's law, needed to extend or compress a spring by some distance is proportional to that distance (Carvalho and Santos, 2012). In the Hooke's law, "*F"* is the force sensed by the tip, "*k"* the spring constant of the cantilever, and "*Δx"* the deflection of the cantilever (Carvalho and Santos, 2012):

$$F = k\,\Delta x$$

Most AFMs use an optical system to precisely detect cantilever deflection. A laser diode beam is directed to the back of the cantilever in correspondence of the tip, and it is reflected to a four quadrants photodiode detector (position sensitive detectors). A cantilever deflection of few nanometres is transformed into a shift of the laser spot of many micrometres on the photodiode detector by means of an optical lever. Then, this signal is transformed into a current signal, which represents the tip-surface interaction forces. During AFM imaging a *XY* scanner (single module parallel-kinematics flexure stage) is used to move the sample in these directions, while a piezoelectric scanner, connected to a feedback controller, moves the sample or the probe (based on the AFM brand used) in the *Z* axis. In standard imaging modes, the Z-scanner position is adjusted point by point during an XY raster scanning by the feedback system, in order to map the constant force profile of the surface, which reflects its topography. The main elements of an AFM instrument are shown in **Figure 12.**

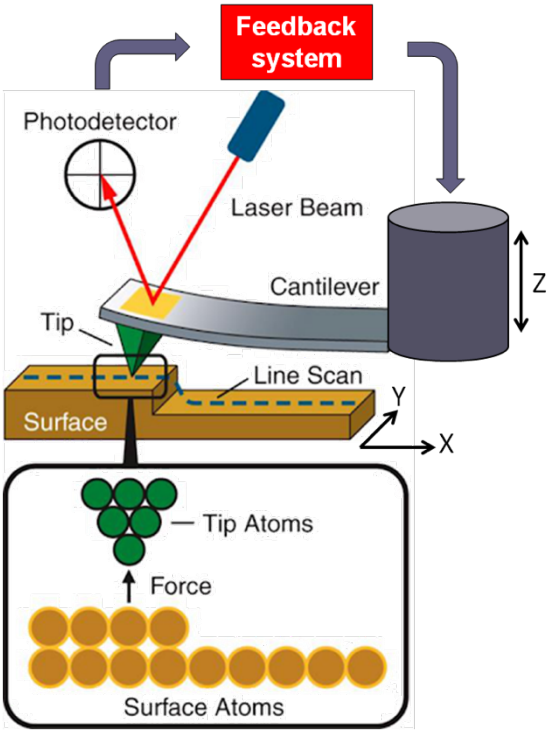

Figure 12. Main elements of an Atomic Force Microscopy instrumentation.

Force Spectroscopy Atomic Force Microscopy to measure cell stiffness

Force spectroscopy Atomic Force Microscopy (AFM) was used to evaluate the stiffness (described as Young's modulus or elastic modulus) of cells.

In force spectroscopy, the tip does not scan the sample surface, but moves only in vertical direction (*Z* axis), towards the cell and, then, away from it: the tip is pushed into the cell surface until it reaches a well-defined indentation depth (Luo *et al.*, 2016).

During this procedure the cantilever deflection is recorded with respect to the sample-tip distance, or, in reality, with respect to vertical displacement of the piezoscanner (which corresponds indeed to sample-cantilever distance). The output of the analysis of each cell is, therefore, a cantilever deflection versus scanner displacement curve. This curve is converted into a force-distance curve applying the Hooke's law introduced before.

The overall tip-sample interactions in force spectroscopy are dominated by relative short range attracting forces, such as van der Waals and capillary forces (in air) (Stylianou *et al.*, 2019) and, at shorter relative distances, by repulsive forces, all balanced by the elastic forces exerted by the cantilever. At a given tip-sample distance, the attractive forces exceed the value of the cantilever spring constant and the tip can "jump" into contact with the surface. From the contact point onwards, as the tip continues to press on the cell, both the positive deflection of the cantilever and the repulsive contact forces (electrostatic and polymer-brush forces) increase (a representative force-distance curve is shown in **Figure 13**). The cantilever by pushing into the

sample with some well-defined force can investigate the viscoelastic properties of the sample itself, obtaining in this way the value of the Young's modulus (approach force-distance curve). Reversely, when the cantilever begins to retract from the cell, it often remains in contact with the sample (retracting force-distance curve). In this phase adhesion forces can be measured (Carvalho and Santos, 2012).

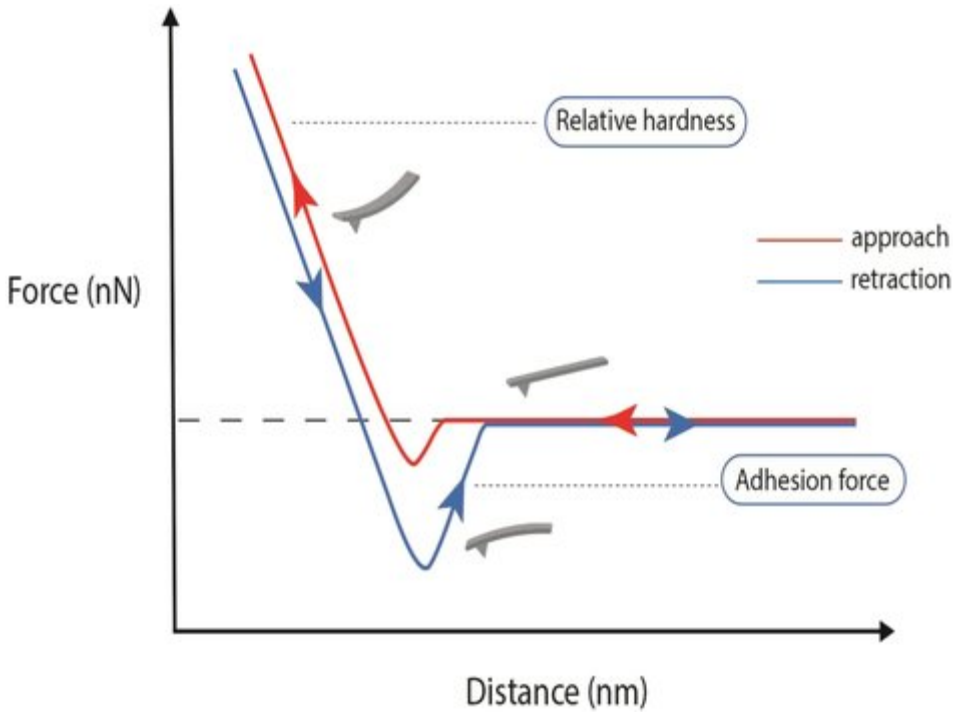

Figure 13. Schematic force-distance curve of AFM force spectroscopy: initially there is no interaction between tip and sample and they are far; then, the tip "jump to contact" with the sample, approaches further to sample that leads to a positive deflection of the cantilever due to repulsive forces (in red the approach force-distance curve). Subsequently, the cantilever moves toward the opposite direction and, at the beginning, the behaviour is similar to that described for the approach, while then the cantilever deflects negatively for the adhesion between tip and sample (in blue the retracting one). At last, adhesion forces are overcome by cantilever restoring forces and the tip is detached from the sample (Liu and Yang, 2019).

The force-distance experiment can be performed both in air and in liquid environment. For experiment in air usually adhesion forces are due to capillary forces between the tip and the sample. When the tip and the surface are immersed in water, the adhesion forces are actually reduced (capillary forces are almost eliminated, while van der Waals forces do not change). Measurements can be performed on a variety of specimen. If the specimen is of biological interest, the interaction force (the SetPoint) is usually not above 1 nN to maintain the integrity of soft biological samples.

When dealing with cells, which are extremely non-homogeneous samples, stiffness is expected to be dependent on the specific subcellular compartment in contact with the tip. In order to capture the global stiffness/Young's modulus, or the integrated stiffness of the subcellular structures under the cell surface, a micrometer-size spherical bead is usually used as probe, and is placed in correspondence to the central/nuclear region of cells (Luo *et al.*, 2016). For this reason, for sample preparation DAPI was used to label the nuclei of cells analysed obtaining reliable cell stiffness values. The use of a spherical tip also prevents the risk of sample damaging. In fact, in case of a tip-like penetrator, the contact area is not constant but function of the applied force. As a consequence, the sample is subjected to a stress where the effective strain is connected to the ratio between the contact radius and the sphere radius (10 μm) (Atkins and Tabor, 1965).

Force-distance curve analysis

The first step in biomechanical analysis is the calibration of the spring constant of the cantilever. Cantilever deflection is known as a distance x (in nanometers) and in order to convert this value into a quantitative value of force F (known as SetPoint, nN), using the Hooke's law (already mentioned above), it is essential to calculate the spring constant (k, nN/nm). This is an interaction force that increases when the cantilever pushing towards the sample surface. Spring constant can be calculated from the cantilever geometry and from the knowledge of the Young's modulus of the material. A thermal-tune method is used to determine the spring constant of the cantilever: a thermal vibration of the cantilever beam, away from the sample, is recorded and after few seconds of data acquisition the software performs a fit to find the fundamental resonance peak, which corresponds to the spring constant.

Moreover, the InvOLS (Inverse Optical Lever Sensitivity, Volts/nm), also referred as sensitivity (S), of the experimental setup must be calculated. This parameter describes the amount of photodiode response (Volts) per nanometer of cantilever deflection. The cantilever deflection is obtained by a displacement of the laser on the photodetector, and at the beginning it is expressed in Volts and after it is converted in nanometers. The cantilever deflection depends on type of cantilever, on the optical path of the AFM detection laser, and on how the cantilever is mounted in the instrument. In order to calibrate the sensitivity of the AFM system, it is necessary to measure the force-distance curve between a cantilever tip and a bare hard surface (as glass slide). The repulsive contact region is linear for the interaction between a tip and a hard substrate, as shown in **Figure 14** (dotted line).

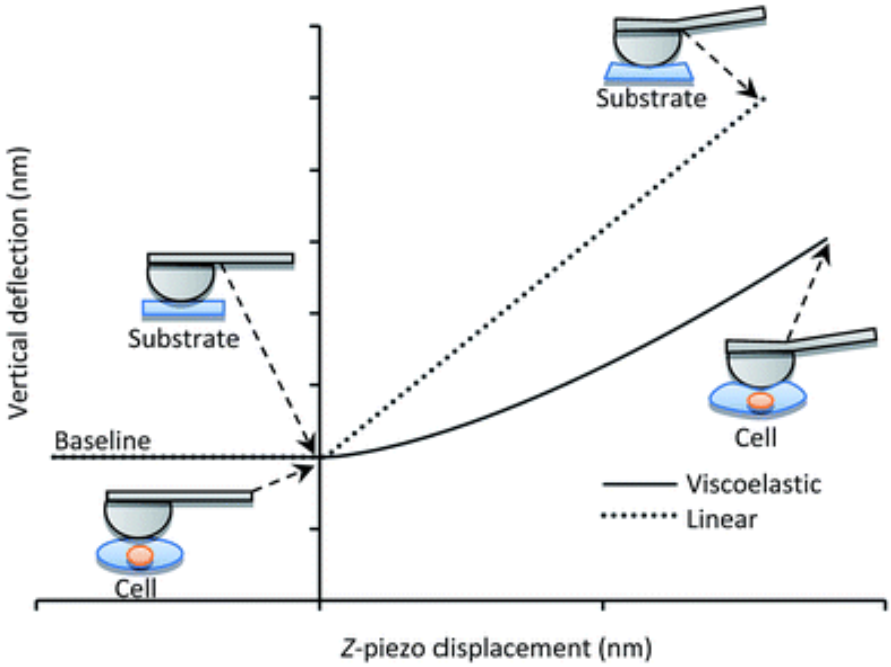

Figure 14. Cantilever vertical deflection *versus* *z*-piezo displacement during indentation of an incompressible substrate as glass (dotted line) and of a single cell (solid line). In the second case the sample is indented and for the same cantilever deflection the z-piezo movement is less than for the case of a rigid sample. The two curves have been aligned in order to have the same contact point (Fortier *et al.*, 2016).

Therefore, the software by performing a linear fit to find the slope can determine the factor for converting deflection expressed in Volts (V) into deflection expressed in nanometers (x):

$$x = V / S$$

When the sample of interest is analyzed (at least one force curve for each cell) the sensitivity value is used to calibrate the applied forces.

The response of the cells to the indentation (shown in "d" of **Figure 15**) is governed by the plastic, elastic, viscosity and adhesion properties of the cells.

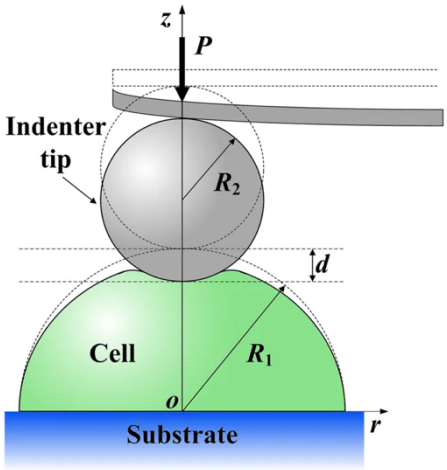

Figure 15. Cell indentation with spherical AFM tip. The indentation into the cell is indicated by the letter "*d*" (Sen, Subramanian and Discher, 2005)**.**

When the tip indents the cell, there is a minor cantilever deflection for the same z-piezo movement compared to that of the hard sample (Alessandrini and Facci, 2005). As it is shown in **Figure 14,** the shape of the force curves of living cells is often different to that of hard surfaces: curves show a more gradual pattern compared to that of hard surface. The repulsive contact region has a gradient that may not be constant. Indeed, the stiffness of a sample may change and for a given change in force changes in indentation depth. When the tip indents a soft surface, as a cell, the tip-sample contact area will change, so a micron-sized sphere with a well-known shape is attached to the tip giving a more reproducible contact area (Chen, 2014).

Hertz model

Contact mechanics models are used to model tip-sample interaction and extract biomechanical information as the sample Young's modulus. Among those is the Hertz model, which assumes that the sample is elastic and homogeneous and to use a spherical and not deformable tip. Such approximation in the case of cells is valid only when the indentation depth is well below the cell height (Chen and Lu, 2012). The Hertz model, as well as other contact mechanics models, put in correlation the force with the indentation values in order to extract the Young's modulus. In the Hertz contact model:

$$P = \frac{4E_{cell}R^{1/2}}{3(1-\nu^2)}\delta^{3/2}, \quad E_{tip} >> E_{cell}$$

"E" is the Young's modulus, "P" the force, "R" the contact radius (radius of the spherical indenter), "v" the Poisson ratio (0.5 in this case), and "δ" (m) the indentation depth. The subscripts ''tip'' and ''cell'' refer to the parameters for the indenter tip and cell, respectively.
The indentation value is calculated from the piezo displacement value, minus the deviation from the contact point **(www.jpk.com**) (Thomas *et al.*, 2013), as indicated in **Figure 16a**. In **Figure 16b** is represented the force-indentation curve derived from data of **Figure 16a**. Such curve is generally fitted by means of the Hertz model.

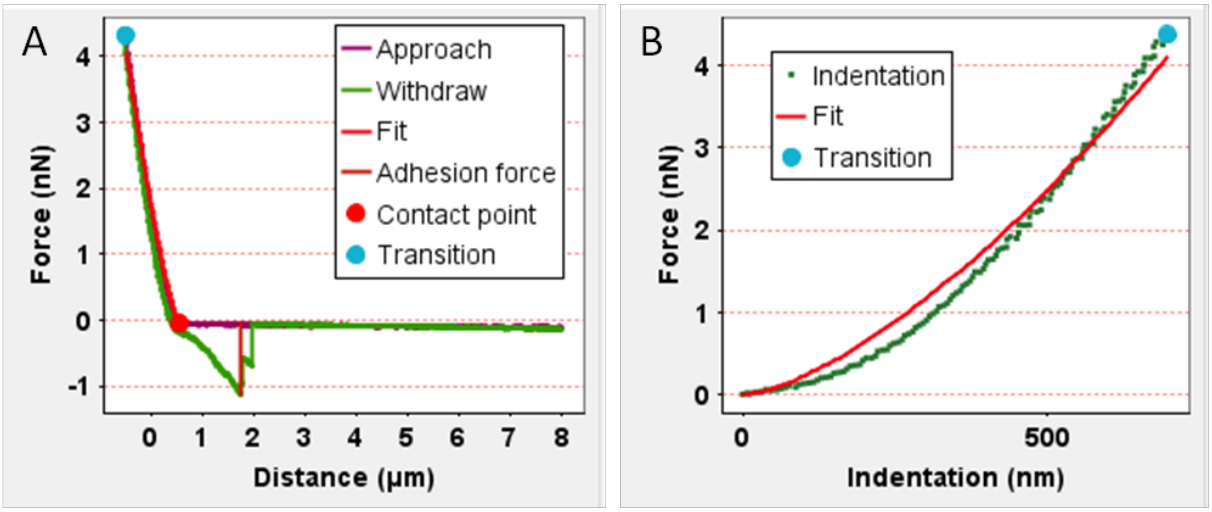

Figure 16. a) Representative force-distance curve and b) force-indentation curve on MCF7 cell.

As mentioned before, the Hertz model becomes invalid when the indentation depth is comparable to cell height (Chen and Lu, 2012). For this reason, height of cells analysed with Force spectroscopy were measured with a non-Contact mode AFM analysis. The height (as shown in **Figure 25a** of section Results) of cells is around 5 µm for both cell lines analysed (MCF7 and MDA-MB-231 cells), so the indentation interval chosen for force spectroscopy analyses was of 500 nm (10% of the total cell height). The small depth of indentation allows to avoid the stiffness contribution of the substrate (glass) to the measurement and to avoid stiffness changes due to the contribution of organelles or layered structures, typical of biological systems at increasing indentation depth. The majority of cells have a surface covered with various membrane protrusions and corrugations (such as microvilli, microridges, filopodia) and a glycocalyx, which is called a pericellular "brush". Next, there is the cell membrane (whose viscous components could influence the viscosity of the system) supported by the actin and/or tubulin cytoskeleton, which surrounds cellular organelles including the cell nucleus. The cytoskeleton components deformability of the nucleus could play a role in cell elasticity (Abidine *et al.*, 2018). It has been demonstrated that a typical indentation curve of cell in some cases does not present a simple power shape; on the contrary, the indentation curve can reveal two slopes: the first slope can represent the plasma membrane stiffness and includes a contribution from the sub-membrane cortical cytoskeleton (highly variable from a few nanometers to several hundred nanometers), whereas the second slope represents the stiffness of the inner bulk of the cell, as the others cytoskeleton elements and the nucleus (Rusaczonek *et al.*, 2019).

As was demonstrated, the Hertz model does not take into account neither the "brush" contribution to the cell mechanics nor the multi-layer nature of the investigated materials, but it considers the global stiffness of each cell (Guz *et al.*, 2014).

Therefore, considering spring constant and sensitivity values, cell force curves were fitted with Hertz model and cellular Young's modulus values were obtained (Demichelis *et al.*, 2015)(Demichelis *et al.*, 2015).

AIM AND HYPOTHESIS OF THE STUDY

Triple negative breast cancer (TNBC) is one of the most aggressive breast cancer subtype and with a poor prognosis. Nowadays, the chemotherapy is the main treatment in both early and advanced stage of the TNBC, but patients without complete response to conventional chemotherapy are approximately 80%. In light of that, clarifying biological mechanisms of the metastatic process is crucial in finding new therapeutic approaches for effective interventions.

Metastasis is thought to be easier for more deformable and, therefore, soft cancer cells, which can migrate through narrow pores of the matrix and vessels. Extracellular vesicles derived from triple-negative breast cancer, by sharing oncogenic molecules, have been shown to promote proliferation, drug resistance, migration, and metastatic capability in target cells in proportion to properties of donor cell.

Considering all these evidences, we wondered if TNBC-derived small-EVs, in particular, could transfer information to target cells about the biomechanical properties of the cell from which they originate. Our hypothesis is that TNBC-derived small-EVs, in addition to modify biomolecular pathways of target cells (by making them more aggressive, motile, invasive and metastatic), could also alter their biophysical properties modulating their stiffness to facilitate their spreading to other sites and create metastases. We believe that this mechanism can be expanded also to other cell lines and that all EVs could represent a way to transfer biomechanical information between cells.

Therefore, we set out to investigate if and how small-EVs derived from the MDA-MB-231 cell line (TNBC) can modulate biomechanical properties (stiffness/Young's modulus), cytoskeleton and nuclear morphology of MCF7 cell line (Luminal A) as target cell.

MATERIALS AND METHODS

Cell cultures

Culture conditions and cell lines

MDA-MB-231 and MCF7 breast cancer cell lines were cultivated in DMEM (Dulbecco's Modified Eagle's Medium High Glucose with Sodium Pyruvate with L-Glutamine, EuroClone, #ECM0728L) supplemented with 10% FBS (Fetal Bovine Serum South America origin EU, EuroClone, #ECS0180L) and 1% Penicillin/Streptomicin (100X, EuroClone, #ECB3001D). Cell lines were grown at 37°C in humidified 5% CO_2 incubator and split every 2-3 days according to their confluence. Adherent cells were detached by 5 minutes incubation with Tripsin-EDTA (1X in PBS w/o Calcium w/o Magnesium w/o Phenol Red., EuroClone, #ECB3052D) at 37°C, which is in turn neutralized by culture medium. Cells were centrifuged (at 25°C 200 xg for 5 minutes) and resuspended in fresh culture medium to be further seeded at desired confluence. Cells were resuspended in FBS with 5% DMSO (Dimethyl sulfoxide Cell culture grade, Euroclone, #EMR385100) and conserved in cryovials at -80°C or liquid nitrogen for long-term storage.

Cell lines used are:

- MDA-MB-231 (triple-negative breast cancer, TNBC): an epithelial human breast cancer cell line with an elongated fibroblast-like morphology but distinct from fibroblasts that grows randomly (Cailleau, Olivé and Cruciger, 1978); this cell line was established from a pleural effusion of a 51-year-old caucasian female with a metastatic mammary adeno-carcinoma and is one of the most commonly used breast cancer cell lines in medical research laboratories. MDA-MB-231 is a poorly differentiated triple-negative breast cancer (TNBC) cell line as it lacks oestrogen receptor (ER), progesterone receptor (PR) and HER2 (human epidermal growth factor receptor 2) (Holliday and Speirs, 2011). The highly aggressive MDA-MB-231 breast cancer cell line is characterized by a high proliferation rate, motility, invasiveness and, therefore, high metastatic rate (Islam and Resat, 2017). The metastatic potential of breast cancer cells is associated with the expression levels of numerous proteins, including matrix metalloproteinases (MMPs), nitric oxide synthase, plasminogen activator (PA), and cyclooxygenase (COX) (Lee *et al.*, 2014). Even though this type of tumour has been widely investigated, the exact circumstances of the metastatic process and related changes are still not fully understood.

- MCF7 (Luminal A breast cancer): a widely studied epithelial human breast cancer cell line with epithelial-like phenotype with strong cell-cell adhesion. This cell line was established from the pleural effusion from a 69 year female caucasian suffering from a breast adeno-carcinoma. MCF7 is a rather unaggressive non-invasive cell line, generally considered as having low metastatic potential. A feature of MCF7 cells is their capability to form domes and to grow in monolayers like epithelial cells. MCF7 cell line expresses both ER and PR, but is HER2 (human epidermal growth factor receptor 2) negative (Holliday and Speirs, 2011). The rather unaggressive MCF7 breast cancer cell line does not usually migrate to other sites or invade tissues (Gest *et al.*, 2013)(H. *et al.*, 2011), so it is considered to have low/non-metastatic potential.

Cell counting

Cells in suspension were counted with the Bürker Chamber, which is composed by a crystal slide with two chambers of counting areas that can be loaded independently. Each counting grid has 9 large squares (1 mm^2 each), divided by double lines into 16 small squares. Cells are placed in suspension with Trypan blue 0.5 % (p/v) in PBS (EuroClone, #ECM0990D) in an equal volume, and load in a cell counting area. The cells of 6 large squares (identified by the triple line) were counted, considering only two sides of the large square in the count. At the end of the procedure the cell concentration is calculated as follows:

$$Cells / mL = Cell\ count \times Dilution\ factor \times 10^4 / number\ of\ large\ squares\ counted$$

The volume of 1 large square is 0.1 µL. In order to estimate the concentration of cells (cells/mL), the number of cells obtained is multiplied for the dilution factor 2 (cells diluted two times in Trypan, 1:1), multiplied for 10^4 (in order to find the cell number in 1 mL) and divided for 6 (the number of all large squares counted).

Small-Extracellular Vesicle Isolation

Experimental cell conditions for vesicle isolation

Two different experimental procedures were tested for the isolation of Small-EVs from MDA-MB-231 cells via ultracentrifuge:

- At first, 2,500,000 cells (MDA-MB-231) were grown in 175 cm^2 flask in DMEM with 10% FBS for 24 hours in order to avoid cellular stress, then cells were washed twice with PBS (Phosphate-buffered saline, Sigma-aldrich); after that, DMEM with 10% of Ultracentrifugated EV-depleted FBS (UC-dFBS) or Ultrafiltrated EV-depleted FBS

(UF-dFBS) were added to cells, which have been left to grow for 48 hours to isolate Small-EVs released in supernatant. UC-dFBS was prepared by 18 hours ultracentrifugation of FBS at 120,000 xg. Only the light-coloured top layers of the supernatant (approx. 9/10 of the total volume) were retained and used in the subsequent analyses. UF-dFBS was obtained by centrifuging FBS in Amicon ultra-15 centrifugal filters (Ultracel-PL PLHK, 100 kDa cutoff, Merck Millipore, #UFC9100) for 40 min at 4,000 xg. We denoted as UF-dFBS the flow of FBS passing through the membrane with pores that, therefore, is depleted of EVs and big contaminant proteins.

- Subsequently, a new protocol of vesicle isolation was fine tuned: 2,500,000 cells (MDA-MB-231) were grown in 175 cm^2 flask in DMEM with 10% FBS for 2-3 days, in order to avoid cellular stress; then, cells were washed twice with PBS and three times with DMEM without FBS (DMEM Ø) to reduce the presence of serum contaminant proteins (i.e. albumin). MDA-MB-231 cells were left to grow for 24 hours in DMEM Ø to collect the vesicles released in supernatant from this cell line.

Ultracentrifuge

Ultracentrifugation by applying high centrifugal speed for sufficient time uses centrifugal force to separate EVs from other molecules that travel the length of the tube until the creation of the pellet (Brennan *et al.*, 2020). Then, the supernatant is removed and the pellet is then resuspended into PBS.

Supernatant of the MDA-MB-231 cells seeded for 24 hours or 48 hours was centrifuged at 300 xg at 4°C for 10 minutes in order to eliminate cellular debris. Then, the supernatant was filtered using a 0.2 µm filter to remove the bigger proteins or large-EVs. The filtered supernatant was transferred into Amicon Ultra-15 centrifugal filters (Ultracel-PL PLHK, 100kDa cutoff, Merck Millipore, #UFC9100) and centrifuged at 4,000 xg and at 4°C for 40 minutes in order to concentrate the medium to use ultracentrifuge tubes with a reduced volume capacity. Small-EVs will not pass through the filter pores, since they have much larger diameters than 8 nm, which corresponds approximately to the 100 kDa cutoff. The concentrated medium was placed in the polypropylene centrifuge tubes (OptiSeal Polypropylene Centrifuge Tubes, Beckman Coulter, #361623) after addition of PBS to reach the tube volume**.** The solution was ultracentrifuged at 120,000 xg at 4°C for 1 hours (Ultracentrifuge Optima XPN-90, Beckman coulter, #A94468). Finally, the supernatant was removed, and the pellet was resuspended in 100-200 µL of PBS and stored at -20°C. At each isolation of small-EVs, six 175 cm^2 flasks were used to seed the

MDA-MB-231 and vesicles derived from 1 or 2 flasks were inserted into an ultracentrifuge tube, resuspended independently and then joined together. Usually, one isolation experiment (6 flasks 175 cm^2 = 600 µL of PBS) was used for 1 or 2 functional experiment (vesicle uptake).

Small-Extracellular Vesicle Characterization

Atomic Force Microscopy

Atomic Force Microscopy (AFM) technique was used to characterize small-EVs from a morphological and dimensional (vesicle height and diameter) point of view in physiological conditions (liquid). We exploited several protocols of EV immobilization for AFM imaging in liquid and air. We used two different substrates (mica and glass slides) and different functionalizations of these scaffolds (plasma cleaning, APTES and vesicle antibodies); finally, we decided to use a protocol based on Poly-Lysine-coated mica, since it guarantees a simple and reproducible protocol with fewer artifacts. Moreover, we measured the same batch of vesicles both in liquid and in air conditions by using the Poly-Lysine based protocol: we observed in images acquired in air an increase in diameter and a decrease in height of small-EVs compared to that obtained in liquid. Therefore, we opted to use Poly-Lysine based protocol in liquid conditions.

The tip of AFM can be modified in several methods and there are many ways to study surface properties, including measuring friction, adhesion forces and viscoelastic properties, magnetic or electrostatic properties (Vahabi, Nazemi Salman and Javanmard, 2013). The resolution of the images depends on the geometry of the tip (e.g. sharp-conical, spherical or pyramidal tip) and on elastic and vibrational characteristics of the cantilever.

According to the applications and the interactions to be observed, AFM technique has three main scanning modes: static modes (contact mode), dynamic modes (non-contact mode), and tapping mode (semi-contact mode), as shown in **Figure 17**. These modes differ in the tip-sample average distance and are dominated by different forces.

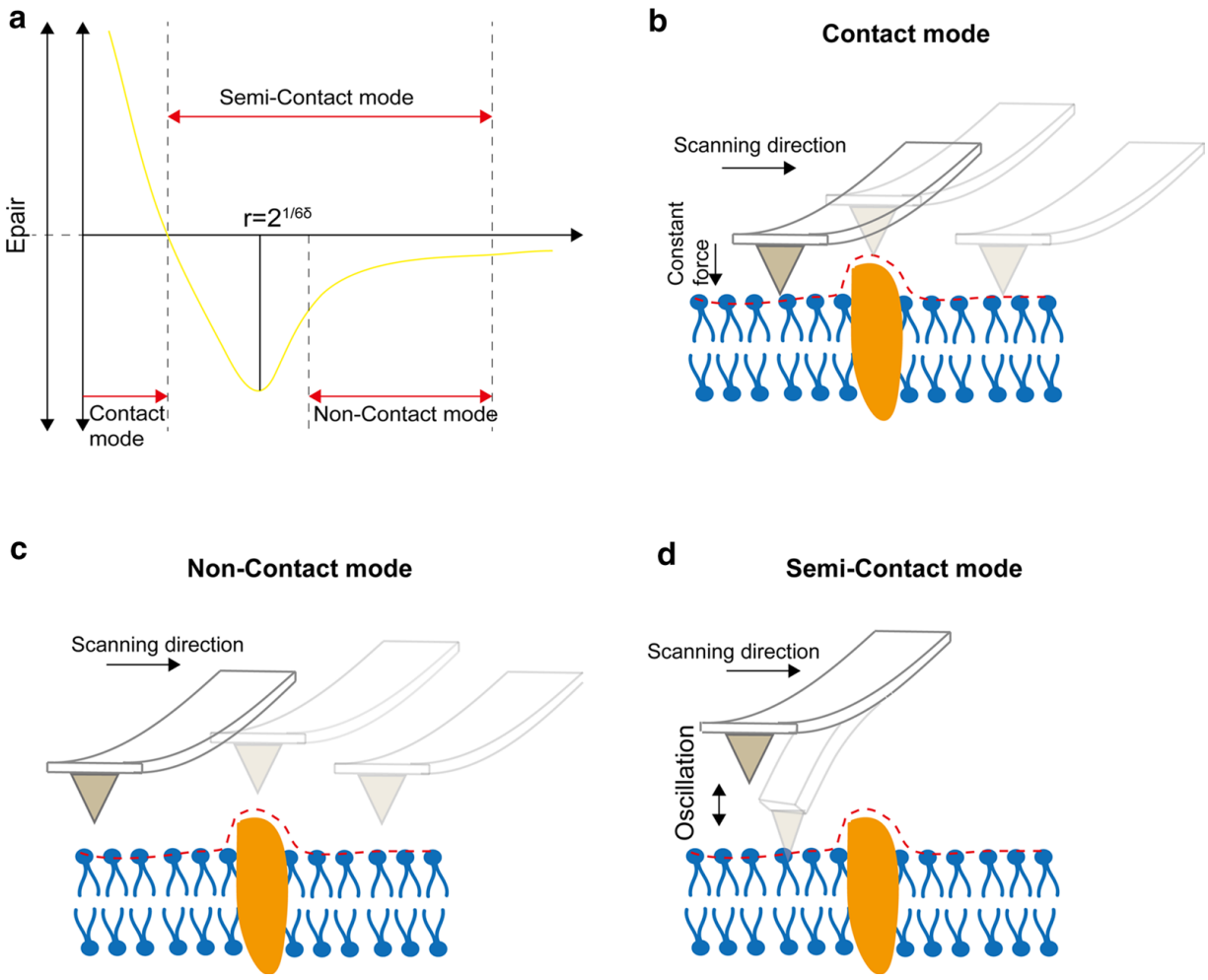

Figure 17. Three basic working modes of AFM. **a)** The curve of both interatomic force and intervals relation. The contact mode, in which the probe is always slightly in contact with the sample and scanned in a constant force mode is showed in **b)** In the contact mode the tip is moved very close to the sample (tip-sample distances < 1 nm), in a quasi-contact regime, where repulsive tip-sample forces dominate. **c)** In the non-contact mode the tip of the needle always vibrates on the surface of the sample, but it is never contact with the sample. **d)** In the tapping mode or semi-contact mode the micro cantilever is subjected to stress vibration near its resonant frequency, and the oscillating needle tip gently strikes the surface of the sample, intermittently making contact with it (Deng *et al.*, 2018).

For the AFM imaging of the Small-EVs derived from MDA-MB-231 sample, freshly cleaved muscovite mica sheets (Ruby Muscovite Mica Scratch Free Grade V-1, Nanoandmore GMBH, USA) were incubated with a drop of Poly-L-Lysine (Sigma-Aldrich) for 15 minutes at room temperature. Subsequently, the excess poly-lysine was removed by performing two washes with H_2O Milli-Q. A drop of small-EVs suspended in PBS was applied to the Poly-Lysine-coated mica surfaces at room temperature for 15 minutes to allow EVs to bind the surface via electrostatic interactions. In fact, the positive charges of Poly-Lysine improve the stability of vesicle immobilization during the imaging in liquid. A drop of buffer phosphate was then added,

in order to measure the vesicles with the AFM in liquid mode, in a physiological condition. The PBS was used as negative control. AFM images were acquired in dynamic AC-mode using a tetrahedral tips with Resonant frequency of 110kHz and Spring constant of 0.09 N/m (BL-AC40TS-C2 OLYMPUS). For each sample, 5 images with an area of 10 x 10 μm and with a sampling of 1024 x 1024 pixels (each pixel size ~ 10 x 10 nm) for a precise dimensional characterization of the substrate were acquired. The AFM images were analysed via Gwyddion® software, as described following. AFM images were subjected to background substraction. Vesicle shape was originally spherical, but it was altered upon the electrostatic interactions with the surface. Therefore, we reported both the height and diameter values to better characterize the observed spheroid shape. The vesicle heights and diameters (obtained from the equivalent radii) were obtained by applying to the images a threshold in height (10 nm) and evaluating, then, the grain distributions. This threshold corresponds to about half the height of most small-EVs; therefore, by using this threshold the diameter measured by the equivalent radius is a good approximation of the Full Width at Half Maximum (FWHM). Moreover, 10 nm was chosen as threshold in order to avoid including in the analyses proteins or other small debris that are below this threshold.

Scanning electron microscope

All measurements were performed in collaboration with Dr. Nicola Cefarin, Istituto Officina dei Materiali Consiglio Nazionale delle Ricerche, TASC, Trieste, Italy.

Scanning electron microscope (SEM) technique was used to characterize small-EVs from a morphological and dimensional (vesicle diameter) point of view in dry conditions.

SEM is a scanning probe technique that exploits the scansion of a focused electron beam on a surface to create an image. The electrons interacting with atoms at various depths of the sample produce various signals that can be used to obtain information about the surface topography and composition. Accelerated electrons of SEM carry significant amounts of kinetic energy, and this energy is dissipated as a variety of signals produced by electron-sample interactions when the incident electrons are decelerated in the solid sample. Various types of signals are produced including secondary electrons (SEs), backscattered electrons, diffracted backscattered electrons, photons, visible light. Secondary electrons and backscattered electrons are commonly used for imaging samples: secondary electrons are most valuable for showing morphology and topography on samples, while backscattered electrons for illustrating differences in composition of samples. For the vesicles imaging, secondary and backscattered electron signals were acquired, but only SE images were used for the extraction of vesicle diameter. An image of the

surface is then constructed based on the number of SEs collected for each pixel during scanning. Thus, the *Z*-axis data are only related to signal intensity (greyscale) giving no metrological information.

For the preparation of the samples, silica slides were cleaned and cut with a diamond tip; a drop of Poly-lysine was added to them, in order to facilitate the capture of small-EVs via electrostatic charge. Subsequently, the excess poly-lysine was removed by performing two washes with H_2O Milli-Q. Then 10 µL of small-EVs were spotted on silica slides. In the meantime, also 10 µL of 5% glutaraldehyde in PBS was added to small-EVs (incubation of 30 minutes) to allow the vesicle fixation. The silica slides were washed by performing two washes with PBS and two washes with H_2O Milli-Q. Finally, the sample was dehydrated with increasing ethanol solution (40%-60%-80%-98%-100%), and then dried at room temperature. Then, sample were sputtered coated with a thin layer of Au (thickness of approximately 5 nm), to make the sample conductive (Kondratov *et al.*, 2017). All SEM images were acquired with a Zeiss Supra40 SEM. A low current was used for the acquisition to reduce the sample damage. Imaging was performed at low acceleration voltage (5 keV) by detecting secondary electrons. For each sample, 10 images with an area of 14x10 µm were acquired. The SEM images were analysed with Gwyddion® software, as described for AFM analyses.

Nanoparticle tracking analysis

All measurements were performed in collaboration with the group of Prof. Daniela Cesselli, Department of Medical and Biological Sciences and Anatomical Pathology, University of Udine, Italy.

Nanoparticle tracking analysis (NTA) technique was used to characterize small-EVs from a concentration and dimensional (vesicle size distribution) point of view in physiological conditions (liquid).

The principle of NTA is based on the ability to track the characteristic movement of (nano)particles in solution according to the Brownian motion. A typical NTA device is composed of a laser beam, a microscope connected to a camera (sensitive charge-coupled device, *CCD*, or complementary metal–oxide–semiconductor, *CMOS*), a hydraulic pump and a measuring chamber. The scheme of the NTA technique is presented in **Figure 18**.

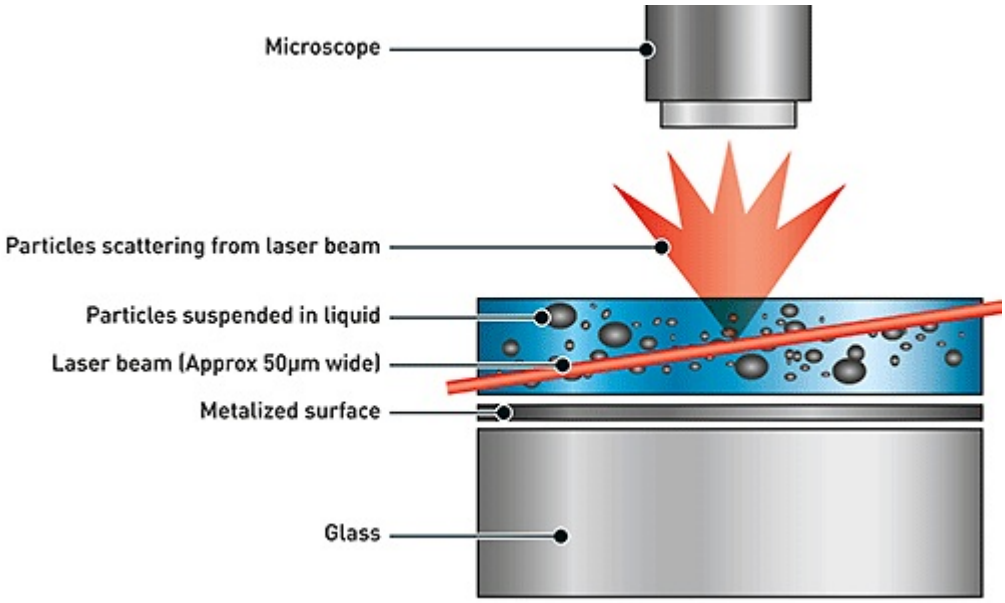

Figure 18. Nanoparticle Tracking Analysis instrument configuration (**https://www.azonano.com/article.aspx?ArticleID=4062**).

The hydraulic pump puts vesicles present in sample suspension into motion by injecting them into the measuring chamber. The tracking of the single particles in the chamber is documented by the camera that captures the scatter light upon illumination of the particles with the laser. From the acquired video recording, the movement of each particle is tracked and plotted as a function of time; the calculation of particle size distribution is obtained by applying the two-dimensional Stokes-Einstein equation. Basic data concerning the small-EVs analyzed with this method include average size, concentration, and size distribution (Szatanek *et al.*, 2017).

For the NTA analysis of Small-EVs derived from MDA-MB-231, the vesicles in PBS were diluted (1: 40/50) in H_2O Milli-Q, in order to obtain the optimal particle concentration for NTA measurements (in the range of 2×10^8 to 20×10^8/mL). Then, the small-EV size distribution and the estimated concentration (particles/ml) were obtained by analyzing with the NTA 3.2 software videos acquired with Nanosight (LM10, Malvern system Ltd., U.K.), equipped with a 405 nm laser. The sample was recorded for 60 s with a detection threshold set at maximum. Temperature was monitored throughout the measurements.

SDS-PolyAcrylamide Gel Electrophoresis

All measurements were performed by me in collaboration with the group of Prof. Riccardo Sgarra, Department of Life Science, University of Trieste, Italy.

SDS-PolyAcrylamide Gel Electrophoresis (SDS-PAGE) technique was used to separate vesicle proteins based on their molecular weight.

SDS-PAGE is an electrophoresis technique that allows protein separation according to their molecular weight. SDS (Sodium Dodecyl Sulphate) is an anionic detergent that linearizes and confers a prominent negative charge to proteins, by binding with the stoichiometry of roughly one molecule of SDS per 2 aminoacids, and making negligible their own charges (mass/charge ratio of proteins is approximately the same). In this way, proteins migrate only according to their steric hindrance. In SDS-PAGE system used, gels are discontinuous and, therefore, include an accumulation phase, called "stacking gel" with low polyacrylamide concentration, and a separation phase, called "running gel", with higher polyacrylamide concentration, where actually proteins are separated. Accumulation of proteins occurs at 20 mA for 30 minutes, while separation at 50 mA for about 1 hour.

Stacking gel: polyacrylamide gel (T = 5%, C = 3.3%) in 1.15 M Tris/HCl pH 8.45, 0.11% (w/v) SDS, 1 mg/mL ammonium persulfate (APS) and TEMED (2 uL for 1 mL solution) for polymerization.

Running gel: polyacrylamide gel (T = 15%, C = 3.3%) in 1.6 M Tris/HCl pH 8.45, 0.16% SDS, 1 mg/mL APS and TEMED (4uL for 10 mL solution).

Gel thickness: 0.75 mm. Gel width: 8 cm. Length of stacking gel: 0.5 cm and length of running gel: 8 cm. Cathode running buffer: 0.1 M Tris, 0.1 M Tricine, 0.1% (w/v) SDS, pH 8.25. Anode running buffer: 0.1 M Tris/HCl, pH 8.9. SDS loading buffer: 1% (w/v) SDS, 15% glycerol, 5% di-thio-threitol (DTT), 0.1% bromophenol blue, 0.13 M Tris/HCl pH 6.8.

Before the sample running SDS sample buffer (125 mM Tris/HCl pH 6.8, 4% w/v SDS, 20% glycerol, traces of bromophenol blue and 0.2 M DTT) was added and then samples were boiled for 5 minutes at 96 °C to favor reducing agent action (DTT) and denature proteins.

Coomassie Blue staining and Western blot

All measurements were performed by me in collaboration with the group of Prof. Riccardo Sgarra, Department of Life Science, University of Trieste, Italy.

Following electrophoresis, the gel was stained with Coomassie Brillant Blue in order to allow visualization of the separated vesicle proteins.

Comassie Blueis a solution used to stain proteins analysed in SDS-PAGE that consist of methanol/water/acetic acid solution (in a 5/4/1 volume ratio) containing 0.05% (w/v) Coomassie Brillant Blue R 250. This technique is simple and cheap and allows to visualize and quantify proteins, although with less sensitivity than others staining-methods. In detail, gel is washed

once with H_2O mQ in order to eliminate SDS excess, then stained with Coomassie Blue for 2-16 hours and de-stained with 10% (v/v) acetic acid, so as to visualize proteins, which retain dye better than gel matrix. Gel is then washed with H_2O mQ and scanned by using Image Scanner (Amersham Pharmacia Biotech).

Otherwise, following electrophoresis, the gel was used to perform Western blot technique, which allows to perform a biomolecular characterization of small-EVs (vesicle marker proteins or contaminants).
Western blot is an analytical technique that consists of a simple procedure through which a specific protein could be detected from a complex mixture of proteins. Data produced by western blot are considered semi-quantitative because this method provides a comparison of protein levels but lacks an absolute quantity determination.
Proteins separated by SDS-PAGE were transferred to a nitrocellulose membrane (Ø 0.2 µm GE Healthcare, Whatman, #10401396) through a wet transfer system (transfer buffer: 20% methanol, 25 mM Tris, 200 mM Glycine) and kept at 4 °C for 16 hours. The transfer was done exploiting an electric field, perpendicular to gel, which causes the migration of negatively conditioned proteins (trapped in gel matrix) toward the positive electrode, where membrane is located. To visualize the correct protein transfer, membrane was stained with Red Ponceau solution (0.2% Red Ponceau S, 3% trichloroacetic acid, 3% sulfosalicylic acid) incubated in agitation for 10 minutes. Blocking is an important step that prevents antibodies from non-specifically binding to the membrane. Blocking was made by shaking incubation of the membrane with blocking solution (5% NFDM – nonfat dry milk (w/v) and 0.1% (v/v) Tween 20 in PBS) for 1 hour at room temperature. Later on, membrane was shaking incubated with primary antibody (diluted in blocking solution) for 1 hour at room temperature and then washed with blocking solution three times for 5 minutes. Washing is very important because minimizes background and removes unbound antibody. The membrane was then shaking incubated with horseradish peroxidase-conjugated secondary antibodies (diluted in blocking solution) for 1 hour and washed with blocking solution three times (5 minutes) and with PBS two times (1 minute and 10 minutes respectively). The secondary antibody, bound to the primary antibody, was labelled with a peroxidase which oxidizes luminol emitting light and impressing an autoradiography films (GE Healthcare, #28-9068-48) in a position that corresponds to the one of the target protein; reaction was performed and enhanced with a ECL kit (Thermo Scientific, #2106).

Primary antibodies used are:

- α-CD63 (MX-49.129.5) (mouse monoclonal, Santa Cruz Biotechnology, #sc-5275) [1:50] [without reducing conditions]
- α-Tsg101 (C-2) (mouse monoclonal, Santa Cruz Biotechnology, #sc-7964) [1:80]
- α-Albumin (F-8) (mouse monoclonal, Santa Cruz Biotechnology, #sc-374670) [1:50]
- α-Calnexin (AF18) (mouse monoclonal, Santa Cruz Biotechnology, #sc-23954) [1:50]

Secondary antibodies used are:

- α-Mouse IgG (Whole molecule) Peroxidase conjugate (Sigma, #A9044) [1:5000]

All measurements were performed in collaboration with the group of Prof. Riccardo Sgarra, Department of Life Science, University of Trieste, Italy.

Bradford assay

Bradford assay was used to quantify proteins of small-EVs derived from MDA-MB-231 and, therefore, to get a rough idea of the amount of isolated vesicles.

Bradford assay is based on the binding of Coomassie blue G-250 dye to proteins and the production of a colored solution in the visible spectrum in response to the amount of protein. The Coomassie Brilliant Blue G-250 dye exists in three forms: anionic (blue), neutral (green), and cationic (red). Under acidic conditions, the dye is red (solution brown) in its protonated state. The red form is converted into the blue one when it makes electrostatic and hydrophobic interactions with protein molecules, and the anionic (−1 net charge) blue form of the dye is stabilized (Brady and Macnaughtan, 2015) (**Figure 19**). The intensity of the colour formed by these assays is measured by a spectrophotometer at 595 nm and Beer's law may be applied for an accurate protein quantification.

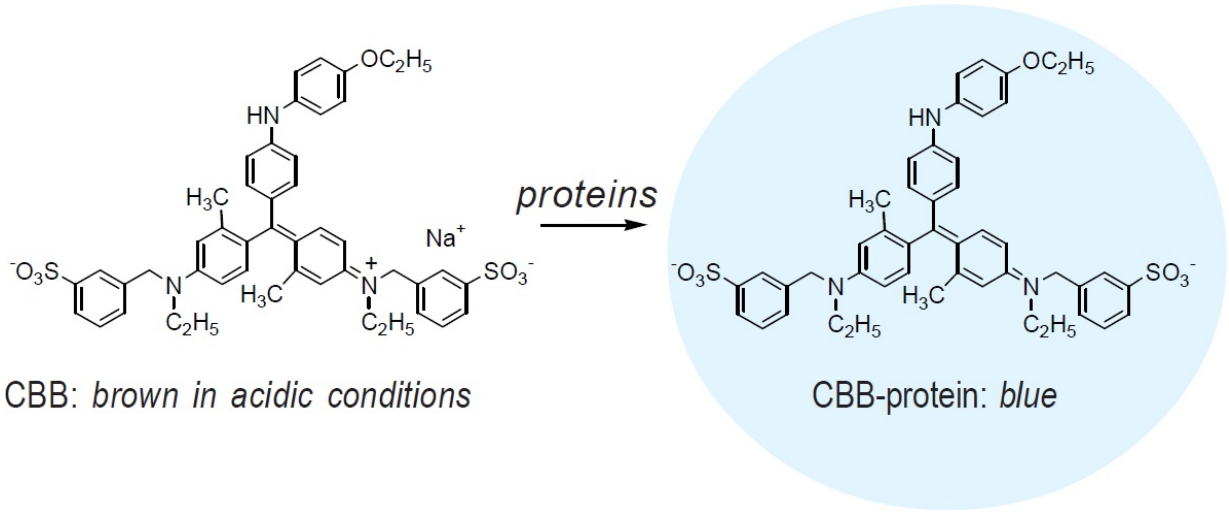

Figure 19. Reaction among protein and Blu Brillante Coomassie G-250, which causes the color change.

The Bradford assay is linear over a short range, typically from 100 µg/mL to 2000 µg/mL; often dilutions of a sample are necessary before analysis. Standard solution of bovine serum albumin (BSA) (Sigma Aldrich) is used to produce a calibration curve of absorbance versus mass concentration. Assuming the analyte-proteins react in the same manner as the BSA standard, the unknown concentration can be determined.

In order to quantify proteins of Small-EVs derived from MDA-MB-231, seven dilutions of the BSA were prepared. For the sample preparation, the same volume of RIPA 2X was added to the volume of small-EVs in PBS, in order to lysate vesicles and detect all the vesicle proteins. The solution was kept in ice for 15 minutes to allow the RIPA activity. Then, solution was centrifuged at 14,000 xg for 10 minutes, and the supernatant was recovered avoiding the pellet composed of cell/lipid debris. A small volume of all samples (different BSA solutions and unknown sample) was put on a 96-well plate. The RIPA buffer was used as blank sample for each experiment. Protein solutions are normally assayed in duplicate or triplicate. Then, the Comassie dye (200 µL) (Bradford-Solution for protein determination, EuroClone, #APA69320500) was added to each wells and left to incubate for 10 minutes. Finally, absorbance was read at 595 nm using TECAN infinite F200 PRO (Tecan Trading AG, Switzerland) spectrophotometer. To obtain the concentration, the triplicate were averaged, the absorbance value of the blank was subtracted, and the quantity of vesicle proteins were obtained from the interpolation of the absorbance value to the equation of the BSA calibration curve.

Functional Experiments

Cell proliferation assay

Cell proliferation assay was used to test both cell viability and cell proliferation.

Cell proliferation assay used is based on the Trypan blue dye uptake, by providing a direct information on the number of cells present in the solution. The uptake of Trypan blue in cells allows to determine the number of viable cells present in a cell suspension. This is an exclusion test based on the principle that live cells have intact cell membranes that exclude the dye, whereas dead cells do not. Therefore, a viable cell will have a bright cytoplasm whereas a nonviable cell a blue one (Strober, 2001). This method consists of 'real-time' counting of proliferation-positive cells using a Bürker chamber, as described above.

In detail, the MCF7 cells were seed in 24-well plate and were left to grow for 24 hours. After that, cells were washed and Small-EVs derived from MDA-MB-231 at different concentrations (0.5 µg/µL, 0.1 µg/µL, 0.2 µg/µL) were added to the medium. PBS was used as negative control (Ctrl). Each sample was analysed in triplicate (in three different wells). MCF7 cells were left to incubate with vesicles for 24or 48 hours. Then, target cells were collected and counted (as described above).

Force Spectroscopy Atomic Force Microscopy

Force spectroscopy Atomic Force Microscopy (AFM) was used to evaluate the stiffness (described as Young's modulus or elastic modulus) of cells analysed, as described in Introduction section.

Force spectroscopy analysis of cells was carried out using Smena AFM (NT-MDT Co., Moscow, Russia) mounted on an inverted fluorescence microscope (Nikon Eclipse Ti-U).
For the sample preparation, MDA-MB-231 and MCF7 cells were seeded on glass of 13 mm of diameter (low density in order to prevent cell overlapping, which could alters the stiffness value of single cell). The MCF7 cells were incubated with Small-EVs derived from MDA-MB-231 as described above (in "Cell proliferation assay" paragraph). Cells were washed with PBS three times and fixed with PFA 4% for 20 minutes by shaking. Then, cells were washed with PBS three times and conserved in PBS with 1% penicillin/streptomycin at 4°C for short periods. To visualize nuclei, cells are stained with DAPI (Sigma Aldrich) in PBS for 10 minutes. Cells are washed with PBS three times. Then, cells were analyzed with the Atomic Force Microscopy in contact mode in liquid solution (PBS). For AFM force spectroscopy, silicon spherical tip with a diameter of 20 µm (Tip: CSG01 cantilever from NT-MDT Smena, k = 0.006-0.012 N/m) was used, in order to collect the global stiffness of the cells. A force of 0.7 nN, an indentation rate of 2 µm/sec (low enough to avoid hydrodynamic effects), and an indentation of -500 nm were used. For each sample, 30-60 cells were analysed. Elastic modulus values (E), in kPa, were determined by fitting the obtained force-displacement curves with a Hertz model by using AtomicJ® software.

Indirect immunofluorescence

Immunofluorescence technique was used to evaluate cytoskeleton and nuclear rearrangements of cells.

Indirect immunofluorescence is a commonly used technique in research and clinical diagnostic, in which visualization of a specific protein or antigen in fixed cells is indirectly done. This technique thanks to a fluorescence microscope allows the detection of the antigen of interest in a highly specific way through a primary antibody. The interaction between the immunoglobulin and its antigen is detected by a secondary antibody conjugated with a marker (or by a primary antibody already conjugated with a marker). The fluorescence emitted by the excited fluorophore is indicative of the presence of protein or antigen. Marker used is a fluorophore that absorbs light energy of a specific wavelength and, when excited, emits light at a different wavelength. The indirect immunofluorescence represents a method to visualize the cytoskeleton elements (Banuett, 2010). Since the cytoskeleton is very dynamic it is also sensitive to disruption by chemical or mechanical means, therefore care must be taken in handling the material throughout the procedure.

For the sample preparation, cells were grown on glass of 13 mm of diameter and were harvested at sub-confluence condition. Medium was removed and cells were then washed twice in PBS and fixed with the cross-linking agent 4% (v/v) paraformaldhehyde (PFA) in PBS for 20 minutes. Cells were washed again with PBS twice and stored at 4 °C for short period. The plasma membrane is impermeable to antibodies and is commonly permeabilized by treatment with the detergent TWEEN. Therefore, 0.5% PBS-TWEEN was added to the cells for ten minutes and 0.1% PBS-TWEEN for 5 minutes (three times). Then blocking solution (1% BSA in 0.1% PBS-TWEEN) was added to them for 1 hour in order to block the aspecific autofluorescence and the aspecific sites of the sample. Cells were incubated in a humidified chamber with primary antibody (diluited in blocking solution) for several minutes (different time for each antibody) and were washed with PBS three times. Then, cells were incubated in a humidified chamber with secondary antibody (diluited in blocking solution) for 1 hour and were washed with PBS three times. Nuclei were stained by incubation with DAPI (Sigma Aldrich) in PBS for 5 minutes. Cells are washed two times in PBS and, finally, the mounting medium was used to retard the photobleaching.
For indirect immunofluorescence analyses a microscope (Inverted Research Microscope Eclipse Ti, Nikon) equipped with an epi-fluorescence illuminator or a 488 nm laser for Total Internal Reflection Fluorescence application was used. All images were analyzed using ImageJ® software.
Primary antibodies used are:
- α-alpha-Tubulin (Abcam, #ab52866) for 1 hour [1:500]
- Phalloidin (Invitrogen, #A12381) for 45 minutes [1:40]

- α-Vinculin (Invitrogen, #42H89L44) for 2 hours [1:20]
- anti-pFAK (Cell signaling, #3283S) for 2 hours [1:75]
- anti-Lamin A (Abcam, #ab26300) for 45 minutes [1:40]

Secondary antibodies used are:

- α-Rabbit Alexa Fluor 488 (Invitrogen, #A11008) for 1 hour [1:500]
- α-Mouse Alexa Fluor 594 (Invitrogen, #A11005) for 1 hour [1:500]

RNA extraction and Real Time-qPCR

All measurements were performed in collaboration with the group of Prof. Licio Collavin, Department of Life Science, University of Trieste, Italy.

Real time PCR technique was used to quantify gene expression of Yap downstream genes (CTGF, CYR61, and ANKRD1) in cells.

RNA was extracted using EuroGOLD TriFast reagent (Euroclone), according to manufacturer's instructions. Purified RNA samples were quantified at Nanodrop Spectrophotometer device, by evaluating ng/µl concentration and protein and phenol/ethanol contaminations. The integrity of extract material was detected analyzing the coil and supercoil strips formation. For RNA expression analysis, 0.5 µg of total RNA sample (100 ng/µl) was reverse-transcribed in stable cDNA with iScript™ Advanced cDNA Synthesis Kit (Biorad). The genes of interest were amplified with Itaq UniversSYBR Green (Biorad), according to manufacturer's instructions. A CFX Connect™ Real-Time PCR System (Biorad) was used to perform Real-Time PCR. Primers used are the following:

TARGET	*SEQUENCE*
CTGF	Forward 5'-AGG AGT GGG TGT GTG ACG A-3'
	Reverse 5'-CCA GGC AGT TGG CTC TAA TC-3'
CYR61	Forward 5'-AGC CTC GCA TCC TAT ACA ACC-3'
	Reverse 5'-TTC TTT CAC AAG GCG GCA CTC-3'
ANKRD1	Forward 5'-CAC TTC TAG CCC ACC CTG TGA-3'
	Reverse 5'-CCA CAG GTT CCG TAA TGA TTT-3'
H3	Forward 5'-GAA GAA ACC TCA TCG TTA CAG GCC TGG T-3'
	Reverse 5'-CTG CAA AGC ACC AAT AGC TGC ACT CTG GAA- 3'

Data and statistical analysis

Student's t-test was used to test the significance of the differences in functional assay measurements and immunofluorescence. This test is used to determine if there is a significant difference in the means of two indipendent and identically distributed datasets. If the p-value is < of 0.05, two samples are significantly different. Instead, normality of Young's modulus distributions was checked by Shapiro-Wilk test. In this test the null hypothesis is that the population is normally distributed. If the p-value obtained is > of 0.05, null hypothesis is accepted. Since most of the distributions were observed no-normally distributed, the nonparametric Wilcoxon test was used to compare datasets of force spectroscopy analyses. The test essentially calculates the difference between each set of pairs and analyzes these differences. This test is commonly used as an alternative to the Student's t-test when the distributions can not be assumed to be normally distributed. The null hypothesis of Wilcoxon test is that a randomly selected value from one sample will be less than or greater than a randomly selected value from a second sample is equally likely. Also in this case, if the p-value is < of 0.05, two samples are significantly different.

* = p-value < 0.05; ** = p-value < 0.01; *** = p-value < 0.001; **** = p-value < 0.0001

RESULTS

Triple negative breast cancer (TNBC) is one of the most aggressive breast cancer subtype and with a poor prognosis due to the high propensity for metastatic progression and absence of specific targeted treatments (lack of ER and PR expression and no over-expression of HER2) (Yeo, 2015). Nowadays, chemotherapy is the main treatment in both early and advanced stage of the TNBC (Shang *et al.*, 2018). Unfortunately, TNBC patients without complete response to conventional chemotherapy are approximately 80% and recurrence and metastases frequently occur after the surgery (Jhan and Andrechek, 2017; Nakashoji *et al.*, 2017). In light of that, clarifying biological mechanisms of the metastatic process is crucial in finding new therapeutic approaches for effective interventions.

The development of metastasis requires a series of stages (invasion of extracellular matrix, intravasation and extravasation from vessels and formation of pre-metastatic niche) that, finally, lead to the formation of secondary tumour sites in distant organs (Martin *et al.*, 2014). All these processes are thought to be easier for more deformable and, therefore, soft cancer cells, which can migrate through narrow pores of extracellular matrix and vessels. As a matter of fact, several papers provided evidences for a direct correlation between the metastatic potential of cancer cells and their biomechanical properties: invasive cancer cells appear to be softer than non-invasive one or normal cells (Lekka, 2016; Luo *et al.*, 2016; Alibert, Goud and Manneville, 2017). The reason of those biomechanical differences is still to be completely understood. Several cellular elements are involved in cellular biomechanical changes, including cellular microenvironment, cytoskeleton, nucleus, and plasma membrane (Alibert, Goud and Manneville, 2017). Moreover, the metastatic potential of cancer cells is directly related to their motility, which is a bidirectional interplay between the actin and microtubules organization and expression (Etienne-Manneville, 2004). Extracellular vesicles derived from triple-negative breast cancer have been shown to promote proliferation and drug resistance in non-tumorigenic breast cancer (Ozawa *et al.*, 2018) and to induce an increase in migration of target cell proportional to the metastatic potential of the donor cell (Harris *et al.*, 2015). Moreover, EVs derived from stromal cells of breast cancer have found to promote proliferation and migration via Hippo signalling pathway in non-invasive breast cancer cells (Nardone *et al.*, 2017).

Considering all these evidences, we wondered if small-EVs could also transfer information about biomechanical properties, key step in metastasis, to target cells.

To this end, we examined the effects of small-EVs derived from the MDA-MB-231 cell line (TNBC) on biomechanical properties (stiffness/Young's modulus), cytoskeleton, nucleus, and Yap activity of MCF7 cell line (Luminal A). In order to investigate the role of released vesicles on cellular biomechanics, we decided to use these two commonly used breast cancer cell lines that have different well-defined metastatic potentials: MDA-MB-231 cells are metastatic, whereas MCF7 cells are tumorigenic but considered low/non-metastatic.

Isolation of Small-Extracellular Vesicles derived from MDA-MB-231 cells

Optimization of cell culture conditions for vesicle isolation

Experimental procedures were fined tune and standardized, as much as possible, in order to maximize the number of known, reportable parameters for the vesicle isolation: the same culture and harvesting conditions (e.g. passage number and seeding confluence) were maintained and regular checks for Mycoplasma contamination were performed, as suggested by MISEV2018 (Thery *et al.*, 2018).

At the beginning two different EV-depleted FBS protocols for the growth of MDA-MB-231 cells for vesicle isolation were tested and compared with the control (10% FBS):
MDA-MB-231 cells were grown in DMEM with 10% of Ultracentrifugated EV-depleted FBS (UC-dFBS) in order to isolate Small-EVs released in the supernatant. UC-dFBS was prepared by 18 hours ultracentrifugation of FBS at 120,000 xg.
MDA-MB-231 cells were grown in DMEM with 10% of Ultrafiltrated EV-depleted FBS (UF-dFBS) in order to isolate Small-EVs released in the supernatant. UF-dFBS was obtained by centrifuging FBS in Amicon ultra-15 centrifugal filters (100kDa cutoff) for 55 min at 3,000 xg.
Although MDA-MB-231 cells grown with UF-dFBS appear to be fewer than others, cells seeded with both two different EV-depleted FBS protocols have not significant differences in proliferation when compared with their control, as **Figure 20** shows.

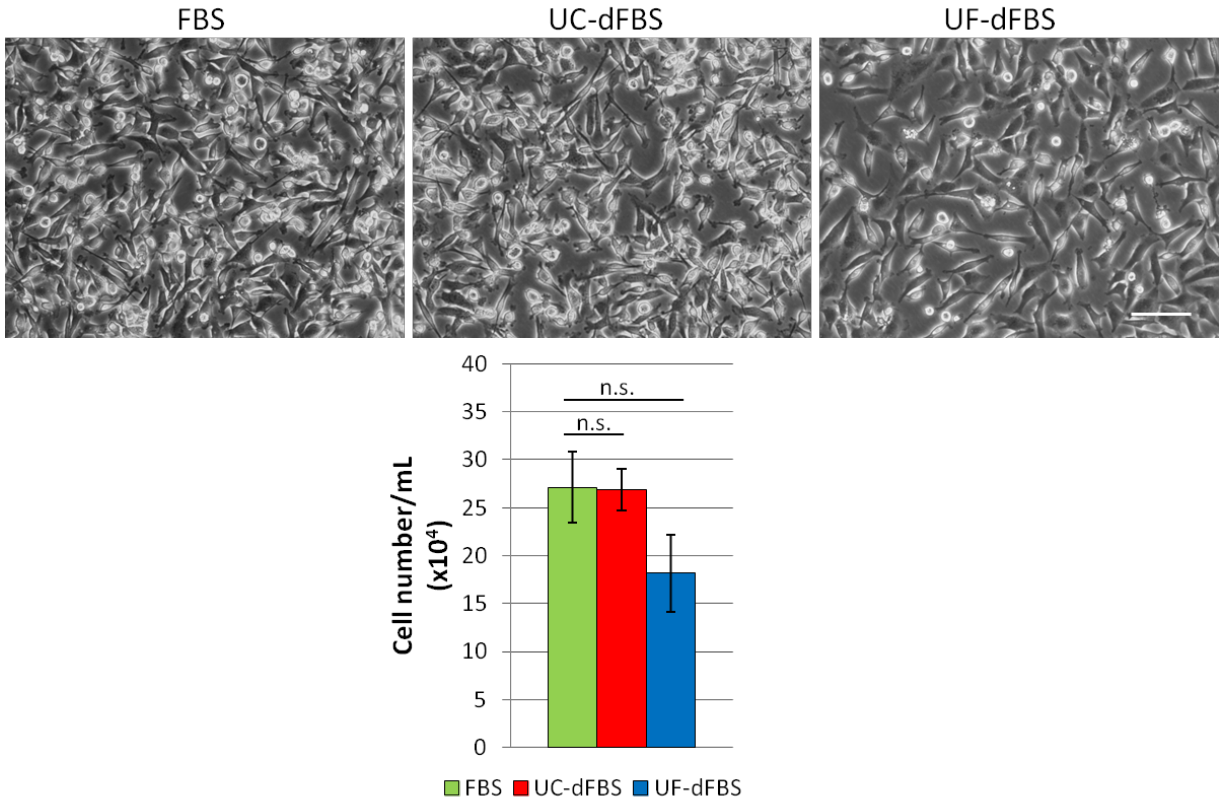

Figure 20. MDA-MB-231 cells cultured with different FBS conditions (FBS, UC-dFBS or UF-dFBS): representative optical images on top and cell proliferation results on bottom. Data are expressed as mean ± SD. Significance of data differences was established via two-tailed Student's t-test. Scale bar indicates 10 µm. N.s. indicates not significant.

As MDA-MB-231 cells are able to grow with both types of depleted FBS, small-EVs derived from MDA-MB-231 cells (hereinafter referred to as "231_sEVs") seeded with these two different EV-depleted FBS conditions were isolated via ultracentrifuge from cell supernatant. In **Figure 21**, 231_sEVs UC and UF indicate 231_sEVs isolated from cells grown with UC- and UF-dFBS, respectively.

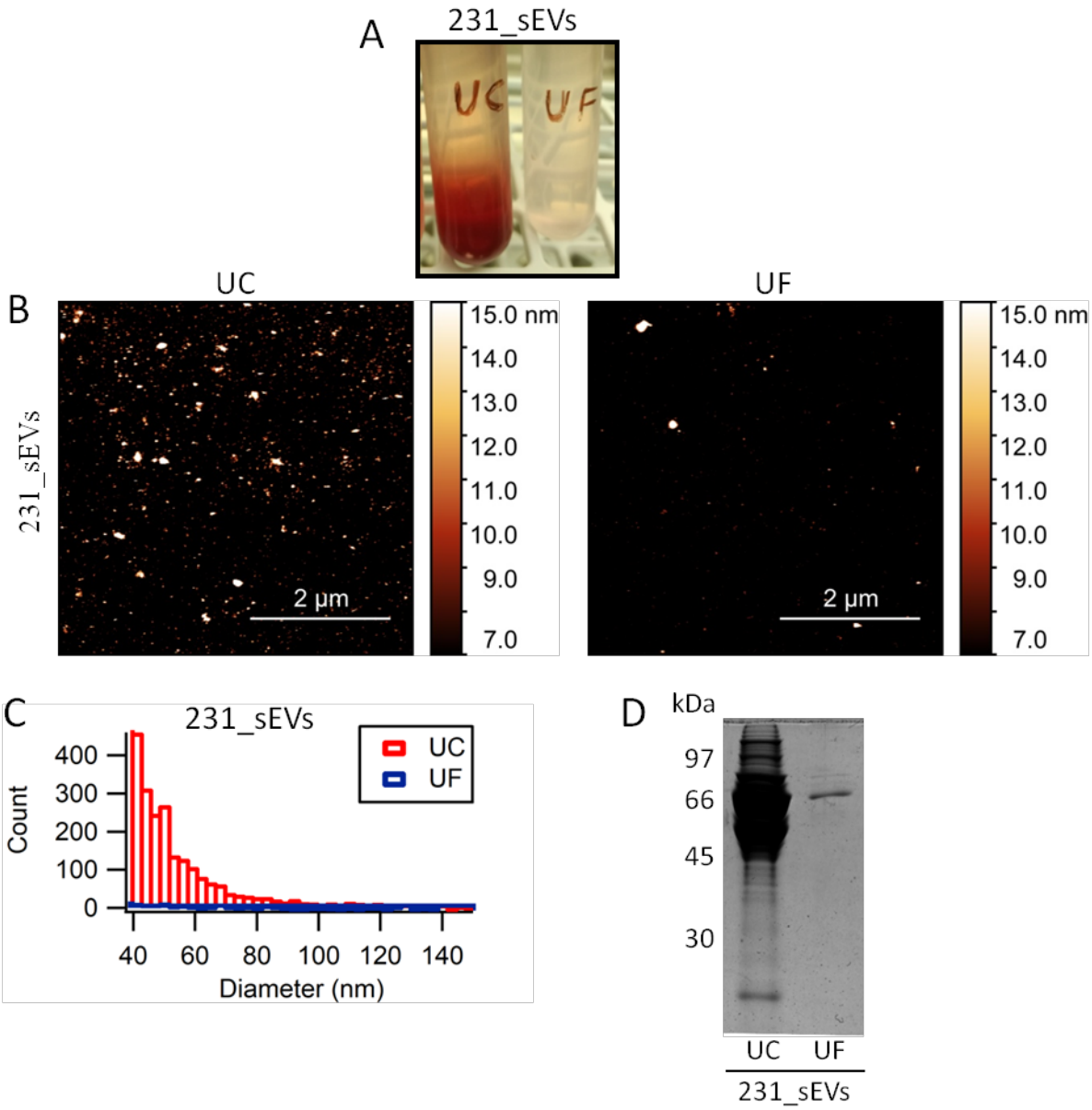

Figure 21. Small-EVs derived from MDA-MB-231 cells cultured with two different FBS conditions (UC-dFBS or UF-dFBS): a) ultracentrifuge tubes, **b**) representative AFM images, **c**) diameter histogram of vesicles obtained from the analysis of AFM images and **d**) representative Coomassie Brilliant Blue-stained SDS-PAGE gel.

From a macroscopic point of view, colorimetric differences can be clearly noted between the two different experimental procedures (**Figure 21, panel a**). Solution obtained from growing cells with EV-depleted FBS via UC is much more turbid than that obtained via UF; this result could be due to the presence of residual proteins and EV contamination of FBS, which could not be eliminated with ultracentrifuge. In fact, AFM images (**Figure 21, panel b**) and diameter histogram obtained from the analysis of AFM images (**Figure 21, panel c**) show a massive presence of small particles, with the same dimensions of EVs, in 231_sEVs UC if compared with UF sample. Since only the method used for EV-depletion of FBS changes between these

two sample preparations, small particles abundant in UC could correspond to FBS contaminants (i.e. proteins or EVs) co-isolated with 231_sEVs. Moreover, SDS-PAGE gel stained with Coomassie Brilliant Blue shows that 231_sEVs UC contain also many more protein bands, when compared with the 231_sEVs UF sample (**Figure 21, panel d**). Protein bands observed in both samples could be attributed to an albumin (with 70 kDa as molecular weight (Haudenschild *et al.*, 2014)) contamination derived from the FBS. Considering that the final aim of this thesis project is to perform functional experiments in target cells, we decided to set aside both UC and UF-dFBS preparation for 231_sEVs isolation, in order to avoid bias or unreliable results due to FBS protein contaminants.

Subsequently, a new protocol for vesicle isolation was fined tune: MDA-MB-231 cells were left to grow for 24 hours in serum-free medium (DMEM Ø) to collect, via ultracentrifuge, vesicles released in supernatant from this cell line, as performed from Méndez et al. for secretome sample preparation (Mendez *et al.*, 2018). Cell metabolic activity of MDA-MB-231 cells was tested via the colorimetric MTT assay after 24, 48, or 72 hours without FBS in the medium (**Supplementary 1**). We did not observed significant differences only between MDA-MB-231 cells cultured without FBS and the control after 24 hours. Cell viability of MDA-MB-231 cells cultured with this new protocol for vesicle isolation was investigated via cell proliferation assay. Optical images (**Figure 22 panel a**) and cell proliferation assay results (**Figure 22 panel b**) demonstrated that MDA-MB-231 cells after 48 hours in normal and 24 hours in serum-free medium can proliferate as the control (cells with 10% FBS), while this is not possible for cells cultured without FBS for 72 hours. Moreover, SDS-PAGE gel stained with Coomassie Brilliant Blue (**Figure 22 panel c**) shows that 231_sEVs isolated from MDA-MB-231 cells cultured with the new protocol do not have the band ascribable to the FBS albumin, which was present in previous vesicle preparations (231_sEVs UC and UF). Unfortunately, since the new cell culture protocol allows to collect small-EVs released from cells only in one day and since the sample is purer and free of FBS protein contamination, the final yield is very low (5-10 times less the amount of 231_sEVs UF). As a matter of fact, even after various efforts to increase vesicle and protein concentration, protein bands of the 231_sEVs obtained with the new method have rarely been observed after the staining with Coomassie Brilliant Blue or Red Ponceau.

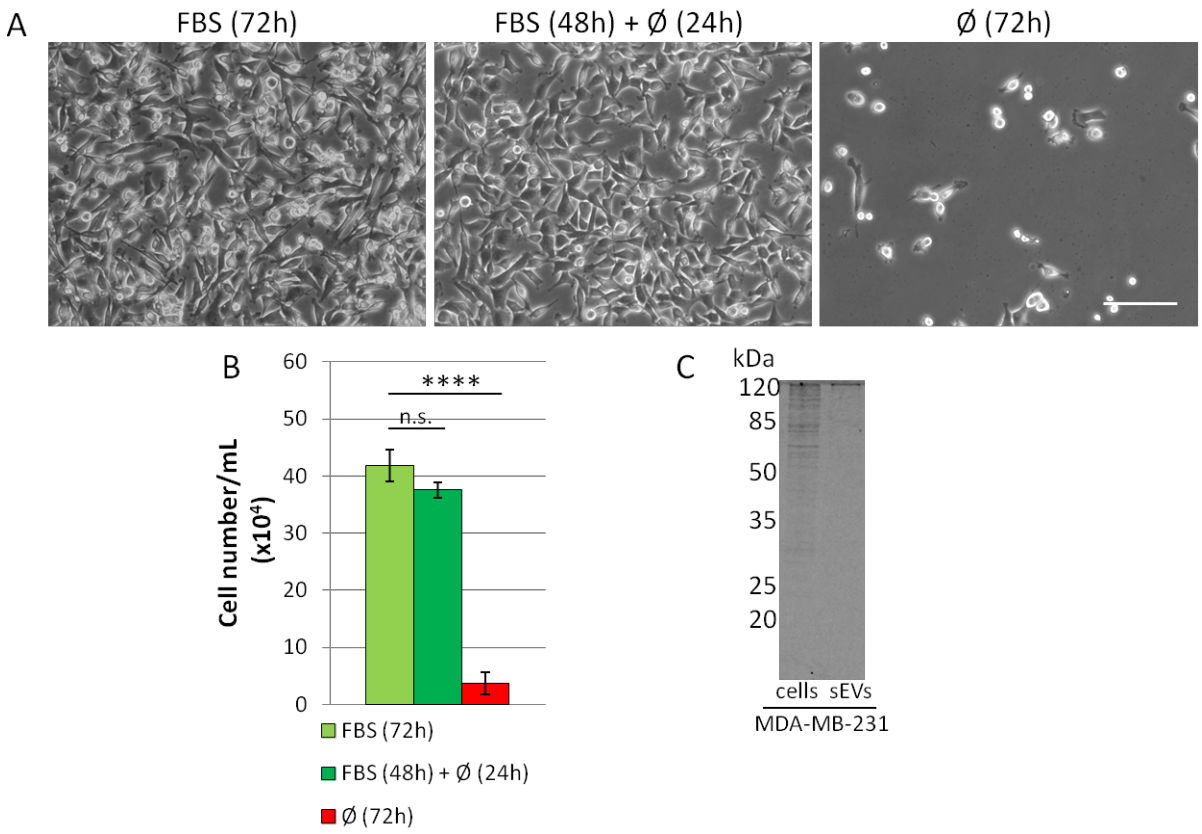

Figure 22. MDA-MB-231 cells cultured with the new cell cultured protocol for small-EVs isolation. a) Representative optical images and **b**) cell proliferation results of MDA-MB-231 cells. **c**) Representative Coomassie Brilliant Blue-stained SDS-PAGE gel of 231_sEVs isolated from MDA-MB-231 cells cultured with the new methods. Data are expressed as mean ± SD. Significance of data differences was established via two-tailed Student's t-test. Scale bar indicates 10 µm. N.s. indicates not significant.

Characterization of Small-Extracellular Vesicles derived from MDA-MB-231 cells

Small-Extracellular Vesicle characterization

Small-EVs isolated via UC from MDA-MB-231 (231_sEVs) were characterized from a morphological, dimensional and biomolecular point of view. Scanning Electron Microscopy (SEM) images (as shown in **Figure 23a**) allowed to recognize the typical rounded structure and the typical diameter ranging from 40 to 200 nm (as shown in **Figure 23c**), obtained from the analysis of the SEM images, of the small-EVs. The spherical shape of 231_sEVs was confirmed also through Atomic Force Microscopy (AFM) images (**Figure 23b**); also the vesicle height and diameter derived from the analysis of the AFM images (ranging from 10 to 60 nm and 30 to 160 nm, respectively) are conform with those obtained in AFM literature studies (**Figure 23d**).

Nanoparticle Tracking Analysis (NTA) measurements showed vesicle concentration and size distribution with a modal value ~150 nm (**Figure 23e**), which falls within the typical small-EV diameter range, of 231_sEVs.

Western blot showed the absence of serum contaminant albumin, but the presence of typical small-EV marker protein CD63 in both MDA-MB-231 cell lysate and 231_sEVs and TSG101 only in cell lysate; moreover, the cellular specific marker calnexin was observed only in MDA-MB-231 cellular lysate (**Figure 23f**).

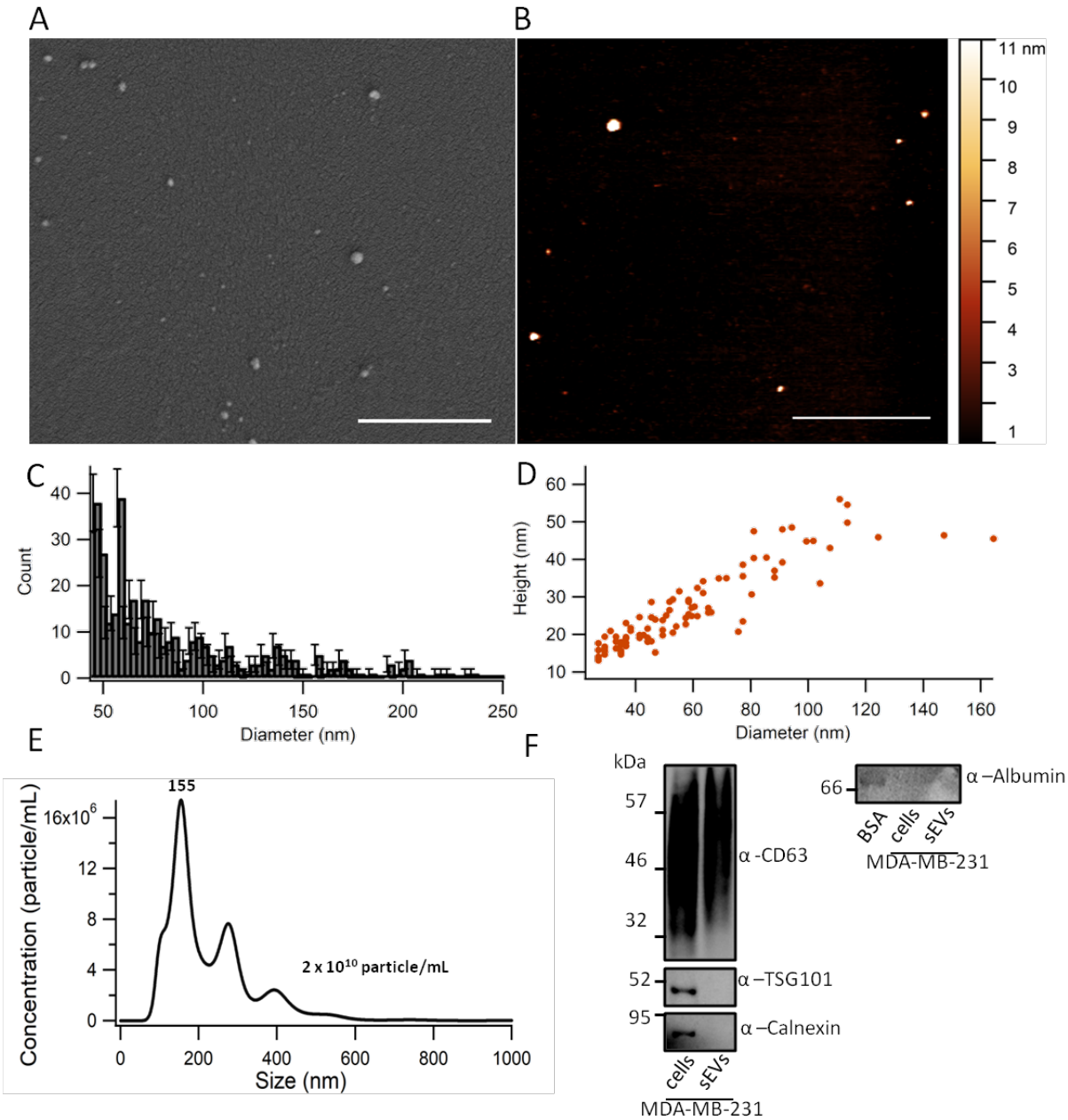

Figure 23. MDA-MB-231-derived small extracellular vesicles (231_sEVs) characterization. a) A representative SEM image of 231_sEVs. **b**) A representative AFM image of 231_sEVs. **c**) Diameter histogram of vesicles obtained from the analysis of SEM images (Poisson error bars).**d**) Scatterplot of height and diameter

vesicles obtained from the analysis of AFM images. **e**) Nanoparticle concentration and size distribution of 231_sEVs obtained via NTA. **f**) Western blot analysis of vesicle markers (CD63 and TSG101) and cellular (Calnexin) and serum (Albumin) contaminants in both MDA-MB-231 cellular lysate and 231_sEVs. Scale bar indicates 1 μm.

Functional experiments: addition of MDA-MB-231-derived small-EVs to MCF7 cells

For all functional experiments performed, 231_sEVs were quantified via Bradford assay. We tested if the RIPA or PBS could affect Bradford results and, finally, we did not observed any differences with water.

Moreover, taking into account that the two breast cell lines, MCF7 and MDA-MB-231, have different characteristics, we have chosen, for almost all functional experiments, to not compare the two different cell lines together with the MCF7 treated with 231_sEVs; conversely, we decided to optimize conditions and parameters in order to observe differences first between the two cell lines and, then, between MCF7 cells upon small-EV uptake and their control.

Small-EVs derived from MDA-MB-231 promote proliferation in MCF7 cells

Cell proliferation assay based on Trypan blue dye was used to investigate proliferation rate of MCF7 target cells upon vesicle uptake, in relation with their control.

It is known from literature that cell proliferation of MDA-MB-231 is significantly higher than proliferation of MCF7 cells (**Figure 24a**). Therefore, the activity and functionality of the isolated small extracellular vesicles were verified by evaluating the effects of 231_sEVs on MCF7 cell proliferation.

In order to optimize cellular treatment, we evaluated the MCF7 cell proliferation after the addition of 231_sEVs at three different vesicle concentrations (0.05 μg/μl, 0.1 μg/μl and 0.2 μg/μl) and at two different incubation time (24 or 48 hours). A significant increase in cellular proliferation rate was observed in MCF7 cells treated with 0.1 μg/μl and 0.2 μg/μl of 231_sEVs for 48 hours when compared to negative control, PBS (as shown in **Figure 24b)**. No significant increase in cellular proliferation was observed for other conditions. This increase in cell proliferation of MCF7 cells, in agreement with literature, showed that small-EVs isolated are active and can transfer molecular characteristics of the donor cell to the target cells.

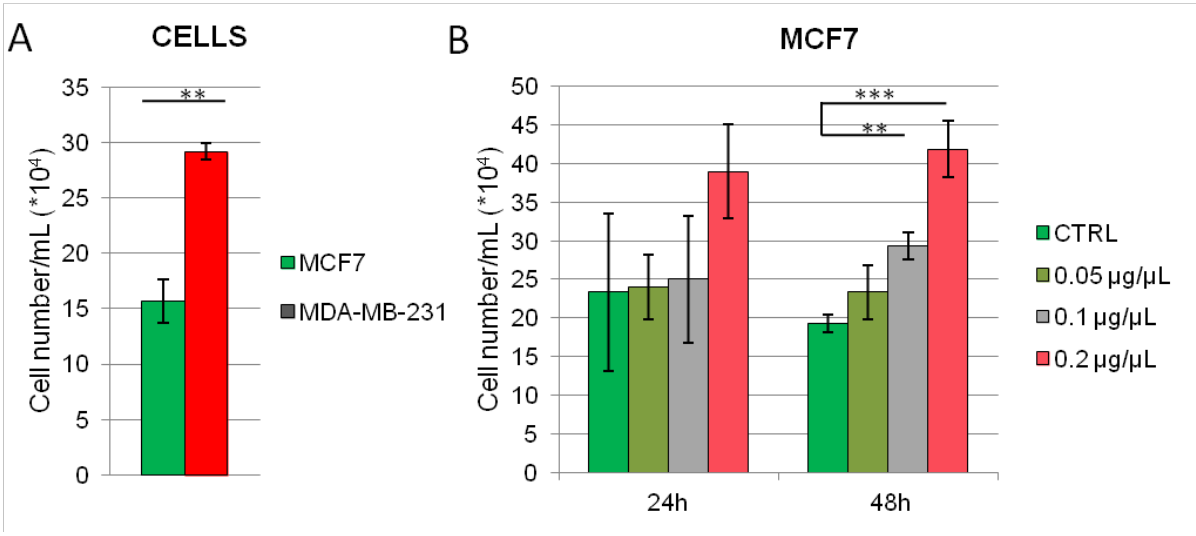

Figure 24. **Effects of small-EVs derived from MDA-MB-231 on the MCF7 cell proliferation. a**) Cell proliferation of MCF7 and MDA-MB-231 cells in comparison. **b**) Cell proliferation assay of MCF7 cells treated different concentrations of 231_sEVs for 24 or 48 hours in relation to the negative control. Data are expressed as mean ± SD. Significance of data differences was established via two-tailed Student's t-test.

Small-EVs derived from MDA-MB-231 induce cell stiffness changes in MCF7 cells

Cell stiffness of MDA-MB-231 cells and MCF7 cells were investigated through Force Spectroscopy AFM. After measuring the height of cells (~ 5 µm) (in **Figure 25a**), we decided to perform an indentation of – 500 nm on single cell (10 % of the total height, in order to perform the fitting via Hertz model). For these measurements, we used a silicon spherical bead (20 µm of diameter), in order to obtain one global elastic modulus for each single cell. As expected, MDA-MB-231 cells resulted to be significantly softer than MCF7 cells (**Figure 25b**). Then, we measured MCF7 cells upon the addition of the 231_sEVs at the same condition as before. In almost all conditions MCF7 cells stiffness decreases upon 231_sEV uptake, but significantly for cells treated with 0.2 µg/µl of 231_sEVs for both 24 and 48 hours, as shown in **Figure 25c**.

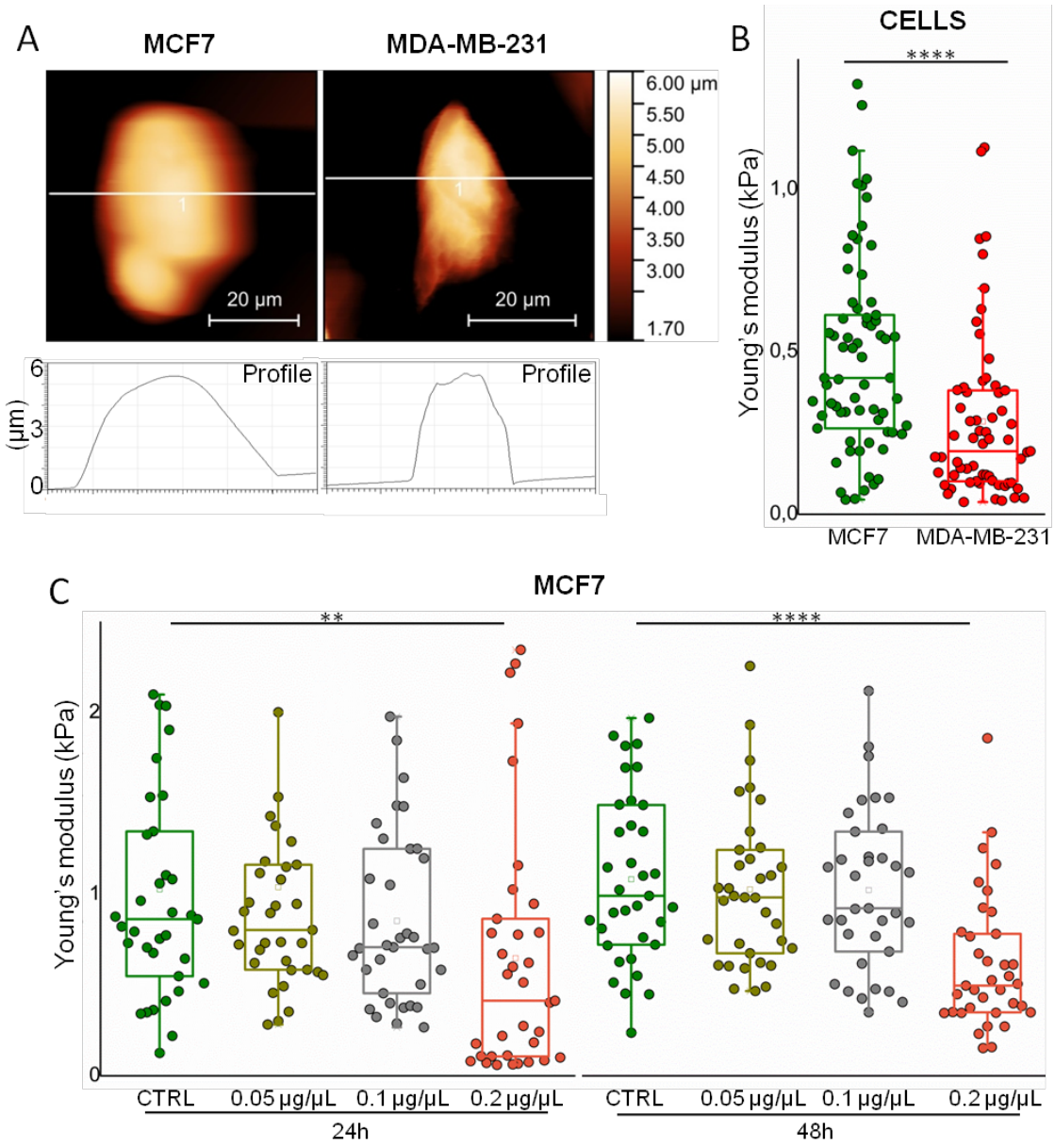

Figure 25. Effects of small-EVs derived from MDA-MB-231 on the MCF7 cell stiffness. a) Representative AFM images with relative height profile of MCF7 and MDA-MB-231 cells. Boxplot showing the Young's modulus distributions of MCF7 and MDA-MB-231 single cells (**b**) and after the addition of 231_sEVs at different conditions, in relation to the relative negative control (**c**). The lower and the upper boundaries of the box represent Q1 (25 percentile) and Q3 (75 percentile) of the data, respectively; the ▫ symbol and the horizontal bar inside the box represent the mean and medium, respectively. Significance of data differences was established via Wilcoxon test, considering that some Young's modulus distributions are no-normally distributed (investigated via Shapiro-Wilk test).

We investigated the regulation of biomechanical properties of target cells by EVs also in other experimental models. We investigated via AFM force spectroscopy cell stiffness of the MCF10A healthy breast cells and MCF7 and MDA-MB-231 as target cells after the addition of umbilical cord mesenchymal stromal cell-derived EVs, MSC_EVs (obtained in collaboration

with prof. Mario Gimona's lab at the Paracelsus Medical University Salzburg). The Young's modulus values of breast healthy and cancer cells significantly decrease upon MSC_EV addition, as shown in **Figure 26.**

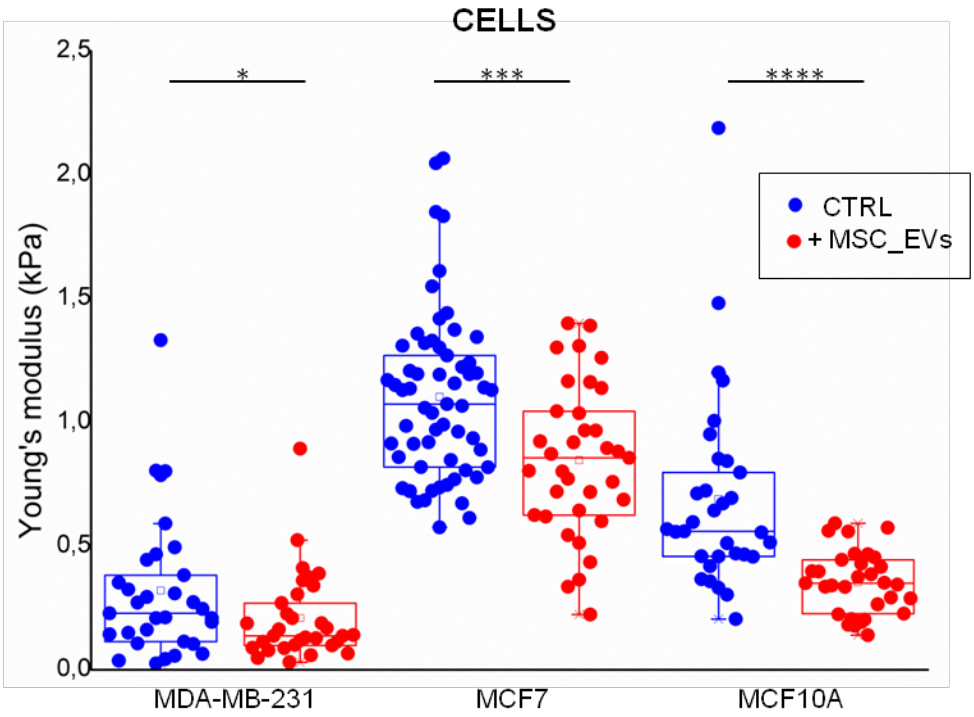

Figure 26. Effects of EVs derived from MSC on cell stiffness of breast healthy or cancer cells. Boxplot showing the Young's modulus distributions of single cells, in relation to the relative negative control. The lower and the upper boundaries of the box represent Q1 (25 percentile) and Q3 (75 percentile) of the data, respectively; the ▫ symbol and the horizontal bar inside the box represent the mean and medium, respectively. Significance of data differences was established via Wilcoxon test, considering that some Young's modulus distributions are no-normally distributed (investigated via Shapiro-Wilk test).

Furthermore, we tested the biomechanical response of the U87MG glioblastoma as target cells after treatment with small-EVs derived from Glioma-Associated Stem Cells (GASC) (obtained in collaboration with Daniela Cesselli's group at University of Udine). Results in **Figure 27a** shows that U87 cells are softer if compared with GASC ones. AFM force spectroscopy results in **Figure 27b** show an increase in the cell stiffness of U87 cells after the treatment with GASC-derived small-EVs. Moreover, in the same study AFM force spectroscopy results were used to investigate routes of small-EV internalization. We measured cell stiffness of U87 cells treated with 3 different drugs as inhibitors of the main routes of vesicle uptake, in order to interfere with internalization of GASC-derived small-EVs. A blocker of endocytosis was tested: Chlorpromazine (CPZ) that prevents formation of clathrin-coated vesicles at the plasma

membrane interfering with clathrin-dependent endocytosis. Moreover, we used Chloroquine (CRC), inhibitor of the Na+/H+ exchanger which is a key player of micropinocytosis, and Filipin (FIL), an cholesterol reducing agent responsible of disruption of lipid rafts-mediated endocytosis. We observed an overall similar behaviour, with the increase in young's modulus values of cells treated with GASC-derived small-EVs despite the presence of the drugs. CRC seems to be the more effective in reducing the vesicle activity on the biomechanical response (the stiffness increases less), while CPZ and FIL seem to have less effect on the interference of vesicle activity (as can be seen in **Figure 27**).

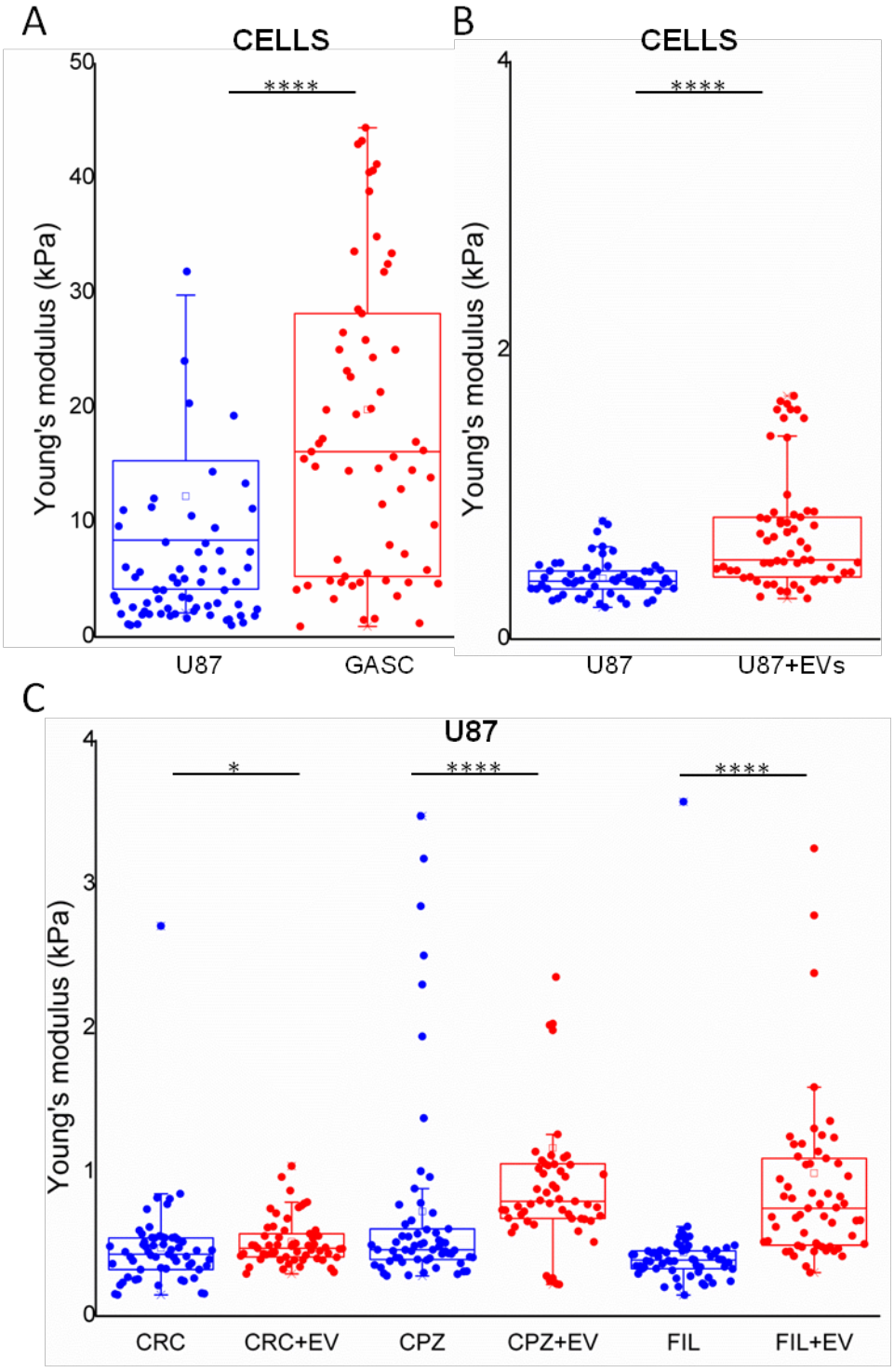

Figure 27. a) Cell stiffness of GASC and U87 cells; b) effects of small-EVs derived from GASC on cell stiffness of glioblastoma U87 cells and c) on cell stiffness of glioblastoma U87 cells treated with 3 different drugs. Boxplot showing the Young's modulus distributions of single cells, in relation to the relative negative control. The lower and the upper boundaries of the box represent Q1 (25 percentile) and Q3 (75 percentile) of the data, respectively; the ▫ symbol and the horizontal bar inside the box represent the mean and medium, respectively. Significance of data differences was established via Wilcoxon test, considering that some Young's modulus distributions are no-normally distributed (investigated via Shapiro-Wilk test).

Small-EVs derived from MDA-MB-231 induce cytoskeleton rearrangements in MCF7 cells

Cytoskeleton and nuclear properties of MDA-MB-231 and MCF7 breast cancer cells have already been extensively analysed. Nevertheless, considering the contradictory results, we decided to investigate through epifluorescence and Total Internal Reflection Fluorescence (TIRF) analyses the cytoskeleton differences and the nuclear characteristics in these two breast cancer cells for a complete and immediate overview. Then, we explored cytoskeleton, nuclear lamin A and nuclear morphology of MCF7 cells treated or not with 231_sEVs, in order to correlate the observed biomechanical changes with cytoskeleton and nuclear rearrangements.

Significantly higher levels of α-tubulin expression were observed in MDA-MB-231 if compared with MCF7 cells, as shown in **Figure 28a**. The same trend, so a significant increase of α-tubulin expression, was observed also in MCF7 cells upon the 231_sEVs addition if compared with the control, as showed in **Figure 28b**. Therefore, the 231_sEV activity makes α-tubulin expression of the MCF7 cells similar to that of MDA-MB-231 cells. No significant differences were observed in F-actin structures, neither comparing the MCF7 to the MDA-MB-231 cells, nor the MCF7 cells treated or not with 231_sEVs.

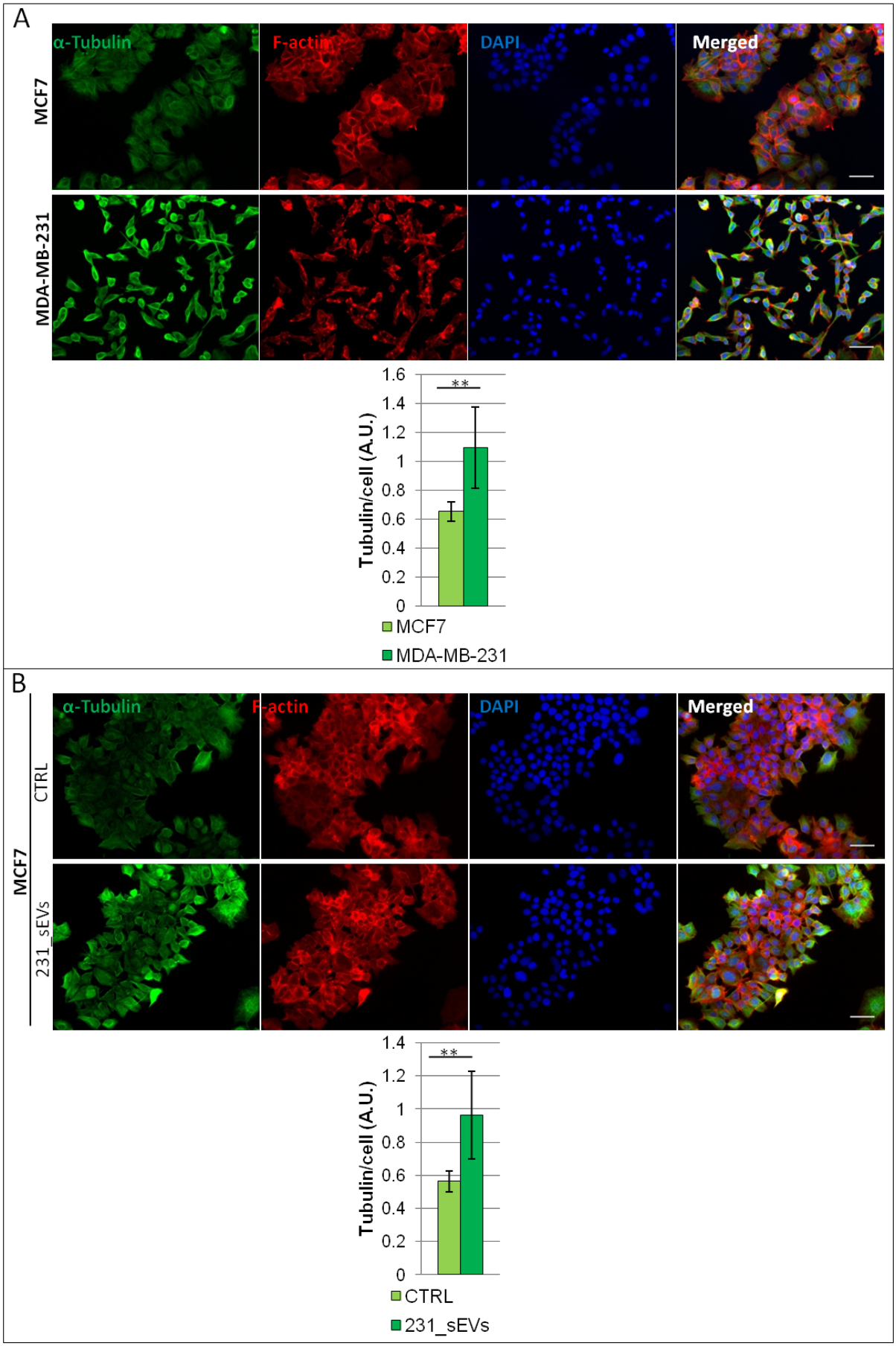
A
α-Tubulin
F-actin
DAPI
Merged
MCF7
MDA-MB-231
Tubulin/cell (A.U.)
1.6
1.4
1.2
1
0.8
0.6
0.4
0.2
0
**
MCF7
MDA-MB-231
B
α-Tubulin
F-actin
DAPI
Merged
MCF7
CTRL
231_sEVs
Tubulin/cell (A.U.)
1.4
1.2
1
0.8
0.6
0.4
0.2
0
**
CTRL
231_sEVs

Figure 28. Effects of MDA-MB-231-derived small-EVs on α-tubulin expression of MCF7 cells. a) Representative epifluorescence images on top and relative histograms on bottom, showing the α-tubulin expression of MCF7 and MDA-MB-231 cells and **b**) in MCF7 after the addition of 231_sEVs, in relation to the relative negative control. Data are expressed as mean ± SD. Significance of data differences was established via two-tailed Student's t-test. Scale bar indicates 50 μm.

MDA-MB-231 cells show significant lower densities of focal adhesions, as detected by TIRF imaging of Vinculin and pFAK, and significant lower adhesion size, as detected by pFAK imaging, if compared with MCF7 cells (**Figure 29a-b**). Contrary, MCF7 cells upon the 231_sEV addition have significant higher densities and size of focal adhesions when compared with their control (**Figure 29c-d**).

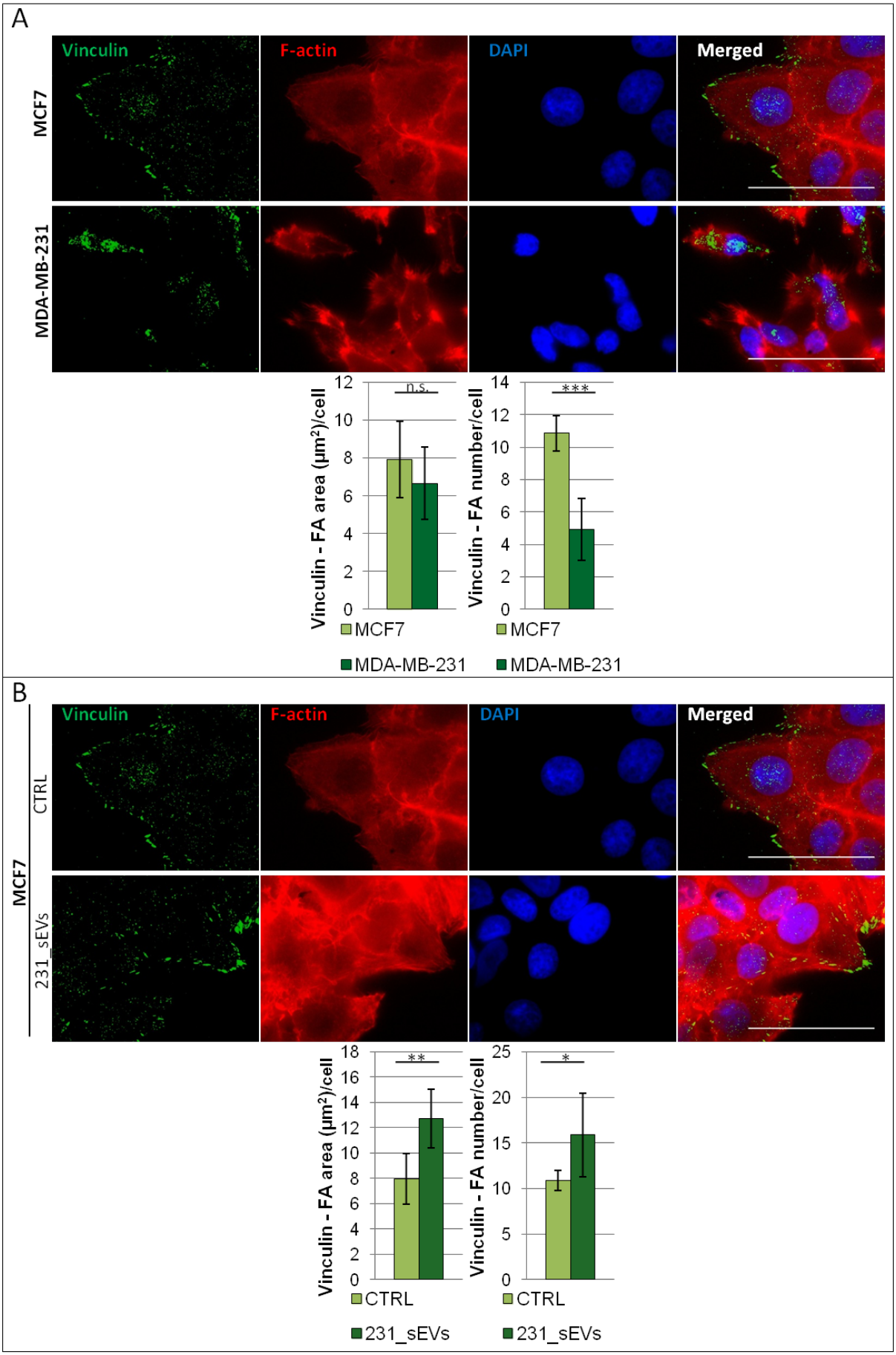
A
Vinculin
F-actin
DAPI
Merged
MCF7
MDA-MB-231
Vinculin - FA area (µm²)/cell
n.s.
Vinculin - FA number/cell
***
MCF7
MDA-MB-231
B
CTRL
231_sEVs
**
*
CTRL
231_sEVs

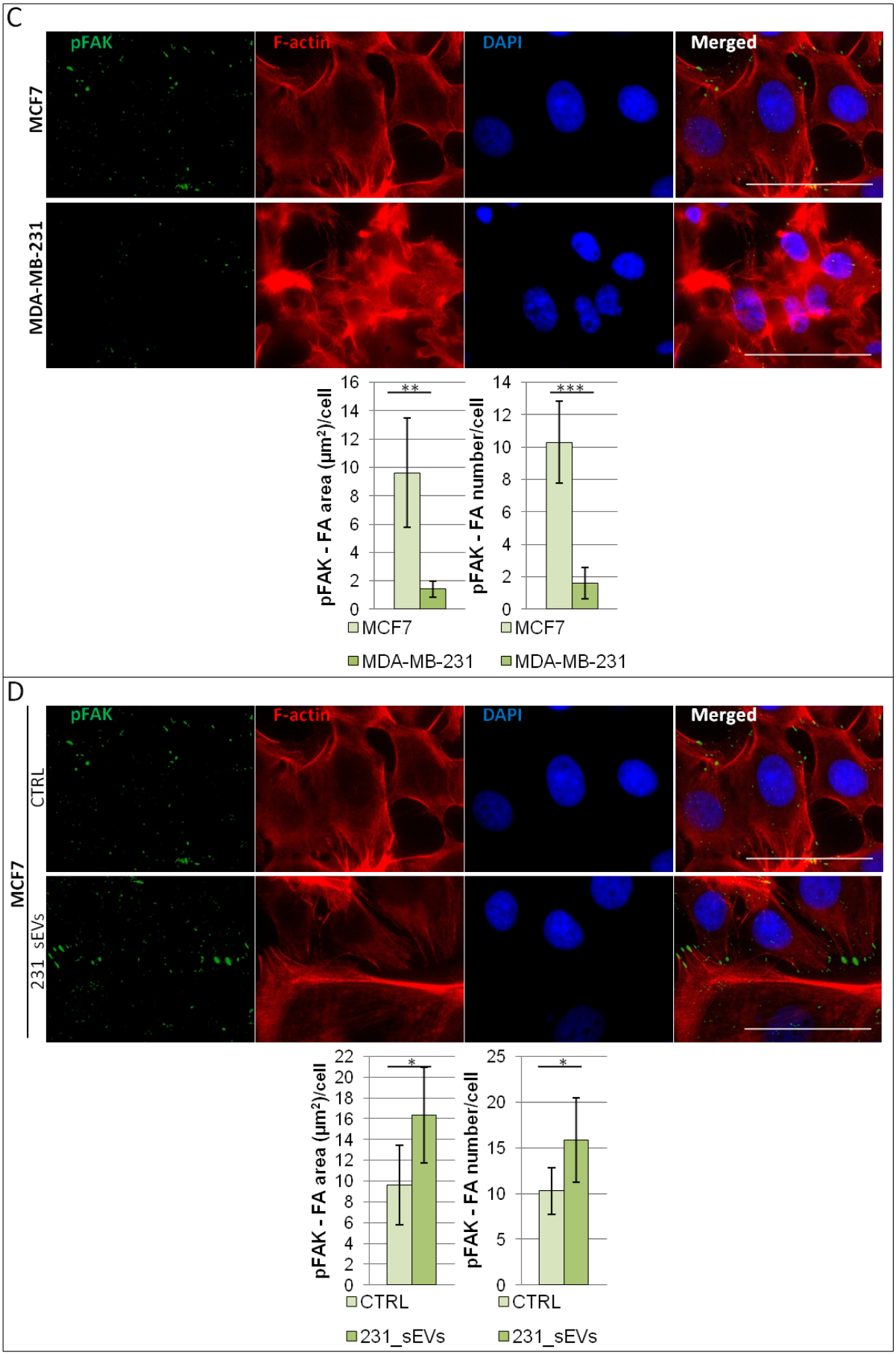
C
pFAK
F-actin
DAPI
Merged
MCF7
MDA-MB-231
pFAK - FA area (µm²)/cell
pFAK - FA number/cell
**
***
MCF7
MDA-MB-231
D
CTRL
231 sEVs
*
231_sEVs

Figure 29. Effects of small-EVs derived from MDA-MB-231 on focal adhesions of MCF7 cells. (**a-c**) Representative Total Internal Reflection Fluorescence (Vinculin and pFAK) and epifluorescence (F-actin and DAPI) images on top and relative histograms on bottom, showing the area, density, and activity of FAs in MCF7 and MDA-MB-231 cells; (**b-d**). Representative Total Internal Reflection Fluorescence (Vinculin and pFAK) and epifluorescence (F-actin and DAPI) images on top and relative histograms on bottom, showing the area, density, and activity of FAs in MCF7 cells treated with 231_sEVs in relation to their negative control. Data are expressed as mean ± SD. Significance of data differences was established via two-tailed Student's t-test. Scale bar indicates 50 μm. N.s. indicates not significant.

Then, we investigated also the nuclear characteristics and Lamin A expression of the cells. Significant smaller nuclear area and circularity and significant higher Lamin A expression were observed in MDA-MB-231 than MCF7 cells, as shown in **Figure 30a**. The 231_sEVs addition leads to a significant reduction in nuclear size and circularity and an increase of Lamin A expression in the MCF7 cells treated when compared with the control (**Figure 30b**).

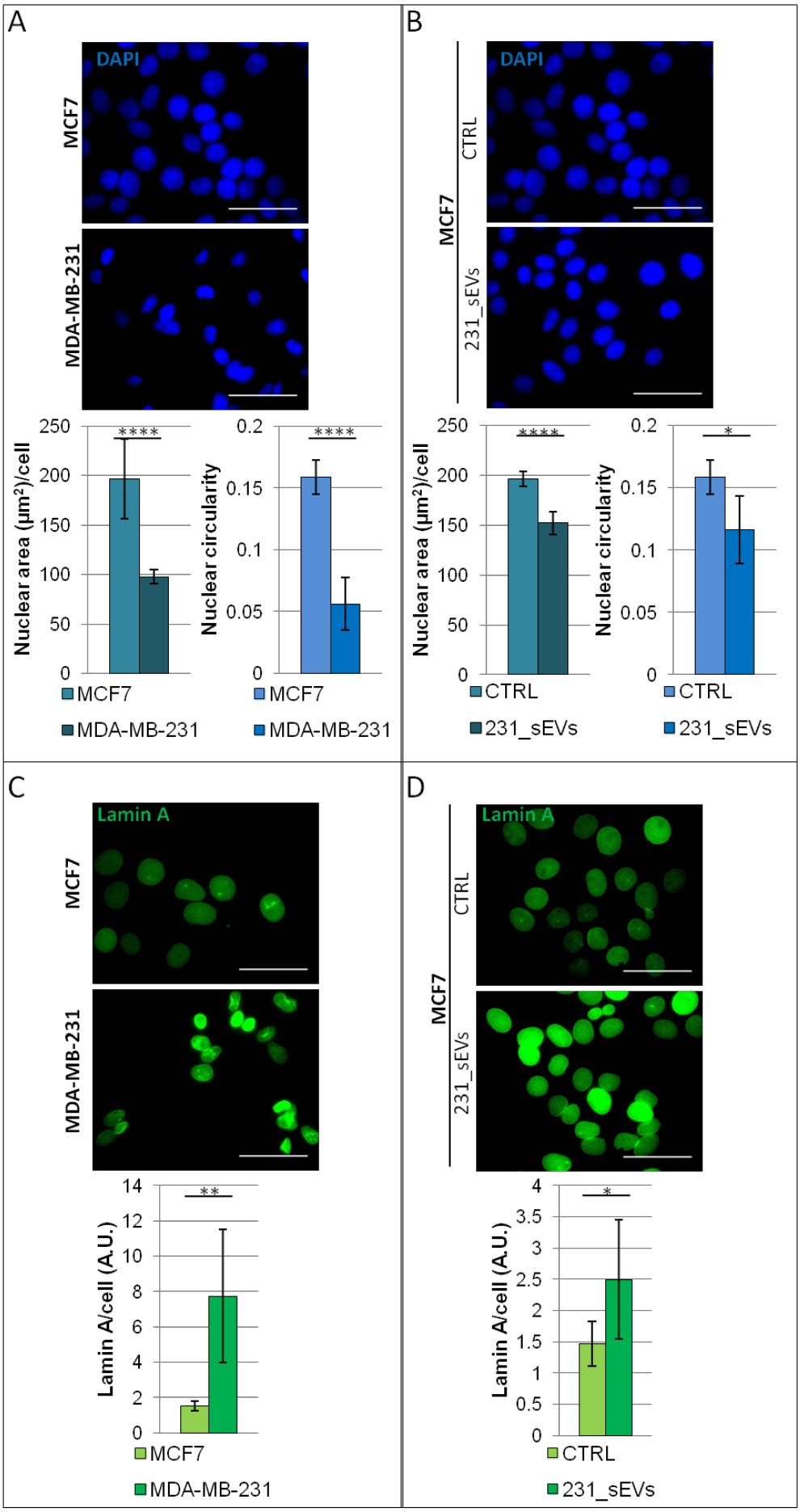
A
DAPI
MCF7
MDA-MB-231
Nuclear area (µm²)/cell
250
200
150
100
50
0
****
Nuclear circularity
0.2
0.15
0.1
0.05
0
****
MCF7
MDA-MB-231
B
DAPI
CTRL
MCF7
231_sEVs
Nuclear area (µm²)/cell
****
Nuclear circularity
*
CTRL
231_sEVs
C
Lamin A
MCF7
MDA-MB-231
Lamin A/cell (A.U.)
14
12
10
8
6
4
2
0
**
MCF7
MDA-MB-231
D
Lamin A
CTRL
MCF7
231_sEVs
Lamin A/cell (A.U.)
4
3.5
3
2.5
2
1.5
1
0.5
0
*
CTRL
231_sEVs

Figure 30. Effects of 231_sEVs on nuclear morphology and nuclear protein Lamin A expression of MCF7 cells. (**a-c**) Representative epifluorescence images on top and relative histograms on bottom, showing the nuclear area and circularity and Lamin A expression in MCF7 and MDA-MB-231 cells. (**b-d**) Representative epifluorescence images on top and relative histograms on bottom, showing the nuclear area and circularity and Lamin A expression in MCF7 cells treated with 231_sEVs in relation to their negative control. Data are expressed as mean ± SD. Significance of data differences was established via two-tailed Student's t-test. Scale bar indicates 50 µm.

Preliminary results: Small-EVs derived from MDA-MB-231 increase gene expression of Yap downstream genes in MCF7 cells

The expression level of Yap downstream genes (CTGF, CYR61, and ANKRD1) were investigated through RT-qPCR in cells. In agreement with literature (Shen *et al.*, 2018), Yap is minimally expressed in MCF7 cells, whereas Yap is overexpressed in MDA-MB-231 cells (**Figure 31a**). Transcription of Yap target genes CTGF and ANKRD1 in MCF7 cells was activated by 231_sEV treatment (**Figure 31b**). This result could be associated to the transportation into the nucleus of YAP (key transcription factor of the Hippo signaling pathway), where it activates transcription of the downstream genes, such as CTGF and ANKDR1. No changes in the transcription of CYR61 gene were observed in MCF7 cells after the treatment with 231_sEVs (**Figure 31b**). This RT-qPCR experiment must be repeated and confirmed.

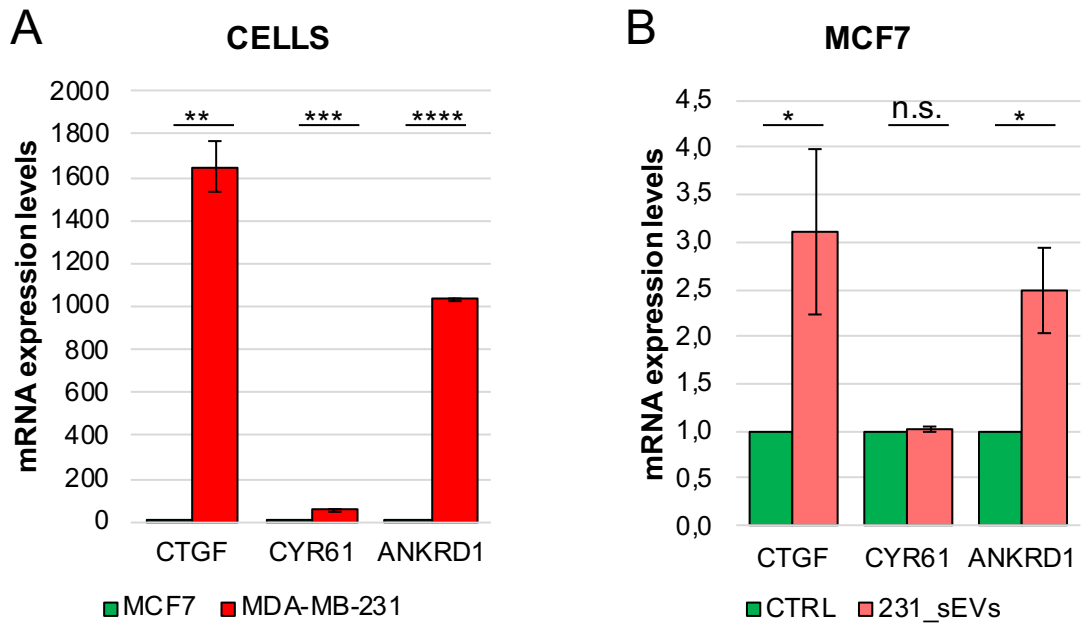

Figure 31. Effects of small-EVs derived from MDA-MB-231 on gene expression of Yap downstream genes of MCF7 cell. a) Expression of Yap downstream genes measured by RT-qPCR in MCF7 and MDA-MB-231 cells; **b**) Yap downstream gene expression in MCF7 cells treated with 231_sEVs in relation to their negative control. Data normalized on histone H3. Data are expressed as mean ± SD. Significance of data differences was established via two-tailed Student's t-test. N.s. indicates not significant.

DISCUSSION

Phenomena of metastasis in cancer are responsible for approximately 90% of cancer-related deaths (Kozłowski, Kozłowska and Kocki, 2015). Triple negative breast cancer (TNBC) is a particularly aggressive, invasive, and with a poor prognosis breast cancer subtype, whose treatment is limited due to the lack of well-defined molecular targets (Yeo, 2015). Despite the constant progress in this field, development of metastases in TNBC remains a highly complex and poorly understood process with a relatively poor outcome (Al-Mahmood *et al.*, 2018). Metastasis is a complex multi-step process: cancer cells need to disseminate from primary tumor site, enter and survive in the circulation, and extravasate in order to create, then, pre-metastatic niche (Shibue and Weinberg, 2017). More deformable and softer cancer cells have greater metastatic ability, since they can pass more easily through the narrow pores of the extracellular matrix, vessels, and create secondary tumor sites (Rudzka *et al.*, 2019). It is known that extracellular vesicles released by triple-negative breast cancer cells can transfer oncogenic proteins, mRNAs, and miRNAs to target cells promoting cell proliferation, tumor growth, cancer cell invasion, and metastasis (Green *et al.*, 2015). TNBC-derived EVs have gained increasing attention as excellent cancer biomarkers and therapeutic targets (Goh *et al.*, 2020). As EVs circulating in body fluids are likely to have been derived from various tissues throughout the body, analysis of cell specific EVs can gives information on early diagnosis, progression, and therapy monitoring of the disease (Boukouris and Mathivanan, 2015). Moreover, the release of EVs in extracellular space provides the opportunity to detect vesicles in a non-invasive manner in body fluids (Boukouris and Mathivanan, 2015). In light of that, it is important to obtain as much information as possible on how EVs can regulate metastatic processes. Previous studies suggested that small-EVs could directly modify biological processes related to cellular adhesion, migration and motility and consequently focal adhesions, cytoskeleton, and biomechanics. In fact, breast cancer-derived extracellular vesicles, accurately reflecting the donor cell, contain proteins that have key roles in regulation of cellular adhesion and cytoskeleton (Rontogianni *et al.*, 2019)(Kruger *et al.*, 2014). One study found that the secretion of small-extracellular vesicles is required for directionally persistent and efficient in vivo movement of cancer cells (Sung *et al.*, 2015). The integrin ITGB3, which is required for metastasis of MDA-MB-231 cells, and its interaction and activation of FAK seem to have fundamental roles in extracellular vesicle biogenesis and vesicle uptake in breast cancer (Altei *et al.*, 2020)(Fuentes *et al.*, 2020). Breast cancer-derived extracellular vesicles have been seen to contribute to metastasis by altering tissue mechanics of distant organs in order to support

tumor cell invasion and seeding (Barenholz-Cohen *et al.*, 2020). Moreover, one study discovered that small-EVs secreted by mesenchymal stromal/stem cell-derived adipocytes can promote breast cancer cell growth by regulating Hippo signaling pathway (Wang *et al.*, 2019). Nevertheless, to our knowledge, there is no evidence showing that small-EVs can directly modulate biomechanics of target cells. Therefore, the purpose of this project is precisely to investigate this mechanism.

Small Extracellular Vesicle isolation

First of all, different cell culture conditions were tested and the final protocol for small-EV isolation was optimized. Initially, two method were used in order to deplete FBS-derived EVs: Ultracentrifugated EV-depleted FBS (UC-dFBS) and Ultrafiltrated EV-depleted FBS (UF-dFBS). The most widely used supplement for cell culture is the serum (Fetal Bovine Serum, FBS), which is essential for cell growth, metabolism, and proliferation. FBS contains its own extracellular vesicles, which are morphologically, and largely also content-wise, similar to the EVs of cultured cells and, therefore, can be co-isolated with cellular EVs (Kornilov *et al.*, 2018). Also other elements, including albumin, are present in the FBS and, therefore, if co-isolated they could alter EV characterization and downstream functional experiments (Thery *et al.*, 2018). Currently, there are no standardized protocols for eliminating contaminants (i.e. EVs and albumin) from FBS. Ultracentrifugation (UC) at 100,000–200,000 xg for ~ 18 hours is the most widely used method for this purpose (Kornilov *et al.*, 2018)(Thery *et al.*, 2018). Both methods used for FBS-derived EV depletion, by still having contaminants proved unsuitable for the purpose of the study: perform functional experiments in target cells. Therefore, we decided to set aside both UC and UF-dFBS preparation for 231_sEVs isolation and a new protocol was fined tune: MDA-MB-231 cells were left to grow in normal medium and then, after several washes, for 24 hours in serum-free medium (DMEM Ø). These results underline the importance of choose the right EV depletion protocol from FBS depending on the final goal and, moreover, stress the complementarity of techniques used for EV characterization.

Small-EVs derived from the breast cancer cell line MDA-MB-231 have been isolated via ultracentrifuge from cell supernatant. Several techniques have been described in literature to isolate small-EVs from cell culture supernatant. Nevertheless, vesicle research is plagued by the lack of standardized isolation strategy, due to their heterogeneity in size, origin and content. To this end, a variety of small-EV isolation protocols were considered and have been taken into account as regards their efficiency, yield and purity of isolated vesicles. Ultracentrifugation

remains the most commonly used isolation method (81%) (Royo *et al.*, 2020)(Gardiner *et al.*, 2016). The two commonly used techniques for isolation of small-EVs are the ultracentrifugation (UC) and size-exclusion chromatography (SEC) (Royo *et al.*, 2020)(Gardiner *et al.*, 2016). Takov et al. demonstrated that small-EVs isolated through SEC had higher particle number, protein content, particle/protein ratios and EV marker signal than small-EVs obtained via UC. However, small-EVs isolated with SEC also contained greater amounts of contaminants (such as APOB+ lipoproteins and large quantities of non-EV protein) (Takov, Yellon and Davidson, 2019). Moreover, the ultracentrifuge-based method of isolation is cheap, user-friendly and have a good reproducibility. Therefore, we have opted to use this method for small-EV isolation.

Small Extracellular Vesicle characterization

The isolated small-EVs (231_sEVs) were characterized by using a multi-technique approach, in order to identify the typical shape, dimension, and biomolecular properties of vesicles. Due to their intrinsic heterogeneity in origin, dimensions, and contents, and for the absence of suitable techniques for this purpose, vesicle characterization represents a critical step in vesicle studies. In fact, in this thesis we demonstrated and underlined the complementarity and the importance of using multiple techniques (AFM, SEM, NTA) to get, in particular, an estimation of the vesicle size. SEM images give only dimensions of small-EVs extracted from *XY*-plane, with a high resolution of few nanometers. SEM images do not give reliable quantitative information about vesicle height; the main reason is that in single SEM images the exact correlation between image brightness and surface height is not well known and some impressions could also be misleading (Burnstock and Jones, 2000). Moreover, SEM analyses must be carried out in dry, which could squeeze vesicles and overestimate diameters (Crouzier *et al.*, 2019). Conversely, AFM images allow to perform analyses in physiological conditions (liquid) and obtain height information. Nevertheless, AFM images are always affected by artifacts arising from tip convolution effects (Shen *et al.*, 2017), resulting in a decrease in the lateral resolution of this technique, especially if compared with SEM technique. This effect would lead to an overestimation of vesicle diameter, if the width at the base of small-EVs was considered. Therefore, this problem has been partially overcome by setting a threshold that corresponds to about half the height of most small-EVs (10 nm) and that allows to measure with a good approximation the FWHM of small-EVs. SEM and AFM technique for the analysis of vesicles can cause a shrinkage and an artificial cupshaped morphology of small-EVs due to dehydration (SEM) or to electrostatic interactions (positive charges of Poly-Lysine both in SEM and AFM) used to immobilize them on the

surface. Moreover, these techniques can not estimate the EV concentration and, capturing narrow EV sections of the sample, might fail to reflect the nature of very heterogeneous EV fractions. Instead, NTA is commonly used to determine concentration and diameter of small-EVs on a single particle-level by following the scattering (Bachurski *et al.*, 2019). Moreover, sample acquisition is performed in a liquid phase, which ensures no modifications to small-EV dimensions. Unfortunately, this technique has also some limitations. One of them is that, as other methods based on the Brownian motion principle, the masking of smaller particles by larger ones can obscure smaller particles, making them undetectable (Gardiner *et al.*, 2013). Moreover, NTA is based on the light scattering intensity and, for specific composition properties of EVs, it can not detect vesicles smaller than 60-70 nm (Bachurski *et al.*, 2019), which instead are measured through AFM and SEM techniques. As of matter of fact, NTA results of 231_sEVs did not showed smallest particles (< 75nm), which instead have been detected by SEM and AFM. These results highlight the complementarity of these techniques for size vesicle characterization.

Small Extracellular Vesicle uptake in target cells

A protein quantification assay was used to obtain the estimation of the quantity of Small-EVs to perform functional experiments. The determination of protein amount is one of the most straightforward and fastest ways to obtain an estimation of the quantity of extracellular vesicles. Total protein content can easily be assessed using the Bradford assay, a standard colorimetric protein assay (Hartjes *et al.*, 2019). Although in this analysis protein contaminants (i.e. protein complexes and lipoproteins) could compromise the accuracy of the measurement, using the same protocol for the same isolation condition can give information about the quantity of vesicles isolated for downstream applications.

The activity and different vesicle conditions (concentrations and time incubations) of 231_sEVs were verified and tested in MCF7 cells through proliferation assay. Methods used to determine cell proliferation may monitor the number of cells over time, the number of cellular divisions, metabolic activity, or DNA synthesis. For the type of biological studies, it is important to choose the optimal assay, considering the specific questions that are asked (Adan, Kiraz and Baran, 2016). Cell proliferation assay based on Trypan blue dye, by providing direct information on the cell number present in solution, it is the most frequently method used in vesicle studies to test the cell proliferation.

Functional experiments in target cells

Cell stiffness changes

Cellular biomechanics is often related with metastatic spreading and, therefore, with cancer malignancy. It is known that stiffness (which can be parameterized as Young's modulus, E) of single cancer cells is lower when compared to normal ones for various cancer (Lekka, 2016). Indeed, it should be easier for soft, deformable cells to migrate through tight pores or intertwined matrix fibres and, thus, lead to metastatic processes. Therefore, we tried to understand if also small-EVs could affect in some way cell stiffness properties of target cells.

AFM force spectroscopy results demonstrated that MDA-MB-231-derived small-EVs can directly modulate cell stiffness of the MCF7 target cells, by making them softer (like donor cells), thus, more deformable and with a greater metastatic potential. Therefore, our hypothesis was confirmed: donor cells by using small-EVs can transfer molecular information to target cells that gives them a biomechanical phenotype similar to that of donor cells.

Furthermore, AFM force spectroscopy data confirmed those of cell proliferation: concentration at which the small-EVs isolated are functional is 0.2 µg/µl and there are more differences with the control after an incubation time of 48 hours. In light of these results, subsequent functional experiments were carried out by using the 231_sEVs condition that appears to have most effects on MCF7 cells: 0.2 µg/µl for 48 hours.

The function of Extracellular Vesicles as stiffness modulator of target cells can be extended to small extracellular vesicles derived from other cell lines as well. As a matter of fact, we investigated the activity of EVs in regulation of biomechanical properties of target cells also in other experimental models.

Umbilical cord mesenchymal stromal cell-derived EVs (MSC_EVs) are known to significantly enhance proliferation, migration, and invasion of the MDA-MB-231 and MCF7 human breast cancer cells as target cells (Zhou *et al.*, 2019). Our preliminary AFM force spectroscopy results demonstrated that MSC_EVs can directly modulate cell stiffness of the MCF10A healthy breast cells and MCF7 and MDA-MB-231 as target cells, by making them softer, thus, more deformable and with a greater invasive potential.

Furthermore, small extracellular vesicles derived from Glioma-Associated Stem Cells (GASC) are known to significantly increase growth kinetic, migration ability, and anchorage-independent growth of glioblastoma cells (Bourkoula *et al.*, 2014). The increase in cell stiffness observed via AFM force spectroscopy results in U87 cells after vesicle addition could be related to the nature of the GASC-derived small-EVs, which can "transfer" part of the biomechanical

behaviour of their more rigid originating cell. This data and the previous one is in agreement with our hypothesis that EVs do not decrease stiffness of target cells in a non-specific way, but they modify cell stiffness bringing with them the same biomechanical information of the donor cell. Moreover, AFM force spectroscopy results were used to investigate routes of GASC-derived small-EV internalization. It is shown that cells take up small-EVs by a variety of endocytic pathways, such as clathrin dependent endocytosis, caveolin-mediated endocytosis, macropinocytosis, phagocytosis, lipid-rafts mediated internalization, as well as by fusion with the membrane of recipient cell and specific ligand- receptor interactions (Mulcahy, Pink and Carter, 2014). Moreover, it seems that EVs can use more than one route to efficiently enter cells and that the mechanism of uptake may depend on the molecular composition of both vesicles and target cells. Our results suggested that none of the drugs tested was able to completely block the vesicle uptake and activity, but the preferential pathway for the uptake of GASC-derived small-EVs into U87 cells is the micropinocytosis. Such preliminary findings need to be confirmed with further experiments, but represent another confirmation of the strong effects of small-EV activity on the biomechanical response of recipient cells.

Cytoskeleton rearrangements

After that, we wondered if TNBC-derived small-EVs, in addition to biomechanical phenotype, could modulate also cytoskeleton and nucleus, important elements in biomechanical modulation, and so in metastasis (Alibert, Goud and Manneville, 2017)(Fritsch *et al.*, 2010)(Senigagliesi *et al.*, 2019)(Chiotaki, Polioudaki and Theodoropoulos, 2014)(Fischer, Hayn and Mierke, 2020). It has been known for a long time that changes in cellular cytoskeleton (Alibert, Goud and Manneville, 2017)(Fritsch *et al.*, 2010) and nuclear morphology and stiffness (Senigagliesi *et al.*, 2019)(Chiotaki, Polioudaki and Theodoropoulos, 2014)(Fischer, Hayn and Mierke, 2020) are associated to malignant transformation, as well as to important role in cellular biomechanical modulation.

Epifluorescence results showed that MDA-MB-231-derived small-EVs are capable of transferring molecular information to MCF7 cells that makes its cytoskeleton (α-tubulin), nuclear morphology and nuclear Lamin A protein similar to donor cells (MDA-MB-231). Although actin filaments are softer than microtubules, high concentrations of actin stress fibres promote the assembly of highly organized rigid structures (Fletcher and Mullins, 2010) that increase and are proportional to cell stiffness (Rajagopal et al., 2018). Unfortunately, no significant differences were observed in actin structures, neither comparing MCF7 to MDA-MB-231 cells, nor MCF7 cells treated or not with 231_sEVs. This lack of actin differences

between the two cell lines agrees with the study of Calzado-Martín. Results of this article demonstrated that actin stress fibres (present at apical regions) provide a dominant contribution to stiffness only in healthy cells, while cell stiffness of MCF7 and MDA-MB-231 cells appears not predominantly determined by these structures (mainly in the basal regions) (Calzado-Martín *et al.*, 2016). Moreover, in contrast to other immunofluorescence results, TIRF results demonstrated that 231_sEVs do not lead the MCF7 cells to have the typical low adhesion of the MDA-MB-231 as donor cells, but they promote an increase in cell adhesion and FA activity in MCF7 cells. Peschetola et al. and Tavares et al. showed that the increase in invasiveness is related with large dynamic adhesion sites and with an increased activation of phospho-FAK (Peschetola *et al.*, 2013)(Tavares *et al.*, 2017). Immunofluorescence technique is subject to variability in sensitivity, specificity, and reproducibility and, therefore, it is considered only a semi-quantitative method. Therefore, Western blot analyses should be performed in order to verify changes observed via immunofluorescence analyses.

Yap activity

Biomechanical and cytoskeleton changes were observed in MCF7 cells upon the activity of small-EVs derived from MDA-MB-231. As mentioned before, biomechanics and cytoskeleton can be modulated by the Hippo component YAP (Nardone *et al.*, 2017)(Shen *et al.*, 2018). Therefore, for the purpose of determining whether Yap could be associated with these biomechanical phenotype changes, we subsequently investigated the expression level of Yap downstream genes (CTGF, CYR61, and ANKRD1) in cells. Preliminary real time-PCR results suggested that the addition of TNBC-derived small-EVs can directly increase the expression of Yap downstream genes in non-invasive MCF7 target cells. Studies of Nardone et al. and Shen et al. found out a correlation between the increase in Yap activity and a marked increase in FA formation and promotion of FAK phosphorylation (Nardone *et al.*, 2017)(Shen *et al.*, 2018). Therefore, the opposite trend obtained regarding cell adhesion (Vinculin) and FA activity (pFAK) in MCF7 cells treated with 231_sEVs could be due to the increase in expression level of Yap downstream genes, and probably also of Yap, that could lead to a consequent increase in size, number, and activity of focal adhesions.

CONCLUSIONS AND FUTURE PERSPECTIVES

Thus, the present project is the first to demonstrate that the activity of TNBC-derived small-EVs can directly modify biomechanical phenotype of non-invasive MCF7 target cells, by modulating cellular stiffness, cytoskeleton and nucleus, and increasing the activity of Yap downstream genes. Currently, it remains largely unknown how TNBC-derived small-EVs influence cell biomechanics. We could assume that small-EVs bind FAs, which being subject to changes, then, consequently modulate Yap activity, cytoskeleton, and biomechanics of target cells. Otherwise, TNBC-derived small-EVs could directly cause an increase in Yap activity, which then leads to cytokeleton, nuclear, motility, and finally biomechanical rearrangements in MCF7 cells. Alternatively, biomechanical and other related changes observed in MCF7 cells treated with vesicles could be mainly due to chromatin condensation that modulates structural and mechanical properties of the nucleus, LINC complex proteins, cytoskeleton, and finally biomechanics. Anyway, this project added a new function to small extracellular vesicles in the regulation of TNBC: MDA-MB-231-derived small-EVs can transfer biophysical information to target cells, making them phenotypically similar to donor cells. This new function could be extended to small extracellular vesicles derived from other cells as well. Furthermore, this project represents a proof in support of studies of Nardone et al. and Shen et al. that showed a correlation between the increase in Yap activity and a marked increase in FA formation and pFAK promotion (Nardone *et al.*, 2017)(Shen *et al.*, 2018). Equally, these results confirmed the study of Qiao et al., in which Yap activation seems to drive the cell softening in cancer cells (Qiao *et al.*, 2017).

In conclusion, we believe to demonstrate with this work that the analysis of the biomechanical response of target cells upon EV uptake could represent a powerful tool to test the functionality of EVs and that could represent an important resource in view of the application of extracellular vesicles in theranostic field for metastatic TNBCs and for other types of cancer.

SUPPLEMENTARY

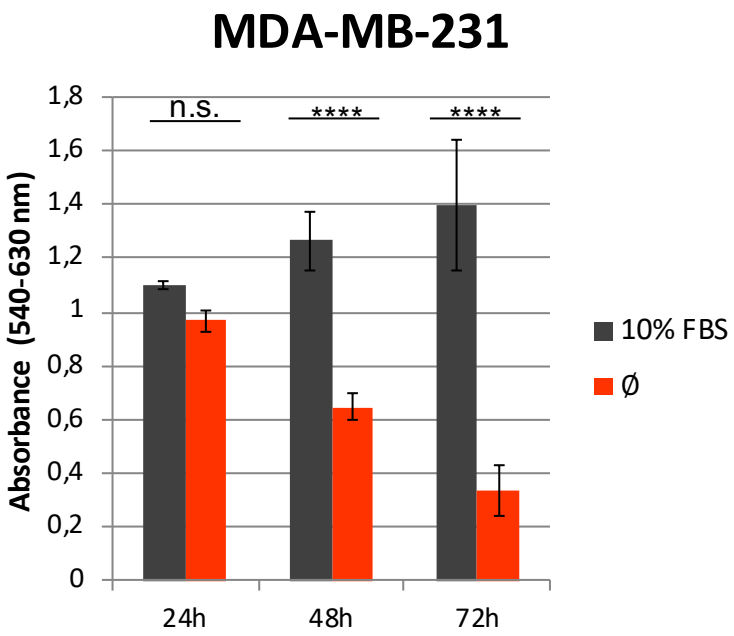

Supplementary figure 1. MTT assay showing MDA-MB-231 cells cultured without FBS for 24, 48 or 72 hours, compared with their control.

BIBLIOGRAPHY

Abidine, Y. *et al.* (2018) 'Mechanosensitivity of Cancer Cells in Contact with Soft Substrates Using AFM', *Biophysical Journal*, 114(5), pp. 1165–1175. doi: 10.1016/j.bpj.2018.01.005.

Adan, A., Kiraz, Y. and Baran, Y. (2016) 'Cell Proliferation and Cytotoxicity Assays', *Current Pharmaceutical Biotechnology*, 17(14), pp. 1213–1221. doi: 10.2174/1389201017666160808160513.

Ahmed, K. A. and Xiang, J. (2011) 'Mechanisms of cellular communication through intercellular protein transfer', *Journal of Cellular and Molecular Medicine*, pp. 1458–1473. doi: 10.1111/j.1582-4934.2010.01008.x.

Al-Mahmood, S. *et al.* (2018) 'Metastatic and triple-negative breast cancer: challenges and treatment options', *Drug Delivery and Translational Research*, pp. 1483–1507. doi: 10.1007/s13346-018-0551-3.

Al-thoubaity, F. K. (2020) 'Molecular classification of breast cancer: A retrospective cohort study', *Annals of Medicine and Surgery*, 49, pp. 44–48. doi: 10.1016/j.amsu.2019.11.021.

Alessandrini, A. and Facci, P. (2005) 'AFM: a versatile tool in biophysics', *Measurement Science and Technology*, 16(6), pp. R65–R92. doi: 10.1088/0957-0233/16/6/R01.

Alibert, C., Goud, B. and Manneville, J. B. (2017) 'Are cancer cells really softer than normal cells?', *Biology of the Cell*, pp. 167–189. doi: 10.1111/boc.201600078.

Allen, T. M. *et al.* (1991) 'Uptake of liposomes by cultured mouse bone marrow macrophages: influence of liposome composition and size', *BBA - Biomembranes*, 1061(1), pp. 56–64. doi: 10.1016/0005-2736(91)90268-D.

Almeria, C. *et al.* (2019) 'Hypoxia Conditioned Mesenchymal Stem Cell-Derived Extracellular Vesicles Induce Increased Vascular Tube Formation in vitro', *Frontiers in Bioengineering and Biotechnology*, 7. doi: 10.3389/fbioe.2019.00292.

Altei, W. F. *et al.* (2020) 'Inhibition of αvβ3 integrin impairs adhesion and uptake of tumor-derived small extracellular vesicles', *Cell Communication and Signaling*, 18(1). doi: 10.1186/s12964-020-00630-w.

Antonyak, M. A., Wilson, K. F. and Cerione, R. A. (2012) 'R(h)oads to microvesicles', *Small GTPases*. doi: 10.4161/sgtp.20755.

Aplin, A. E. *et al.* (1998) 'Signal transduction and signal modulation by cell adhesion receptors: The role of integrins, cadherins, immunoglobulin-cell adhesion molecules, and selectins', *Pharmacological Reviews*, pp. 197–263.

Atkins, A. G. and Tabor, D. (1965) 'Plastic indentation in metals with cones', *Journal of the Mechanics and Physics of Solids*, 13(3), pp. 149–164. doi: 10.1016/0022-5096(65)90018-9.

Bachurski, D. *et al.* (2019) 'Extracellular vesicle measurements with nanoparticle tracking analysis–An accuracy and repeatability comparison between NanoSight NS300 and ZetaView', *Journal of Extracellular Vesicles*, 8(1). doi: 10.1080/20013078.2019.1596016.

Banuett, F. (2010) 'A method to visualize the actin and microtubule cytoskeleton by indirect immunofluorescence.', *Methods in molecular biology (Clifton, N.J.)*, 638, pp. 225–233. doi: 10.1007/978-1-60761-611-5_17.

Barenholz-Cohen, T. *et al.* (2020) 'Lung mechanics modifications facilitating metastasis are mediated in part by breast cancer-derived extracellular vesicles', *International Journal of Cancer*, 147(10), pp. 2924–2933. doi: 10.1002/ijc.33229.

Bebelman, M. P. *et al.* (2018) 'Biogenesis and function of extracellular vesicles in cancer', *Pharmacology and Therapeutics*, pp. 1–11. doi: 10.1016/j.pharmthera.2018.02.013.

Bianchini, G. *et al.* (2016) 'Triple-negative breast cancer: Challenges and opportunities of a heterogeneous disease', *Nature Reviews Clinical Oncology*, pp. 674–690. doi: 10.1038/nrclinonc.2016.66.

Bjørge, I. M. *et al.* (2018) 'Extracellular vesicles, exosomes and shedding vesicles in regenerative medicine-a new paradigm for tissue repair', *Biomaterials Science*, pp. 60–78. doi: 10.1039/c7bm00479f.

Bodega, G. *et al.* (2019) 'Microvesicles: ROS scavengers and ROS producers', *Journal of Extracellular Vesicles*. doi: 10.1080/20013078.2019.1626654.

Boukouris, S. and Mathivanan, S. (2015) 'Exosomes in bodily fluids are a highly stable resource of disease biomarkers', *Proteomics - Clinical Applications*, pp. 358–367. doi: 10.1002/prca.201400114.

Bourkoula, E. *et al.* (2014) 'Glioma-associated stem cells: A novel class of tumor-supporting cells able to predict prognosis of human low-grade gliomas', *Stem Cells*, 32(5), pp. 1239–1253. doi: 10.1002/stem.1605.

Bouzid, T. *et al.* (2019) 'The LINC complex, mechanotransduction, and mesenchymal stem cell function and fate', *Journal of Biological Engineering*. doi: 10.1186/s13036-019-0197-9.

Brady, P. N. and Macnaughtan, M. A. (2015) 'Evaluation of colorimetric assays for analyzing reductively methylated proteins: Biases and mechanistic insights', *Analytical Biochemistry*. doi: 10.1016/j.ab.2015.08.027.

Brennan, K. *et al.* (2020) 'A comparison of methods for the isolation and separation of extracellular vesicles from protein and lipid particles in human serum', *Scientific Reports*, 10(1). doi: 10.1038/s41598-020-57497-7.

Burnouf, T., Agrahari, Vibhuti and Agrahari, Vivek (2019) 'Extracellular vesicles as nanomedicine: Hopes and hurdles in clinical translation', *International Journal of Nanomedicine*, 14, pp. 8847–8859. doi: 10.2147/IJN.S225453.

Burnstock, A. and Jones, C. (2000) 'Scanning electron microscopy techniques for imaging materials from paintings.', in *Radiation in Art and Archeometry*, pp. 202–231. doi: 10.1016/b978-044450487-6/50056-0.

Burridge, K. and Guilluy, C. (2016) 'Focal adhesions, stress fibers and mechanical tension', *Experimental Cell Research*, pp. 14–20. doi: 10.1016/j.yexcr.2015.10.029.

Cailleau, R., Olivé, M. and Cruciger, Q. V. J. (1978) 'Long-term human breast carcinoma cell lines of metastatic origin: Preliminary characterization', *In Vitro*, 14(11), pp. 911–915. doi: 10.1007/BF02616120.

Calzado-Martín, A. *et al.* (2016) 'Effect of Actin Organization on the Stiffness of Living Breast Cancer Cells Revealed by Peak-Force Modulation Atomic Force Microscopy', *ACS Nano*, 10(3), pp. 3365–3374. doi: 10.1021/acsnano.5b07162.

Capo-Chichi, C. D. *et al.* (2011) 'Loss of A-type lamin expression compromises nuclear envelope integrity in breast cancer', *Chinese Journal of Cancer*, 30(6), pp. 415–425. doi: 10.5732/cjc.010.10566.

Caponnetto, F. *et al.* (2017) 'Size-dependent cellular uptake of exosomes', *Nanomedicine: Nanotechnology, Biology and Medicine*, 13(3), pp. 1011–1020. doi: https://doi.org/10.1016/j.nano.2016.12.009.

Carvalho, F. A. and Santos, N. C. (2012) 'Atomic force microscopy-based force spectroscopy - Biological and biomedical applications', *IUBMB Life*, pp. 465–472. doi: 10.1002/iub.1037.

Chen, J. (2014) 'Nanobiomechanics of living cells: A review', *Interface Focus*. doi: 10.1098/rsfs.2013.0055.

Chen, J. and Lu, G. (2012) 'Finite element modelling of nanoindentation based methods for mechanical properties of cells', *Journal of Biomechanics*, 45(16), pp. 2810–2816. doi: 10.1016/j.jbiomech.2012.08.037.

Chernomordik, L. V. and Kozlov, M. M. (2003) 'Protein-Lipid Interplay in Fusion and Fission of Biological Membranes', *Annual Review of Biochemistry*, 72(1), pp. 175–207. doi: 10.1146/annurev.biochem.72.121801.161504.

Chiotaki, R., Polioudaki, H. and Theodoropoulos, P. A. (2014) 'Differential nuclear shape dynamics of invasive andnon-invasive breast cancer cells are associated with actin cytoskeleton organization and stability', *Biochemistry and Cell Biology*, 92(4), pp. 287–295. doi: 10.1139/bcb-2013-0120.

Choi, D. S. *et al.* (2013) 'Proteomics, transcriptomics and lipidomics of exosomes and ectosomes', *Proteomics*, pp. 1554–1571. doi: 10.1002/pmic.201200329.

Ciccocioppo, F. *et al.* (2019) 'The Link Among Neurological Diseases: Extracellular Vesicles as a Possible Brain Injury Footprint', *Neuro-Signals*, 27(1), pp. 25–39. doi: 10.33594/000000116.

Crouzier, L. *et al.* (2019) 'Development of a new hybrid approach combining AFM and SEM for the nanoparticle dimensional metrology', *Beilstein Journal of Nanotechnology*, 10, pp. 1523–1536. doi: 10.3762/bjnano.10.150.

Dasgupta, I. and McCollum, D. (2019) 'Control of cellular responses to mechanical cues through YAP/TAZ regulation', *Journal of Biological Chemistry*, pp. 17693–17706. doi: 10.1074/jbc.REV119.007963.

Demichelis, A. *et al.* (2015) 'Toward the realization of reproducible AFM measurements of elastic modulus in biological samples', *Journal of Biomechanics*. doi: 10.1016/j.jbiomech.2015.01.023.

Deng, X. *et al.* (2018) 'Application of atomic force microscopy in cancer research', *Journal of Nanobiotechnology*, p. V. doi: 10.1186/s12951-018-0428-0.

Van Deun, J. *et al.* (2014) 'The impact of disparate isolation methods for extracellular vesicles on downstream RNA profiling', *Journal of Extracellular Vesicles*, 3(1). doi: 10.3402/jev.v3.24858.

Dobrokhotov, O. *et al.* (2018) 'Mechanoregulation and pathology of YAP/TAZ via Hippo and non-Hippo mechanisms', *Clinical and Translational Medicine*, 7(1). doi: 10.1186/s40169-018-0202-9.

Etienne-Manneville, S. (2004) 'Actin and microtubules in cell motility: Which one is in control?', *Traffic*, pp. 470–477. doi: 10.1111/j.1600-0854.2004.00196.x.

Fabbri, M. *et al.* (2012) 'MicroRNAs bind to Toll-like receptors to induce prometastatic inflammatory response', *Proceedings of the National Academy of Sciences of the United States of America*, 109(31). doi: 10.1073/pnas.1209414109.

Fais, S. *et al.* (2016) 'Evidence-Based Clinical Use of Nanoscale Extracellular Vesicles in Nanomedicine', *ACS Nano*, pp. 3886–3899. doi: 10.1021/acsnano.5b08015.

Fares, J. *et al.* (2020) 'Molecular principles of metastasis: a hallmark of cancer revisited',

Signal Transduction and Targeted Therapy. doi: 10.1038/s41392-020-0134-x.

Feng, D. *et al.* (2010) 'Cellular internalization of exosomes occurs through phagocytosis', *Traffic*, 11(5), pp. 675–687. doi: 10.1111/j.1600-0854.2010.01041.x.

Fischer, T., Hayn, A. and Mierke, C. T. (2020) 'Effect of Nuclear Stiffness on Cell Mechanics and Migration of Human Breast Cancer Cells', *Frontiers in Cell and Developmental Biology*, 8. doi: 10.3389/fcell.2020.00393.

Fletcher, D. A. and Mullins, R. D. (2010) 'Cell mechanics and the cytoskeleton', *Nature*, pp. 485–492. doi: 10.1038/nature08908.

Fortier, H. *et al.* (2016) 'AFM force indentation analysis on leukemia cells', *Analytical Methods*, 8(22), pp. 4421–4431. doi: 10.1039/c6ay00131a.

Fritsch, A. *et al.* (2010) 'Are biomechanical changes necessary for tumour progression?', *Nature Physics*, pp. 730–732. doi: 10.1038/nphys1800.

Fuentes, P. *et al.* (2020) 'ITGB3-mediated uptake of small extracellular vesicles facilitates intercellular communication in breast cancer cells', *Nature Communications*, 11(1). doi: 10.1038/s41467-020-18081-9.

Gad, A. K. B. *et al.* (2012) 'Rho GTPases link cellular contractile force to the density and distribution of nanoscale adhesions', *The FASEB Journal*, 26(6), pp. 2374–2382. doi: 10.1096/fj.11-195800.

Galindo-Hernandez, O. *et al.* (2013) 'Elevated concentration of microvesicles isolated from peripheral blood in breast cancer patients', *Archives of Medical Research*, 44(3), pp. 208–214. doi: 10.1016/j.arcmed.2013.03.002.

Gardiner, C. *et al.* (2013) 'Extracellular vesicle sizing and enumeration by nanoparticle tracking analysis', *Journal of Extracellular Vesicles*, 2(1). doi: 10.3402/jev.v2i0.19671.

Gardiner, C. *et al.* (2016) 'Techniques used for the isolation and characterization of extracellular vesicles: Results of a worldwide survey', *Journal of Extracellular Vesicles*, 5(1). doi: 10.3402/jev.v5.32945.

Gest, C. *et al.* (2013) 'Rac3 induces a molecular pathway triggering breast cancer cell aggressiveness: Differences in MDA-MB-231 and MCF-7 breast cancer cell lines', *BMC Cancer*, 13. doi: 10.1186/1471-2407-13-63.

Goetz, J. G. *et al.* (2011) 'Biomechanical remodeling of the microenvironment by stromal caveolin-1 favors tumor invasion and metastasis', *Cell*, 146(1), pp. 148–163. doi: S0092-8674(11)00645-3 [pii]\r10.1016/j.cell.2011.05.040.

Goh, C. Y. *et al.* (2020) 'Exosomes in triple negative breast cancer: Garbage disposals or Trojan horses?', *Cancer Letters*, pp. 90–97. doi: 10.1016/j.canlet.2019.12.046.

Gorjánácz, M. (2014) 'Nuclear assembly as a target for anti-cancer therapies.', *Nucleus (Austin, Tex.)*, 5(1), pp. 47–55. doi: 10.4161/nucl.27928.

Granger, E. *et al.* (2014) 'The role of the cytoskeleton and molecular motors in endosomal dynamics', *Seminars in Cell and Developmental Biology*, pp. 20–29. doi: 10.1016/j.semcdb.2014.04.011.

Green, T. M. *et al.* (2015) 'Breast cancer-derived extracellular vesicles: Characterization and contribution to the metastatic phenotype', *BioMed Research International*. doi: 10.1155/2015/634865.

Gu, Y. *et al.* (2020) 'Prognostic Value of Site-Specific Metastases and Surgery in De Novo

Stage IV Triple-Negative Breast Cancer: A Population-Based Analysis', *Medical science monitor : international medical journal of experimental and clinical research*, 26, p. e920432. doi: 10.12659/MSM.920432.

Guz, N. *et al.* (2014) 'If Cell Mechanics Can Be Described by Elastic Modulus: Study of Different Models and Probes Used in Indentation Experiments', *Biophysical Journal*, 107(3), pp. 564–575. doi: 10.1016/j.bpj.2014.06.033.

H., F. *et al.* (2011) 'Remarks in Successful Cellular Investigations for Fighting Breast Cancer Using Novel Synthetic Compounds', in *Breast Cancer - Focusing Tumor Microenvironment, Stem cells and Metastasis*. doi: 10.5772/23005.

Ha, D., Yang, N. and Nadithe, V. (2016) 'Exosomes as therapeutic drug carriers and delivery vehicles across biological membranes: current perspectives and future challenges', *Acta Pharmaceutica Sinica B*, pp. 287–296. doi: 10.1016/j.apsb.2016.02.001.

Haffty, B. G. *et al.* (2006) 'Locoregional relapse and distant metastasis in conservatively managed triple negative early-stage breast cancer', *Journal of Clinical Oncology*, 24(36), pp. 5652–5657. doi: 10.1200/JCO.2006.06.5664.

Harris, D. A. *et al.* (2015) 'Exosomes released from breast cancer carcinomas stimulate cell movement', *PLoS ONE*, 10(3). doi: 10.1371/journal.pone.0117495.

Hartjes, T. A. *et al.* (2019) 'Extracellular vesicle quantification and characterization: Common methods and emerging approaches', *Bioengineering*. doi: 10.3390/bioengineering6010007.

Haudenschild, D. R. *et al.* (2014) 'High abundant protein removal from rodent blood for biomarker discovery', *Biochemical and Biophysical Research Communications*, 455(1–2), pp. 84–89. doi: 10.1016/j.bbrc.2014.09.137.

Helmke, A. and Vietinghoff, S. von (2016) 'Extracellular vesicles as mediators of vascular inflammation in kidney disease', *World Journal of Nephrology*, 5(2), p. 125. doi: 10.5527/wjn.v5.i2.125.

Hemler, M. E. (2005) 'Tetraspanin functions and associated microdomains', *Nature Reviews Molecular Cell Biology*, pp. 801–811. doi: 10.1038/nrm1736.

Hessvik, N. P. and Llorente, A. (2018) 'Current knowledge on exosome biogenesis and release', *Cellular and Molecular Life Sciences*, pp. 193–208. doi: 10.1007/s00018-017-2595-9.

Holliday, D. L. and Speirs, V. (2011) 'Choosing the right cell line for breast cancer research.', *Breast cancer research : BCR*, 13, p. 215. doi: 10.1186/bcr2889.

Hortobagyi, G. N. *et al.* (2005) 'The global breast cancer burden: Variations in epidemiology and survival', *Clinical Breast Cancer*, pp. 391–401. doi: 10.3816/CBC.2005.n.043.

Hoshino, A. *et al.* (2015) 'Tumour exosome integrins determine organotropic metastasis', *Nature*, 527(7578), pp. 329–335. doi: 10.1038/nature15756.

Irion, U. and St Johnston, D. (2007) 'bicoid RNA localization requires specific binding of an endosomal sorting complex', *Nature*, 445(7127), pp. 554–558. doi: 10.1038/nature05503.

Islam, T. and Resat, H. (2017) 'Quantitative investigation of MDA-MB-231 breast cancer cell motility: Dependence on epidermal growth factor concentration and its gradient', *Molecular BioSystems*, 13(10), pp. 2069–2082. doi: 10.1039/c7mb00390k.

Jackson, C. E. *et al.* (2017) 'Effects of Inhibiting VPS4 Support a General Role for ESCRTs in Extracellular Vesicle Biogenesis', *Biophysical Journal*, 113(6), pp. 1342–1352. doi: 10.1016/j.bpj.2017.05.032.

Jahn, R. and Südhof, T. C. (1999) 'Membrane Fusion and Exocytosis', *Annual Review of Biochemistry*, 68(1), pp. 863–911. doi: 10.1146/annurev.biochem.68.1.863.

Jeppesen, D. K. *et al.* (2019) 'Reassessment of Exosome Composition', *Cell*, 177(2), pp. 428-445.e18. doi: 10.1016/j.cell.2019.02.029.

Jhan, J. R. and Andrechek, E. R. (2017) 'Triple-negative breast cancer and the potential for targeted therapy', *Pharmacogenomics*, 18(17), pp. 1595–1609. doi: 10.2217/pgs-2017-0117.

Kakarla, R. *et al.* (2020) 'Apoptotic cell-derived exosomes: messages from dying cells', *Experimental and Molecular Medicine*. doi: 10.1038/s12276-019-0362-8.

Kalluri, R. and LeBleu, V. S. (2020) 'The biology, function, and biomedical applications of exosomes', *Science*. doi: 10.1126/science.aau6977.

Kalra, H. *et al.* (2013) 'Comparative proteomics evaluation of plasma exosome isolation techniques and assessment of the stability of exosomes in normal human blood plasma', *PROTEOMICS*, 13(22), pp. 3354–3364. doi: https://doi.org/10.1002/pmic.201300282.

Kawahara, H. and Hanayama, R. (2018) 'The role of exosomes/extracellular vesicles in neural signal transduction', *Biological and Pharmaceutical Bulletin*, pp. 1119–1125. doi: 10.1248/bpb.b18-00167.

Khatun, Z. *et al.* (2016) 'Elucidating diversity of exosomes: biophysical and molecular characterization methods', *Nanomedicine*, 11(17), pp. 2359–2377. doi: 10.2217/nnm-2016-0192.

Kim, C. W. *et al.* (2002) 'Extracellular membrane vesicles from tumor cells promote angiogenesis via sphingomyelin', *Cancer Research*, 62(21), pp. 6312–6317.

Kim, D. K. *et al.* (2013) 'EVpedia: An integrated database of high-throughput data for systemic analyses of extracellular vesicles', *Journal of Extracellular Vesicles*, 2(1). doi: 10.3402/jev.v2i0.20384.

Kogure, A., Kosaka, N. and Ochiya, T. (2019) 'Cross-talk between cancer cells and their neighbors via miRNA in extracellular vesicles: An emerging player in cancer metastasis', *Journal of Biomedical Science*. doi: 10.1186/s12929-019-0500-6.

Kondratov, K. A. *et al.* (2017) 'A study of extracellular vesicles isolated from blood plasma conducted by low-voltage scanning electron microscopy', *Cell and Tissue Biology*, 11(3), pp. 181–190. doi: 10.1134/S1990519X17030051.

Konoshenko, M. Y. *et al.* (2018) 'Isolation of Extracellular Vesicles: General Methodologies and Latest Trends', *BioMed research international*, 2018, p. 8545347. doi: 10.1155/2018/8545347.

Kornilov, R. *et al.* (2018) 'Efficient ultrafiltration-based protocol to deplete extracellular vesicles from fetal bovine serum', *Journal of Extracellular Vesicles*, 7(1). doi: 10.1080/20013078.2017.1422674.

Kozłowski, J., Kozłowska, A. and Kocki, J. (2015) 'Breast cancer metastasis - Insight into selected molecular mechanisms of the phenomenon', *Postepy Higieny i Medycyny Doswiadczalnej*, pp. 447–451. doi: 10.5604/17322693.1148710.

Kraning-Rush, C. M., Califano, J. P. and Reinhart-King, C. A. (2012) 'Cellular traction stresses increase with increasing metastatic potential', *PLoS ONE*, 7(2). doi: 10.1371/journal.pone.0032572.

Kruger, S. *et al.* (2014) 'Molecular characterization of exosome-like vesicles from breast cancer cells', *BMC Cancer*, 14(1). doi: 10.1186/1471-2407-14-44.

Kumeda, N. *et al.* (2017) 'Characterization of Membrane Integrity and Morphological Stability of Human Salivary Exosomes', *Biological and Pharmaceutical Bulletin*, 40(8), pp. 1183–1191. doi: 10.1248/bpb.b16-00891.

Lai, R. C. *et al.* (2013) 'Exosomes for drug delivery - A novel application for the mesenchymal stem cell', *Biotechnology Advances*, pp. 543–551. doi: 10.1016/j.biotechadv.2012.08.008.

Lambrechts, A., Van Troys, M. and Ampe, C. (2004) 'The actin cytoskeleton in normal and pathological cell motility', *International Journal of Biochemistry and Cell Biology*, pp. 1890–1909. doi: 10.1016/j.biocel.2004.01.024.

Laulagnier, K. *et al.* (2004) 'Mast cell- and dendritic cell-derived display a specific lipid composition and an unusual membrane organization', *Biochemical Journal*, 380(1), pp. 161–171. doi: 10.1042/BJ20031594.

Leber, M. F. and Efferth, T. (2009) 'Molecular principles of cancer invasion and metastasis (Review)', *International Journal of Oncology*, pp. 881–895. doi: 10.3892/ijo_00000214.

LeClaire, M., Gimzewski, J. and Sharma, S. (2021) 'A review of the biomechanical properties of single extracellular vesicles', *Nano Select*, 2(1), pp. 1–15. doi: https://doi.org/10.1002/nano.202000129.

Lee, K. S. *et al.* (2014) 'Metastatic potential in MDA-MB-231 human breast cancer cells is inhibited by proton beam irradiation via the Akt/nuclear factor-κB signaling pathway', *Molecular Medicine Reports*, 10(2), pp. 1007–1012. doi: 10.3892/mmr.2014.2259.

Lekka, M. (2016) 'Discrimination Between Normal and Cancerous Cells Using AFM', *BioNanoScience*, 6(1), pp. 65–80. doi: 10.1007/s12668-016-0191-3.

Li, J. *et al.* (2019) 'An update on isolation methods for proteomic studies of extracellular vesicles in biofluids', *Molecules*. doi: 10.3390/molecules24193516.

Liu, Q. and Yang, H. (2019) 'Application of atomic force microscopy in food microorganisms', *Trends in Food Science and Technology*, pp. 73–83. doi: 10.1016/j.tifs.2018.05.010.

Liu, Y. L. *et al.* (2019) 'Assessing metastatic potential of breast cancer cells based on EGFR dynamics', *Scientific Reports*, 9(1). doi: 10.1038/s41598-018-37625-0.

Lötvall, J. *et al.* (2014) 'Minimal experimental requirements for definition of extracellular vesicles and their functions: A position statement from the International Society for Extracellular Vesicles', *Journal of Extracellular Vesicles*. doi: 10.3402/jev.v3.26913.

Luo, M. and Guan, J. L. (2010) 'Focal adhesion kinase: A prominent determinant in breast cancer initiation, progression and metastasis', *Cancer Letters*, pp. 127–139. doi: 10.1016/j.canlet.2009.07.005.

Luo, Q. *et al.* (2016) 'Cell stiffness determined by atomic force microscopy and its correlation with cell motility', *Biochimica et Biophysica Acta - General Subjects*, pp. 1953–1960. doi: 10.1016/j.bbagen.2016.06.010.

Maia, J. *et al.* (2018) 'Exosome-based cell-cell communication in the tumor microenvironment', *Frontiers in Cell and Developmental Biology*. doi: 10.3389/fcell.2018.00018.

Margolis, L. and Sadovsky, Y. (2019) 'The biology of extracellular vesicles: The known unknowns', *PLoS Biology*, 17(7). doi: 10.1371/journal.pbio.3000363.

Martin, T. *et al.* (2014) *Cancer Invasion and Metastasis: Molecular and Cellular Perspective*,

Metastatic Cancer: Clinical and Biological Perspectives.

Mathieu, M. *et al.* (2019) 'Specificities of secretion and uptake of exosomes and other extracellular vesicles for cell-to-cell communication', *Nature Cell Biology*, pp. 9–17. doi: 10.1038/s41556-018-0250-9.

Mendez, O. *et al.* (2018) 'Extracellular HMGA1 promotes tumor invasion and metastasis in triple-negative breast cancer', *Clinical Cancer Research*, 24(24), pp. 6367–6382. doi: 10.1158/1078-0432.CCR-18-0517.

Momen-Heravi, F. *et al.* (2013) 'Current methods for the isolation of extracellular vesicles', *Biological chemistry*, 394(10), pp. 1253–1262. doi: 10.1515/hsz-2013-0141.

Momenimovahed, Z. and Salehiniya, H. (2019) 'Epidemiological characteristics of and risk factors for breast cancer in the world', *Breast Cancer: Targets and Therapy*, pp. 151–164. doi: 10.2147/BCTT.S176070.

Moreau, D. *et al.* (2019) 'Drug-induced increase in lysobisphosphatidic acid reduces the cholesterol overload in Niemann–Pick type C cells and mice', *EMBO reports*, 20(7). doi: 10.15252/embr.201847055.

Morelli, A. E. *et al.* (2004) 'Endocytosis, intracellular sorting, and processing of exosomes by dendritic cells', *Blood*, 104(10), pp. 3257–3266. doi: 10.1182/blood-2004-03-0824.

Morhayim, J., Baroncelli, M. and Van Leeuwen, J. P. (2014) 'Extracellular vesicles: Specialized bone messengers', *Archives of Biochemistry and Biophysics*, pp. 38–45. doi: 10.1016/j.abb.2014.05.011.

Mulcahy, L. A., Pink, R. C. and Carter, D. R. F. (2014) 'Routes and mechanisms of extracellular vesicle uptake', *Journal of Extracellular Vesicles*. doi: 10.3402/jev.v3.24641.

Nakashoji, A. *et al.* (2017) 'Clinical predictors of pathological complete response to neoadjuvant chemotherapy in triple-negative breast cancer', *Oncology Letters*, 14(4), pp. 4135–4141. doi: 10.3892/ol.2017.6692.

Nardone, G. *et al.* (2017) 'YAP regulates cell mechanics by controlling focal adhesion assembly', *Nature Communications*, 8. doi: 10.1038/ncomms15321.

Navarro Vilar, L. *et al.* (2017) 'MR Imaging Findings in Molecular Subtypes of Breast Cancer According to BIRADS System', *The Breast Journal*. doi: 10.1111/tbj.12756.

Nazarenko, I. (2020) 'Extracellular Vesicles: Recent Developments in Technology and Perspectives for Cancer Liquid Biopsy', in *Recent Results in Cancer Research*, pp. 319–344. doi: 10.1007/978-3-030-26439-0_17.

Needham, D. and Nunn, R. S. (1990) 'Elastic deformation and failure of lipid bilayer membranes containing cholesterol', *Biophysical Journal*, 58(4), pp. 997–1009. doi: 10.1016/S0006-3495(90)82444-9.

Ong, M. S. *et al.* (2020) 'Cytoskeletal proteins in cancer and intracellular stress: A therapeutic perspective', *Cancers*. doi: 10.3390/cancers12010238.

Ozawa, P. M. M. *et al.* (2018) 'Extracellular vesicles from triple-negative breast cancer cells promote proliferation and drug resistance in non-tumorigenic breast cells', *Breast Cancer Research and Treatment*, 172(3), pp. 713–723. doi: 10.1007/s10549-018-4925-5.

Panagiotou, N. *et al.* (2018) 'Extracellular Vesicles, Ageing, and Therapeutic Interventions', *Cells*, 7(8), p. 110. doi: 10.3390/cells7080110.

Paolini, L., Zendrini, A. and Radeghieri, A. (2018) 'Biophysical properties of extracellular

vesicles in diagnostics', *Biomarkers in Medicine*, 12(4), pp. 383–391. doi: 10.2217/bmm-2017-0458.

Parker, A. L. *et al.* (2017) 'An emerging role for tubulin isotypes in modulating cancer biology and chemotherapy resistance', *International Journal of Molecular Sciences*. doi: 10.3390/ijms18071434.

Peinado, H., Lavotshkin, S. and Lyden, D. (2011) 'The secreted factors responsible for pre-metastatic niche formation: Old sayings and new thoughts', *Seminars in Cancer Biology*, pp. 139–146. doi: 10.1016/j.semcancer.2011.01.002.

Peng, J. *et al.* (2018) 'Roles of Extracellular Vesicles in Metastatic Breast Cancer', *Breast Cancer: Basic and Clinical Research*. doi: 10.1177/1178223418767666.

Peschetola, V. *et al.* (2013) 'Time-dependent traction force microscopy for cancer cells as a measure of invasiveness', *Cytoskeleton*, 70(4), pp. 201–214. doi: 10.1002/cm.21100.

Pitt, J. M., Kroemer, G. and Zitvogel, L. (2016) 'Extracellular vesicles: Masters of intercellular communication and potential clinical interventions', *Journal of Clinical Investigation*, pp. 1139–1143. doi: 10.1172/JCI87316.

Qiao, Y. *et al.* (2017) 'YAP Regulates Actin Dynamics through ARHGAP29 and Promotes Metastasis', *Cell Reports*, 19(8), pp. 1495–1502. doi: 10.1016/j.celrep.2017.04.075.

Rahbarghazi, R. *et al.* (2019) 'Tumor-derived extracellular vesicles: Reliable tools for Cancer diagnosis and clinical applications', *Cell Communication and Signaling*. doi: 10.1186/s12964-019-0390-y.

Raimondo, F. *et al.* (2011) 'Advances in membranous vesicle and exosome proteomics improving biological understanding and biomarker discovery', *Proteomics*, pp. 709–720. doi: 10.1002/pmic.201000422.

Ramstedt, B. and Slotte, J. P. (2002) 'Membrane properties of sphingomyelins', *FEBS Letters*, pp. 33–37. doi: 10.1016/S0014-5793(02)03406-3.

Raposo, G. and Stahl, P. D. (2019) 'Extracellular vesicles: a new communication paradigm?', *Nature Reviews Molecular Cell Biology*, pp. 509–510. doi: 10.1038/s41580-019-0158-7.

Raposo, G. and Stoorvogel, W. (2013) 'Extracellular vesicles: Exosomes, microvesicles, and friends', *Journal of Cell Biology*, pp. 373–383. doi: 10.1083/jcb.201211138.

Rönnlund, D. *et al.* (2013) 'Spatial organization of proteins in metastasizing cells', *Cytometry Part A*, 83(9), pp. 855–865. doi: 10.1002/cyto.a.22304.

Rontogianni, S. *et al.* (2019) 'Proteomic profiling of extracellular vesicles allows for human breast cancer subtyping', *Communications Biology*, 2(1). doi: 10.1038/s42003-019-0570-8.

Royo, F. *et al.* (2020) 'Methods for Separation and Characterization of Extracellular Vesicles: Results of a Worldwide Survey Performed by the ISEV Rigor and Standardization Subcommittee', *Cells*, 9(9). doi: 10.3390/cells9091955.

Rudzka, D. A. *et al.* (2019) 'Migration through physical constraints is enabled by MAPK-induced cell softening via actin cytoskeleton re-organization', *Journal of Cell Science*, 132(11). doi: 10.1242/jcs.224071.

Rusaczonek, M. *et al.* (2019) 'Application of a layered model for determination of the elasticity of biological systems', *Micron*, 124. doi: 10.1016/j.micron.2019.102705.

Saeedi, S. *et al.* (2019) 'The emerging role of exosomes in mental disorders', *Translational Psychiatry*. doi: 10.1038/s41398-019-0459-9.

Santana, S. M. *et al.* (2014) 'Cancerous epithelial cell lines shed extracellular vesicles with a bimodal size distribution that is sensitive to glutamine inhibition', *Physical biology*, 11(6), p. 65001. doi: 10.1088/1478-3975/11/6/065001.

Schierbaum, N., Rheinlaender, J. and Schäffer, T. E. (2017) 'Viscoelastic properties of normal and cancerous human breast cells are affected differently by contact to adjacent cells', *Acta Biomaterialia*, 55, pp. 239–248. doi: 10.1016/j.actbio.2017.04.006.

Scully, O. J. *et al.* (2012) 'Breast cancer metastasis', *Cancer Genomics and Proteomics*, pp. 311–320. doi: 10.1016/j.ajpath.2013.06.012.

Sen, S., Subramanian, S. and Discher, D. E. (2005) 'Indentation and Adhesive Probing of a Cell Membrane with AFM: Theoretical Model and Experiments', *Biophysical Journal*, 89(5), pp. 3203–3213. doi: 10.1529/biophysj.105.063826.

Senigagliesi, B. *et al.* (2019) 'The high mobility group A1 (HMGA1) chromatin architectural factor modulates nuclear stiffness in breast cancer cells', *International Journal of Molecular Sciences*, 20(11). doi: 10.3390/ijms20112733.

Shang, M. *et al.* (2018) 'Potential management of circulating tumor DNA as a biomarker in triple-negative breast cancer', *Journal of Cancer*, pp. 4627–4634. doi: 10.7150/jca.28458.

Sharma, S. *et al.* (2020) 'Impact of isolation methods on the biophysical heterogeneity of single extracellular vesicles', *Scientific Reports*, 10(1), p. 13327. doi: 10.1038/s41598-020-70245-1.

Shedden, K. *et al.* (2003) 'Expulsion of small molecules in vesicles shed by cancer cells: Association with gene expression and chemosensitivity profiles', *Cancer Research*, 63(15), pp. 4331–4337.

Shen, J. *et al.* (2017) 'AFM tip-sample convolution effects for cylinder protrusions', *Applied Surface Science*, 422, pp. 482–491. doi: 10.1016/j.apsusc.2017.06.053.

Shen, J. *et al.* (2018) 'Hippo component YAP promotes focal adhesion and tumour aggressiveness via transcriptionally activating THBS1/FAK signalling in breast cancer', *Journal of Experimental and Clinical Cancer Research*, 37(1). doi: 10.1186/s13046-018-0850-z.

Shibue, T. and Weinberg, R. A. (2017) 'EMT, CSCs, and drug resistance: The mechanistic link and clinical implications', *Nature Reviews Clinical Oncology*, pp. 611–629. doi: 10.1038/nrclinonc.2017.44.

Simeone, P. *et al.* (2020) 'Extracellular Vesicles as Signaling Mediators and Disease Biomarkers across Biological Barriers', *International Journal of Molecular Sciences*, 21(7), p. 2514. doi: 10.3390/ijms21072514.

Skog, J. *et al.* (2008) 'Glioblastoma microvesicles transport RNA and proteins that promote tumour growth and provide diagnostic biomarkers', *Nature Cell Biology*, 10(12), pp. 1470–1476. doi: 10.1038/ncb1800.

Sokolova, V. *et al.* (2011) 'Characterisation of exosomes derived from human cells by nanoparticle tracking analysis and scanning electron microscopy', *Colloids and Surfaces B: Biointerfaces*, 87(1), pp. 146–150. doi: 10.1016/j.colsurfb.2011.05.013.

Steeg, P. S. (2016) 'Targeting metastasis.', *Nature reviews. Cancer*, 16(4), pp. 201–18. doi: 10.1038/nrc.2016.25.

Stevic, I. *et al.* (2018) 'Specific microRNA signatures in exosomes of triple-negative and HER2-positive breast cancer patients undergoing neoadjuvant therapy within the GeparSixto

trial', *BMC Medicine*, 16(1). doi: 10.1186/s12916-018-1163-y.

Stremersch, S., De Smedt, S. C. and Raemdonck, K. (2016) 'Therapeutic and diagnostic applications of extracellular vesicles', *Journal of Controlled Release*, 244, pp. 167–183. doi: 10.1016/j.jconrel.2016.07.054.

Strober, W. (2001) 'Trypan Blue Exclusion Test of Cell Viability', in *Current Protocols in Immunology*. doi: 10.1002/0471142735.ima03bs21.

Stylianou, A. *et al.* (2019) 'Atomic force microscopy on biological materials related to pathological conditions', *Scanning*, 2019. doi: 10.1155/2019/8452851.

Subra, C. *et al.* (2007) 'Exosome lipidomics unravels lipid sorting at the level of multivesicular bodies', *Biochimie*, pp. 205–212. doi: 10.1016/j.biochi.2006.10.014.

Subra, C. *et al.* (2010) 'Exosomes account for vesicle-mediated transcellular transport of activatable phospholipases and prostaglandins', *Journal of Lipid Research*, 51(8), pp. 2105–2120. doi: 10.1194/jlr.M003657.

Sung, B. H. *et al.* (2015) 'Directional cell movement through tissues is controlled by exosome secretion', *Nature Communications*, 6. doi: 10.1038/ncomms8164.

Sunkara, V., Woo, H. K. and Cho, Y. K. (2016) 'Emerging techniques in the isolation and characterization of extracellular vesicles and their roles in cancer diagnostics and prognostics', *Analyst*, pp. 371–381. doi: 10.1039/c5an01775k.

Szatanek, R. *et al.* (2017) 'The methods of choice for extracellular vesicles (EVs) characterization', *International Journal of Molecular Sciences*. doi: 10.3390/ijms18061153.

Szekeres-Bartho, J., Šućurović, S. and Mulac-Jeričević, B. (2018) 'The Role of Extracellular Vesicles and PIBF in Embryo-Maternal Immune-Interactions', *Frontiers in immunology*, p. 2890. doi: 10.3389/fimmu.2018.02890.

Takov, K., Yellon, D. M. and Davidson, S. M. (2019) 'Comparison of small extracellular vesicles isolated from plasma by ultracentrifugation or size-exclusion chromatography: yield, purity and functional potential', *Journal of Extracellular Vesicles*, 8(1). doi: 10.1080/20013078.2018.1560809.

Tavares, S. *et al.* (2017) 'Actin stress fiber organization promotes cell stiffening and proliferation of pre-invasive breast cancer cells', *Nature Communications*, 8. doi: 10.1038/ncomms15237.

Taylor, D. D. and Shah, S. (2015) 'Methods of isolating extracellular vesicles impact down-stream analyses of their cargoes', *Methods*, pp. 3–10. doi: 10.1016/j.ymeth.2015.02.019.

Thakur, B. K. *et al.* (2014) 'Double-stranded DNA in exosomes: A novel biomarker in cancer detection', *Cell Research*, pp. 766–769. doi: 10.1038/cr.2014.44.

Thery, C. *et al.* (2018) 'Minimal information for studies of extracellular vesicles 2018 (MISEV2018)', *Journal of Extracellular Vesicles*, 7:1535750, pp. 1–47.

Thomas, G. *et al.* (2013) 'Measuring the mechanical properties of living cells using atomic force microscopy', *Journal of visualized experiments : JoVE*, (76). doi: 10.3791/50497.

Toh, K. C., Ramdas, N. M. and Shivashankar, G. V. (2015) 'Actin cytoskeleton differentially alters the dynamics of lamin A, HP1α and H2B core histone proteins to remodel chromatin condensation state in living cells', *Integr. Biol.*, 7(10), pp. 1309–1317. doi: 10.1039/C5IB00027K.

Tschuschke, M. *et al.* (2020) 'Inclusion Biogenesis, Methods of Isolation and Clinical

Application of Human Cellular Exosomes', *Journal of Clinical Medicine*, 9(2), p. 436. doi: 10.3390/jcm9020436.

Turchinovich, A., Drapkina, O. and Tonevitsky, A. (2019) 'Transcriptome of extracellular vesicles: State-of-the-art', *Frontiers in Immunology*, 10(FEB). doi: 10.3389/fimmu.2019.00202.

Vahabi, S., Nazemi Salman, B. and Javanmard, A. (2013) 'Atomic force microscopy application in biological research: A review study', *Iranian Journal of Medical Sciences*, 38(2), pp. 76–83.

Valadi, H. *et al.* (2007) 'Exosome-mediated transfer of mRNAs and microRNAs is a novel mechanism of genetic exchange between cells', *Nature Cell Biology*, 9(6), pp. 654–659. doi: 10.1038/ncb1596.

Vallejos, C. S. *et al.* (2010) 'Breast Cancer Classification According to Immunohistochemistry Markers: Subtypes and Association With Clinicopathologic Variables in a Peruvian Hospital Database', *Clinical Breast Cancer*, 10(4), pp. 294–300. doi: 10.3816/CBC.2010.n.038.

Wang, S. *et al.* (2019) 'Exosomes secreted by mesenchymal stromal/stem cell-derived adipocytes promote breast cancer cell growth via activation of Hippo signaling pathway', *Stem Cell Research and Therapy*, 10(1). doi: 10.1186/s13287-019-1220-2.

Wang, S. *et al.* (2020) 'Recent advances in single extracellular vesicle detection methods', *Biosensors and Bioelectronics*. doi: 10.1016/j.bios.2020.112056.

Wang, Z. *et al.* (2014) 'Interplay of mevalonate and Hippo pathways regulates RHAMM transcription via YAP to modulate breast cancer cell motility', *Proceedings of the National Academy of Sciences of the United States of America*, 111(1). doi: 10.1073/pnas.1319190110.

Whitehead, B. *et al.* (2015) 'Tumour exosomes display differential mechanical and complement activation properties dependent on malignant state: implications in endothelial leakiness', *Journal of extracellular vesicles*, 4, p. 29685. doi: 10.3402/jev.v4.29685.

Willms, E. *et al.* (2018) 'Extracellular vesicle heterogeneity: Subpopulations, isolation techniques, and diverse functions in cancer progression', *Frontiers in Immunology*. doi: 10.3389/fimmu.2018.00738.

Wu, K. *et al.* (2017) 'Extracellular vesicles as emerging targets in cancer: Recent development from bench to bedside', *Biochimica et biophysica acta. Reviews on cancer*. 2017/10/18, 1868(2), pp. 538–563. doi: 10.1016/j.bbcan.2017.10.001.

Wubbolts, R. *et al.* (2003) 'Proteomic and biochemical analyses of human B cell-derived exosomes: Potential implications for their function and multivesicular body formation', *Journal of Biological Chemistry*, 278(13), pp. 10963–10972. doi: 10.1074/jbc.M207550200.

Xie, M. *et al.* (2020) 'Immunoregulatory Effects of Stem Cell-Derived Extracellular Vesicles on Immune Cells', *Frontiers in immunology*, p. 13. doi: 10.3389/fimmu.2020.00013.

Xu, R. *et al.* (2016) 'Extracellular vesicle isolation and characterization: Toward clinical application', *Journal of Clinical Investigation*, pp. 1152–1162. doi: 10.1172/JCI81129.

Yáñez-Mó, M. *et al.* (2015) 'Biological properties of extracellular vesicles and their physiological functions', *Journal of Extracellular Vesicles*, pp. 1–60. doi: 10.3402/jev.v4.27066.

Yeo, W. (2015) 'Treatment horizons for triple-negative breast cancer', *Hong Kong Journal of Radiology*, pp. 111–118. doi: 10.12809/hkjr1515321.

Yoon, Y. J., Kim, O. Y. and Gho, Y. S. (2014) 'Extracellular vesicles as emerging intercellular

communicasomes', *BMB Reports*, pp. 531–539. doi: 10.5483/BMBRep.2014.47.10.164.

Yu, X., Harris, S. L. and Levine, A. J. (2006) 'The regulation of exosome secretion: A novel function of the p53 protein', *Cancer Research*, 66(9), pp. 4795–4801. doi: 10.1158/0008-5472.CAN-05-4579.

Zhang, W. *et al.* (2016) 'Characterization of exosomes derived from ovarian cancer cells and normal ovarian epithelial cells by nanoparticle tracking analysis', *Tumor Biology*, 37(3), pp. 4213–4221. doi: 10.1007/s13277-015-4105-8.

Zheng, Y. *et al.* (2020) 'Extracellular vesicle-derived circ_SLC19A1 promotes prostate cancer cell growth and invasion through the miR-497/septin 2 pathway', *Cell Biology International*, 44(4), pp. 1037–1045. doi: 10.1002/cbin.11303.

Zhou, X. *et al.* (2019) 'Mesenchymal stem cell.derived extracellular vesicles promote the in vitro proliferation and migration of breast cancer cells through the activation of the ERK pathway', *International Journal of Oncology*, 54(5), pp. 1843–1852. doi: 10.3892/ijo.2019.4747.